

**SUPRAMOLECULAR BIOMATERIALS BASED ON  
CYCLODEXTRIN-OLIGOETHYLENIMINE STAR  
POLYMERS FOR DRUG AND GENE DELIVERY**

**ZHAO FENG**

*(M. Med. Sci., Zhejiang University)*

**A THESIS SUBMITTED**

**FOR THE DEGREE OF DOCTOR OF PHILOSOPHY**

**DEPARTMENT OF BIOMEDICAL ENGINEERING**

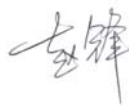
**NATIONAL UNIVERSITY OF SINGAPORE**

**2013**

## **DECLARATION**

I hereby declare that the thesis is my original work and it has been written by me in its entirety. I have duly acknowledged all the sources of information which have been used in the thesis.

This thesis has also not been submitted for any degree in any university previously.



---

Zhao Feng

19 August 2013

## ACKNOLEGEMENT

First and foremost, I owe my deepest gratitude to my supervisor Associate Prof. Li Jun. Thank you for all the support, guidance, and encouragement during my studies. Your insight idea and steady persistence in work has deeply impressed me. Thank you for the hard work during the revision of my papers and thesis. It is hard to express my heartfelt appreciation when I received your emails about my research work at midnight. It has been my great pleasure to study and to do research work under your supervision. The four year PhD study experience is my greatest fortune in my life.

I would like to thank Prof. Li Xiaoping and Associate Prof. Chen Nanguang as members of my PhD Thesis Advisory Committee for their advices and comments. In addition, I would like to thank the National University of Singapore and Department of Bioengineering for offering the Research Scholarship and the facilities and ambience, so that I can smoothly complete my PhD research project.

I would like to thank Dr. Wu Yunlong for his assistance in this project. I learnt lots of lab skills from him, especially the biological experimental skills. I would like to express my heartfelt thanks to all the colleagues and friends in Supramolecular Biomaterials lab at National University of Singapore and Institute of Materials Research and Engineering (IMRE) for their constant assistance and valuable comments during my research work. It is a wonderful

## Acknowledgement

---

experience to work with you. I would like to thank Dr. Zhang Zhongxing for his kind help on the sample measurements at IMRE. Thanks Dr. Yin Hui for her advice and help on biological experiments and reagent ordering. I would like to thank Ms Ni Xiping for her assistance in ordering chemicals from IMRE. Thanks Dr. Zhu Jingling, for your facility booking at IMRE and comments on my project. I would like to express my sincere thanks to Dr. Liu Kerh Li, Loh Xian Jun, Ping Yuan, Liu Chengde, Li Jiajing, She Zhen, Li Zibiao, and Song Xia for their help and suggestions during my research work and life in National University of Singapore.

Special thanks to my friends at AMRI Pte. Ltd., Dr. Wu Xiang, Xiang Kai, Dr. Duan Zhiyong, and Dr. Chen Guihui, for your help during my PhD study.

I would like to express my deeply appreciation to my beloved, Chen Qiaoling. Thanks for being with me and thanks for your consideration and encouragement.

Last but not least, I want to express my heartfelt thanks to my parents for their consistent support and love.

## TABLE OF CONTENTS

<b>DECLARATION.....</b>	<b>i</b>
<b>ACKNOLEGEMENT.....</b>	<b>ii</b>
<b>TABLE OF CONTENTS .....</b>	<b>iv</b>
<b>SUMMARY .....</b>	<b>viii</b>
<b>LIST OF SCHEMES .....</b>	<b>x</b>
<b>LIST OF TABLES .....</b>	<b>xii</b>
<b>LIST OF FIGURES .....</b>	<b>xiii</b>
<b>LIST OF ABBREVIATIONS .....</b>	<b>xx</b>
<b>LIST OF PUBLICATIONS .....</b>	<b>xxiii</b>
<b>CHAPTER 1 INTRODUCTION .....</b>	<b>1</b>
1.1. Background Information .....	1
1.2. Objective and Scope of Study .....	4
1.3. Organization of the Thesis .....	5
1.4. References .....	6
<b>CHAPTER 2 LITERATURE REVIEW .....</b>	<b>10</b>
2.1. Cancer and Cancer Therapy .....	10
2.1.1. Cancer Treatments .....	11
2.1.2. Anticancer Drugs.....	11
2.1.3. Gene Therapy .....	12

## Table of Contents

2.1.4. Drug and Gene Co-delivery .....	13
2.1.5. Gene Delivery Vectors.....	14
2.2. Characteristics of Cyclodextrins .....	18
2.2.1. The Physiochemical Properties of Cyclodextrins.....	19
2.2.2. The Biological Properties of Cyclodextrins .....	20
2.3. Cyclodextrin on Drug Delivery .....	21
2.4. Cyclodextrin on Gene Delivery.....	26
2.4.1. Cyclodextrins as Gene Delivery Enhancers.....	26
2.4.2. Cyclodextrin-based Polymers for Gene Delivery.....	26
2.5. Cyclodextrin-based Polyrotaxanes for Drug and Gene Delivery.....	31
2.6. Target Delivery .....	35
2.6.1. Overview of Folic Acid and Folate Receptor .....	36
2.6.2. Folate-targeted Gene Therapy .....	36
2.6.3. Factors Affecting Folate-targeted Delivery .....	37
2.7. Redox-Sensitive Carriers.....	37
2.8. References .....	40
<b>CHAPTER 3 SOLUBILITY AND ANTITUMOR ACTIVITY OF INCLUSION COMPLEXES OF CYCLODEXTRIN-OLIGOETHYLENIMINES AND PACLITAXEL...50</b>	
3.1. Introduction .....	50
3.2. Experimental Section .....	52
3.2.1. Materials.....	52
3.2.2. Synthesis .....	53
3.2.3. NMR Spectroscopy. ....	56
3.2.4. UV-Vis Spectroscopy.....	56
3.2.5. Fourier Transform Infrared Spectroscopy .....	56
3.2.6. Solubility Test .....	57
3.2.7. Stability Test .....	57
3.2.8. Confocal Microscopy.....	57
3.2.9. Cell Viability Assay .....	58

## Table of Contents

3.3. Results and Discussions .....	58
3.3.1. <i>Synthesis of CD-OEI/PTX Inclusion Complexes</i> .....	59
3.3.2. <i>Water Solubility and Stability</i> .....	62
3.3.3. <i>Cellular Uptake Test</i> .....	64
3.3.4. <i>Cell Viability Test</i> .....	65
3.4. Conclusions .....	66
3.5. References .....	68
 <b>CHAPTER 4     FOLIC ACID MODIFIED CATIONIC</b>	
<b><math>\gamma</math>-CYCLODEXTRIN-OLIGOETHYLENIMINE STAR POLYMER</b>	
<b>WITH BIOREDUCIBLE DISULFIDE LINKER FOR EFFICIENT</b>	
<b>TARGETED GENE DELIVERY.....</b>	
<b>70</b>	
4.1. Introduction .....	70
4.2. Experimental Section .....	73
4.2.1. <i>Materials</i> .....	73
4.2.2. <i>Synthesis Procedure</i> .....	73
4.2.3. <i>Characterization Methods</i> .....	76
4.2.4. <i>Biological Characterization Methods</i> .....	77
4.3. Results and Discussion .....	81
4.3.1. <i>Synthesis of <math>\gamma</math>-CD-OEI-SS-FA</i> .....	81
4.3.2. <i>Formation of <math>\gamma</math>-CD-OEI-SS-FA/DNA Complexes</i> .....	85
4.3.3. <i>Cytotoxicity</i> .....	87
4.3.4. <i>In vitro gene transfection</i> .....	88
4.4. Conclusions .....	93
4.5. References .....	96
 <b>CHAPTER 5     A MULTIFUNCTIONAL SUPRAMOLECULAR</b>	
<b>SELF-ASSEMBLY FORMING A SYNERGISTIC TARGETED AND</b>	
<b>CO-DELIVERY SYSTEM OF GENE AND DRUG FOR POTENTIAL</b>	
<b>CANCER THERAPY.....</b>	
<b>98</b>	
5.1. Introduction .....	98
5.2. Experimental Section .....	100

## Table of Contents

---

5.2.1. <i>Materials</i> .....	100
5.2.2. <i>Preparation of Inclusion Complexes</i> .....	101
5.2.3. <i>Characterization Methods</i> .....	102
5.2.4. <i>Biological Characterization Methods</i> .....	103
5.3. <i>Results and Discussion</i> .....	108
5.3.1. <i>Synthesis of Self-assembled Inclusion Complexes</i> .....	108
5.3.2. <i>Formation of Polyplexes with pDNA</i> .....	112
5.3.3. <i>Cytotoxicity</i> .....	114
5.3.4. <i>In vitro Luciferase Gene Transfection</i> .....	115
5.3.5. <i>Delivery of Wild Type p53 Gene for Cancer Cell Apoptosis</i> .....	122
5.4. <i>Conclusions</i> .....	125
5.5. <i>References</i> .....	127
<b>CHAPTER 6 CONCLUSIONS AND FUTURE WORK</b> .....	<b>130</b>
6.1. <i>Conclusions</i> .....	130
6.2. <i>Future Work</i> .....	132
6.3. <i>References</i> .....	133



## SUMMARY

Cyclodextrins (CDs) are a series of natural cyclic oligosaccharides. The most widely used CDs consist of 6, 7, and 8 D(+)-glucose units connected by  $\alpha$ -1,4-linkages, named  $\alpha$ -,  $\beta$ -, and  $\gamma$ -CD, respectively. The torus structure of CDs is unique with hydrophilic outer surfaces and hydrophobic cavities. The hydrophobic cavities can form inclusion complexes with many hydrophobic drugs to alter their physical, chemical, and biological properties. Furthermore, the hydroxyl groups can be conjugated with cationic polymers for potential gene delivery.

This thesis has four parts. In the first part, we present a literature review of cancer therapy especially chemotherapy, gene therapy, and a combination of drug and gene co-delivery. The properties of CD and CD-based drug delivery, targeted gene delivery, and co-delivery will be presented in this thesis.

In the second part, we synthesized  $\alpha$ -,  $\beta$ -, and  $\gamma$ -CD derivatives by conjugation with short-chain oligoethylenimine arms. These modified cationic cyclodextrin variants can form inclusion complexes with anticancer drug paclitaxel and significantly improve the physiochemical properties, such as solubility. The antitumor activity of paclitaxel in the inclusion complexes is still maintained.

In the third part, we demonstrated synthesis of a new star-shaped cationic

## Summary

---

polymer containing a  $\gamma$ -cyclodextrin core and multiple oligoethylenimine arms. Folic acid was conjugated to the cationic molecules for effective target delivery and a biodegradable disulfide bond was incorporated between the cationic polymer and target group. The new CD-based cationic polymer, named  $\gamma$ -CD-OEI-SS-FA, had low cytotoxicity, and is able to target deliver DNA to specific tumor cells that overexpress folate receptors, as well as smart functions to recover and recycle folate receptors onto cellular membranes to facilitate continuous folate receptor mediated endocytosis to achieve very high levels of gene expression.

In the fourth part, we investigated the synergistic/combined effect by co-delivery of drug and gene to fabricate more effective gene delivery systems. Paclitaxel formed inclusion complexes with previous synthesized cationic polymer  $\gamma$ -CD-OEI-SS-FA. The co-delivery system maintains the target effect and folate receptor recovery function of  $\gamma$ -CD-OEI-SS-FA. Moreover, the unique hydrophobic cavity of  $\gamma$ -CD was used to load paclitaxel with high loading efficiency and high stability and solubility in water. Co-delivery synergistic effect by delivery of tumor suppressor p53 gene was achieved. This co-delivery system could be an efficient strategy for potential cancer gene therapy.

## LIST OF SCHEMES

<b>Scheme 1.1.</b> Synthesis procedures of $\alpha$ -CD-OEI star polymers.....	4
<b>Scheme 2.1.</b> Synthesis of cationic amphiphilic polymer P(MDS- <i>co</i> -CES). ...	14
<b>Scheme 2.2.</b> Conjugation of PEI with crosslinking reagents DSP and DTBP. .....	18
<b>Scheme 2.3.</b> Synthesis of cyclodextrin-containing polycation (CDP, a) and the imidazole-terminated variant (CDPim, b).....	27
<b>Scheme 2.4.</b> Synthesis of $\alpha$ -CD-OEI star-shaped polymers. ....	27
<b>Scheme 2.5.</b> Synthesis of $\beta$ -CD-PEI-FA (a) and HP- $\gamma$ -CD-PEI-P (b). ....	28
<b>Scheme 2.6.</b> Synthesis of the $\beta$ -CD-containing cationic polymers by click chemistry.....	29
<b>Scheme 2.7.</b> Synthesis procedures and structures of cationic polyrotaxanes with multiple OEI-grafted $\beta$ -CD rings. <sup>168</sup> .....	35
<b>Scheme 3.1.</b> Synthesis of $\alpha$ -, $\beta$ -, and $\gamma$ -CD-OEI/PTX inclusion complexes ...	53
<b>Scheme 4.1.</b> Synthesis of FA with disulfide linker FA-SS-COOH (a) and $\gamma$ -CD-OEI-FA and $\gamma$ -CD-OEI-SS-FA (b). ....	82

## List of Schemes

---

<b>Scheme 5.1.</b> (a) Structures of $\gamma$ -CD-OEI-SS-FA. (b) Schematic presentation of the supramolecular self-assembly process for formation of the $\gamma$ -CD-OEI-SS-FA/PTX inclusion complex. (c) Illustration of the concept of the drug and gene co-delivery mediated by the multifunctional supramolecular self-assembly.....	109
---	-----

## LIST OF TABLES

<b>Table 2.1.</b> Structural and physiochemical properties of selected CDs.....	19
<b>Table 2.2.</b> Illustration of CD pharmaceutical products .....	22
<b>Table 2.3.</b> Solubility of PTX in aqueous solutions with different CDs. ....	24
<b>Table 2.4.</b> List of generally used polymers and corresponding CDs .....	32
<b>Table 3.1.</b> Solubility of $\alpha$ -, $\beta$ -, $\gamma$ -CD-OEIs at 25 °C.....	59
<b>Table 3.2.</b> Water solubility of CD-OEI/PTX inclusion complexes at 25 °C...	62
<b>Table 5.1.</b> Cell cycle analysis results of FR-positive KB cells transfected with pCMV-p53 and pCMV-p53mt135 mediated by PEI (25 KDa), $\gamma$ -CD-OEI, $\gamma$ -CD-OEI-FA, $\gamma$ -CD-OEI-SS-FA, $\gamma$ -CD-OEI/PTX, $\gamma$ -CD-OEI-FA/PTX, $\gamma$ -CD-OEI-SS-FA/PTX, and physical mixture of $\gamma$ -CD-OEI-SS-FA and PTX at N/P ratio of 15 in FA-free RPMI 1640 medium. ....	123
<b>Table 5.2.</b> Cell cycle analysis results of FR-negative A549 cells transfected with pCMV-p53 and pCMV-p53mt135 mediated by PEI (25 KDa), $\gamma$ -CD-OEI, $\gamma$ -CD-OEI-FA, $\gamma$ -CD-OEI-SS-FA, $\gamma$ -CD-OEI/PTX, $\gamma$ -CD-OEI-FA/PTX, $\gamma$ -CD-OEI-SS-FA/PTX, and physical mixture of $\gamma$ -CD-OEI-SS-FA and PTX at N/P ratio of 15 in FA-free RPMI 1640 medium. ....	124

## LIST OF FIGURES

<b>Figure 2.1.</b> Illustration of worldwide cancer mortality rates (Referred from WHO GLOBOCAN 2008). .....	11
<b>Figure 2.2.</b> Structure of paclitaxel.....	12
<b>Figure 2.3.</b> Selected cationic polymers as non-viral gene delivery vectors....	16
<b>Figure 2.4.</b> Structure of branched PEI (bPEI) and linear PEI (lPEI). .....	17
<b>Figure 2.5.</b> Illustrated structure of CD and the related profiles. ....	18
<b>Figure 2.6.</b> Illustrated formation of 1:1 CD-drug inclusion complex. ....	21
<b>Figure 2.7.</b> Illustrated structure of $\beta$ -CD dimer. ....	25
<b>Figure 2.8.</b> Illustrated structure of bridged bis( $\beta$ -CD). ....	25
<b>Figure 2.9.</b> Schematic representation of the nanoparticles consists of transferrin-targeted siRNA-CDP/Ad-PEG.....	30
<b>Figure 2.10.</b> Demonstration of CD and polyrotaxane: (a) structure of $\alpha$ -CD, (b) synthesis of polyrotaxane from $\alpha$ -CD and PEO-diamine. <sup>158</sup> .....	31
<b>Figure 2.11.</b> Selective disulfide cross-linking agents. ....	38
<b>Figure 3.1.</b> Illustrated structure of paclitaxel and OEI-grafted cyclodextrins.	52

## List of Figures

<b>Figure 3.2.</b> $^1\text{H}$ NMR spectra of PTX in $\text{CDCl}_3$ (a), $\gamma$ -CD-OEI-2 (b), and $\gamma$ -CD-OEI-2/PTX (c) in $\text{D}_2\text{O}$ .	60
<b>Figure 3.3.</b> $^{13}\text{C}$ NMR spectra of PTX in $\text{CDCl}_3$ (a), $\gamma$ -CD (b), and $\gamma$ -CD-OEI-2/PTX (c) in $\text{D}_2\text{O}$ .	61
<b>Figure 3.4.</b> UV-Visible spectra of $\alpha$ -, $\beta$ -, $\gamma$ -CD-OEI-2 and $\alpha$ -, $\beta$ -, $\gamma$ -CD-OEI-2/PTX on a concentration of 0.2 mg/mL in $\text{H}_2\text{O}$ . The arrow indicates UV absorption of PTX at 230 nm.	61
<b>Figure 3.5.</b> FT-IR spectra of $\gamma$ -CD-OEI-2 (a), PTX (b), and $\gamma$ -CD-OEI-2/PTX inclusion complex (c).	62
<b>Figure 3.6.</b> Stability of $\alpha$ -, $\beta$ -, $\gamma$ -CD-OEI-1/PTX and $\alpha$ -, $\beta$ -, $\gamma$ -CD-OEI-2/PTX in aqueous solution with a concentration of 3 mg/mL from 2 to 72 hours at 25 $^\circ\text{C}$ .	64
<b>Figure 3.7.</b> Confocal microscopy images of PTX-7-FITC (a), $\gamma$ -CD-OEI-2-rhodamine (b), and $\gamma$ -CD-OEI-2-rhodamine/PTX-7-FITC (c) in HeLa cells. The same field of cells was observed by red fluorescent image (left), red and green merged image (middle), and bright field (right).	65
<b>Figure 3.8.</b> Cell viability assay of $\alpha$ -CD-OEI-1, $\alpha$ -CD-OEI-2, $\beta$ -CD-OEI-1, $\beta$ -CD-OEI-2, $\gamma$ -CD-OEI-1, $\gamma$ -CD-OEI-2 in HeLa (a) and MCF-7 cells (c), and $\alpha$ -CD-OEI-1/PTX, $\alpha$ -CD-OEI-2/PTX, $\beta$ -CD-OEI-1/PTX, $\beta$ -CD-OEI-2/PTX, $\gamma$ -CD-OEI-1/PTX, $\gamma$ -CD-OEI-2/PTX in HeLa (b) and MCF-7 cells (d) at various concentrations for 48 hours in DMEM medium. Data represent mean $\pm$ standard deviation (n = 4).	66

## List of Figures

---

<b>Figure 4.1.</b> $^1\text{H}$ NMR spectra of $\gamma$ -CD-OEI (a), $\gamma$ -CD-OEI-FA <sub>1.2</sub> (b), $\gamma$ -CD-OEI-SS-FA <sub>0.8</sub> (c), $\gamma$ -CD-OEI-SS-FA <sub>1.3</sub> (d), and $\gamma$ -CD-OEI-SS-FA <sub>1.7</sub> (e) in D <sub>2</sub> O. ....	83
<b>Figure 4.2.</b> $^{13}\text{C}$ NMR spectra of $\gamma$ -CD-OEI-SS-FA <sub>1.3</sub> in D <sub>2</sub> O. ....	84
<b>Figure 4.3.</b> UV-Visible spectra of FA (0.01 mg/mL), $\gamma$ -CD-OEI (0.1 mg/mL), $\gamma$ -CD-OEI-FA <sub>1.2</sub> (0.1 mg/mL), and $\gamma$ -CD-OEI-SS-FA <sub>1.3</sub> (0.1 mg/mL) in H <sub>2</sub> O. ....	84
<b>Figure 4.4.</b> Release profiles of $\gamma$ -CD-OEI-SS-FA <sub>1.3</sub> in the absence and presence of DTT at 10 $\mu\text{M}$ and 10 mM in PBS buffer (pH 7.4, 1.0 mL) at 37 °C. ....	85
<b>Figure 4.5.</b> Electrophoretic mobility of pDNA in the polyplexes formed with PEI (a), $\gamma$ -CD-OEI (b), $\gamma$ -CD-OEI-FA <sub>1.2</sub> (c), and $\gamma$ -CD-OEI-SS-FA <sub>1.3</sub> (d). The arrows indicate the N/P ratios where the DNA mobility is completely retarded. ....	86
<b>Figure 4.6.</b> Particle size (a) and zeta potential (b) of the pDNA polyplexes with PEI (25 kDa), $\gamma$ -CD-OEI, $\gamma$ -CD-OEI-FA <sub>1.2</sub> , and $\gamma$ -CD-OEI-SS-FA <sub>1.3</sub> , respectively, at various N/P ratios. ....	86
<b>Figure 4.7.</b> Cell viability assay in KB cell line. The cells were treated with PEI (25 kDa), $\gamma$ -CD-OEI, $\gamma$ -CD-OEI-FA <sub>1.2</sub> , and $\gamma$ -CD-OEI-SS-FA <sub>1.3</sub> at various concentrations for 24 hours in the absence (a) and presence (b) of FA (0.001 g/L) in RPMI 1640 medium. Data represent mean $\pm$ standard deviation (n = 5). ....	87



## List of Figures

---

<b>Figure 4.8.</b> <i>In vitro</i> gene transfection efficiency of the pDNA polyplexes with PEI (25 kDa), $\gamma$ -CD-OEI, $\gamma$ -CD-OEI-SS-FA <sub>0.8</sub> , $\gamma$ -CD-OEI-SS-FA <sub>1.3</sub> , and $\gamma$ -CD-OEI-SS-FA <sub>1.7</sub> in KB cells in RPMI 1640 medium in the absence of FA. Data represent mean $\pm$ standard deviation (* <i>P</i> < 0.05, n = 4). .....	88
<b>Figure 4.9.</b> <i>In vitro</i> gene transfection efficiency of the pDNA polyplexes with PEI (25 kDa), $\gamma$ -CD-OEI, $\gamma$ -CD-OEI-FA <sub>1.2</sub> , and $\gamma$ -CD-OEI-SS-FA <sub>1.3</sub> in KB cells (a) and A549 cells (b) in RPMI 1640 medium in the absence of FA. Data represent mean $\pm$ standard deviation (* <i>P</i> < 0.05, n = 4). .....	89
<b>Figure 4.10.</b> <i>In vitro</i> gene transfection efficiency of the pDNA polyplexes with $\gamma$ -CD-OEI, $\gamma$ -CD-OEI-FA <sub>1.2</sub> , and $\gamma$ -CD-OEI-SS-FA <sub>1.3</sub> at N/P ratio of 50 in comparison with pDNA polyplexes with PEI (25 kDa) at N/P ratio of 10 in KB (a) and A549 (b) cells in RPMI 1640 medium treated with FA at different concentrations (0.000, 0.001, 0.010, and 0.100 g/L). Data represent mean $\pm$ standard deviation (* <i>P</i> < 0.05, n = 4). .....	91
<b>Figure 4.11.</b> <i>In vitro</i> gene transfection efficiency of the pDNA polyplexes with PEI (25 kDa) at N/P ratio of 10 and pDNA polyplex with $\gamma$ -CD-OEI, $\gamma$ -CD-OEI-FA <sub>1.2</sub> , and $\gamma$ -CD-OEI-SS-FA <sub>1.3</sub> at N/P ratio of 50 in KB cells in RPMI 1640 medium treated with BSO at different concentrations (0, 50, 250, and 500 $\mu$ M). Data represent mean $\pm$ standard deviation (* <i>P</i> < 0.05, n = 4). .	92
<b>Figure 4.12.</b> Confocal microscopy images of transfected KB cells by the EGFP polyplexes with PEI (25 kDa) (a), $\gamma$ -CD-OEI (b), $\gamma$ -CD-OEI-FA <sub>1.2</sub> (C), and $\gamma$ -CD-OEI-SS-FA <sub>1.3</sub> (d) in RPMI 1640 medium in the absence of FA. N/P ratio	

## List of Figures

was 10 for (a), and 50 for (b) – (d). For each experiment, the same field of cells was observed by fluorescent (left) and bright (right) fields to visualize GFP expression. ....	93
<b>Figure 5.1.</b> Size exclusion chromatography diagrams of $\gamma$ -CD (a), $\gamma$ -CD-OEI (b), $\gamma$ -CD-OEI-SS-FA (c), and $\gamma$ -CD-OEI-SS-FA/PTX (d) recorded with refractive index (RI) and optical rotation (OR). ....	110
<b>Figure 5.2.</b> $^1\text{H}$ NMR spectra of $\gamma$ -CD-OEI (a), $\gamma$ -CD-OEI/PTX (b), $\gamma$ -CD-OEI-FA/PTX (c), $\gamma$ -CD-OEI-SS-FA (d), and $\gamma$ -CD-OEI-SS-FA/PTX (e) in $\text{D}_2\text{O}$ . ....	111
<b>Figure 5.3.</b> UV-vis spectra of $\gamma$ -CD-OEI, $\gamma$ -CD-OEI/PTX, $\gamma$ -CD-OEI-FA, $\gamma$ -CD-OEI-FA/PTX, $\gamma$ -CD-OEI-SS-FA, and $\gamma$ -CD-OEI-SS-FA/PTX at 0.1 mg/mL in $\text{H}_2\text{O}$ . The arrow indicates UV absorption of PTX at 230 nm. ....	112
<b>Figure 5.4.</b> Electrophoretic mobility of pDNA in the polyplexes formed with PEI (a), $\gamma$ -CD-OEI/PTX (b), $\gamma$ -CD-OEI-FA/PTX (c), and $\gamma$ -CD-OEI-SS-FA/PTX (d). The arrows indicate the N/P ratios where the DNA mobility is completely retarded. ....	112
<b>Figure 5.5.</b> Particle size (a) and zeta potential (b) of the pDNA polyplexes with PEI (25 kDa), $\gamma$ -CD-OEI, $\gamma$ -CD-OEI/PTX, $\gamma$ -CD-OEI-FA, $\gamma$ -CD-OEI-FA/PTX, $\gamma$ -CD-OEI-SS-FA, and $\gamma$ -CD-OEI-SS-FA/PTX at various N/P ratios. ....	113
<b>Figure 5.6.</b> Cell viability assay in KB cells. The KB cells were treated with PEI (25 kDa), $\gamma$ -CD-OEI, $\gamma$ -CD-OEI/PTX, $\gamma$ -CD-OEI-FA, $\gamma$ -CD-OEI-FA/PTX, $\gamma$ -CD-OEI-SS-FA, $\gamma$ -CD-OEI-SS-FA/PTX, and physical mixture of	

## List of Figures

---

$\gamma$ -CD-OEI-SS-FA and PTX (denoted by  $\gamma$ -CD-OEI-SS-FA + PTX) at various concentrations for 24 hours in FA-free RPMI 1640 medium. Data represent mean  $\pm$  standard deviation (n = 4). ..... 114

**Figure 5.7.** *In vitro* gene transfection efficiency of the pDNA polyplexes with PEI (25 kDa),  $\gamma$ -CD-OEI,  $\gamma$ -CD-OEI-FA,  $\gamma$ -CD-OEI-SS-FA,  $\gamma$ -CD-OEI/PTX,  $\gamma$ -CD-OEI-FA/PTX,  $\gamma$ -CD-OEI-SS-FA/PTX, and physical mixture of  $\gamma$ -CD-OEI-SS-FA and PTX (denoted by  $\gamma$ -CD-OEI-SS-FA + PTX) at different N/P ratios in KB cells (a) and A549 cells (b) in FA-free RPMI 1640 medium.

Data represent mean  $\pm$  standard deviation (\**P* < 0.005, n = 4). ..... 115

**Figure 5.8.** *In vitro* gene transfection efficiency of the pDNA polyplexes with by PEI (25 kDa),  $\gamma$ -CD-OEI,  $\gamma$ -CD-OEI-FA,  $\gamma$ -CD-OEI-SS-FA,  $\gamma$ -CD-OEI/PTX,  $\gamma$ -CD-OEI-FA/PTX,  $\gamma$ -CD-OEI-SS-FA/PTX, and physical mixture of  $\gamma$ -CD-OEI-SS-FA and PTX (denoted by  $\gamma$ -CD-OEI-SS-FA + PTX) at N/P ratio of 15 in KB cells (a) and A549 cells (b) in the absence and presence of 0.001 g/L of FA in the culture medium. Data represent mean  $\pm$  standard deviation (\**P* < 0.005, n = 4). ..... 118

**Figure 5.9.** *In vitro* gene transfection efficiency of the pDNA polyplexes with PEI (25 kDa),  $\gamma$ -CD-OEI,  $\gamma$ -CD-OEI-FA,  $\gamma$ -CD-OEI-SS-FA,  $\gamma$ -CD-OEI/PTX,  $\gamma$ -CD-OEI-FA/PTX,  $\gamma$ -CD-OEI-SS-FA/PTX, and physical mixture of  $\gamma$ -CD-OEI-SS-FA and PTX (denoted by  $\gamma$ -CD-OEI-SS-FA + PTX) at N/P ratio of 15 in KB cells in the absence and presence of 250  $\mu$ M of BSO in the culture medium. Data represent mean  $\pm$  standard deviation (\**P* < 0.005, n = 4) ..... 119

## List of Figures

---

**Figure 5.10.** Confocal microscopy images of the KB cells transfected by the pDNA polyplexes with  $\gamma$ -CD-OEI-Rhd (a),  $\gamma$ -CD-OEI-Rhd/PTX-FITC (b),  $\gamma$ -CD-OEI-FA-Rhd (c),  $\gamma$ -CD-OEI-FA-Rhd/PTX-FITC (d),  $\gamma$ -CD-OEI-SS-FA-Rhd (e),  $\gamma$ -CD-OEI-SS-FA-Rhd/PTX-FITC (f), and  $\gamma$ -CD-OEI-SS-FA/PTX-FITC (g) at N/P ratio of 15 in FA-free RPMI 1640 medium. PTX and  $\gamma$ -CD-OEI derivatives were labeled with FITC (green) and rhodamine (red), respectively. .... 121

**Figure 5.11.** Representative cell cycle diagrams of KB cells transfected with pCMV-p53 mediated by  $\gamma$ -CD-OEI/PTX (a),  $\gamma$ -CD-OEI-FA/PTX (b),  $\gamma$ -CD-OEI-SS-FA/PTX (c), and transfected with pCMV-p53mt135 mediated by  $\gamma$ -CD-OEI/PTX (d),  $\gamma$ -CD-OEI-FA/PTX (e), and  $\gamma$ -CD-OEI-SS-FA/PTX (f) at N/P ratio of 15 in FA-free RPMI 1640 medium. .... 122

## **LIST OF ABBREVIATIONS**

Ad	Adamantane
BSA	Bovine serum albumin
BSO	Buthionine Sulphoximine
CD	Cyclodextrin
CDI	1,1'-Carbonyldiimidazole
CO <sub>2</sub>	Carbon dioxide
DMEM	Dulbecco's Modified Eagle's Medium
DMF	Dimethylformamide
DMSO	Dimethyl Sulfoxide
DNA	Deoxyribonucleic acid
DOX	Doxorubincin
DTT	Dithiothreitol
EDCI	<i>N</i> -(3-dimethylaminopropyl)- <i>N'</i> -ethylcarbodiimide hydrochloride

### List of Abbreviation

---

FA	Folic acid
FR	Folate receptor
FITC	Fluoresence isothiocyanate
GSH	Glutathione
HOBt	1-hydroxybenzotriazole
MWCO	Molecular weight cut off
MTT	3-(4,5-Dimethylthiazol-2-yl)-2,5-diphenyl tetrazolium bromide
NMR	Nuclear magnetic resonance
NHS	<i>N</i> -hydroxysuccinimide
OEI	Oligoethylenimine
PCL	Polycaprolactone
PEI	Polyethyleneimine
PEG	Poly(ethylene glycol)
PEO	Poly(ethylene oxide)
PPO	Poly(propylene oxide)
PR	Polyrotaxane
PPR	Polypseudorotaxane
PTX	Paclitaxel

### **List of Abbreviation**

---

TNBS      2,4,6-Trinitrobenzene sulfonic acid

TNB      2,4,6-Trinitrobenzene

THF      Tetrahydrofuran

## LIST OF PUBLICATIONS

1. **Feng Zhao**, Hui Yin, Zhongxing Zhang, Jun Li, Folic acid modified cationic  $\gamma$ -cyclodextrin-oligoethylenimine star polymer with bioreducible disulfide linker for efficient targeted gene delivery, *Biomacromolecules*, 2013, 14, 476 – 484.
2. **Feng Zhao**, Hui Yin, Jun Li, Supramolecular self-assembly forming a multifunctional synergistic system for targeted co-delivery of gene and drug, *Biomaterials*, 2014, 35, 1050 – 1062.
3. Jiajing Li, **Feng Zhao**, Jun Li, Polyrotaxanes for applications in life science and biotechnology, *Applied Microbiology and Biotechnology*, 2011, 90, 427 – 443.
4. Jiajing Li, **Feng Zhao**, Jun Li, Supramolecular polymers based on cyclodextrins for drug and gene delivery, *Advances in Biochemical Engineering Biotechnology*, 2011, 125, 207 – 249.
5. Hui Yin, **Feng Zhao**, Yunlong Wu, Daohai Zhang, and Jun Li. CD44-targeted gene delivery via hyaluronic acid conjugated  $\beta$ -cyclodextrin-oligoethylenimine star polymers. *Submitted*.



## **CHAPTER 1 INTRODUCTION**

This thesis contributes to the synthesis of cyclodextrin-based cationic polymers and their application on drug and gene delivery for potential cancer therapy. In this chapter, the background information of cancer therapy, cyclodextrin-based polymers on drug delivery, and cyclodextrin-based non-viral vectors on gene delivery is discussed. In addition, we provide the scope and objective of our study. Finally, the contents and structure of this thesis are listed.

### **1.1. Background Information**

WHO reported that cancer is one of the leading causes of death worldwide and 7.6 million people died because of cancer (around 13% of all deaths) in 2008. Cancer therapy generally includes chemotherapy, radiotherapy, surgery, hormone therapy, immunotherapy, and gene therapy. All the cancer therapy methods have their advantages and disadvantages.

Chemotherapy using anticancer drugs usually kills both tumor cells and normal cells, leading to serious side effects. Paclitaxel (PTX) is one of the most widely used drugs that can efficiently treat ovarian, breast, head and neck, and non-small-cell lung cancers.<sup>1,2</sup> The mechanism of PTX is to bind tubulin and promote tubulin polymerization and stabilization of microtubules

against depolymerization.<sup>3, 4</sup> Thus, PTX-induced microtubule stabilization leads to G2/M cell cycle arrest and cell death.<sup>5</sup> The application of PTX usually hampers by its limited source and poor aqueous solubility.<sup>6-8</sup> Structure modification of PTX and preparation of effective formulations with effective carriers are widely investigated to improve its physiochemical properties and anticancer capability.

Gene therapy is the treatment of diseases using the genetic materials to specific cells of a patient,<sup>9</sup> which has been greatly studied during the last two decades. Nowadays, design and synthesis of safe and effective non-viral vectors to carry and protect oligonucleotides for gene therapy has attracted great interest because of the superior properties of safety, low cytotoxicity, easy to be scale-up and structure modification.<sup>10</sup> Cationic polymer is one of the most investigated non-viral gene delivery materials. Among of them, polyethylenimine (PEI) is one of the most prominent examples of cationic polymers that have been extensively studied as non-viral gene delivery vectors.<sup>11</sup> The DNA polyplexes of PEI can avoid lysosomal trafficking and degradation after internalization into cells due to its buffering capacity.<sup>12</sup> The application of PEI generally hinders due to its high toxicity induced by the aggregation and adherence on the cell surface.<sup>13-15</sup> Structure modification of PEI with poly(ethylene glycol) PEG,<sup>16-18</sup> polycaprolactone (PCL),<sup>19, 20</sup> cyclodextrin,<sup>21</sup> and other formulations are widely investigated.

Cyclodextrins (CDs) are a series of natural cyclic oligosaccharides, which consist by D(+)-glucose units linked by  $\alpha$ -1,4-linkages. The unique structure of CDs is composed of hydrophilic outer surfaces and hydrophobic cavities. The hydrophobic cavities can include some hydrophobic drugs to alter their physical, chemical, and biological properties.<sup>22-24</sup> Inclusion complexes between CD derivatives and PTX have already been greatly investigated in the last two decades to try to solve the undesired side effects induced by the cremophor formulation of PTX.<sup>25-31</sup> CD derivatives, such as dimethyl- $\beta$ -CD,

hydroxypropyl- $\beta$ -CD, bridged dimers, have been greatly studied in the formation of inclusion complex with PTX for drug delivery. However, more stable and efficient CD-based carriers still need to be explored.

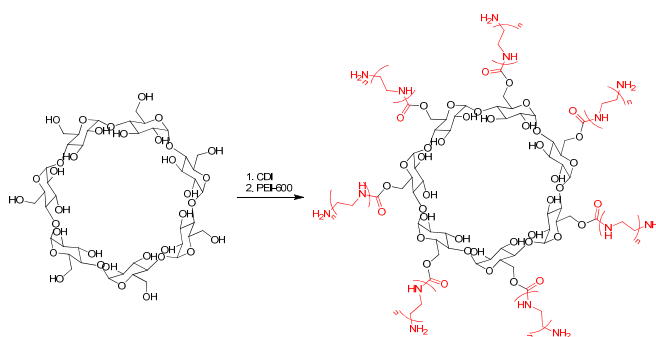
Ligands with specific binding ability to cancer cells that overexpressed corresponding receptors are widely conjugated to gene delivery vectors for targeted delivery. Folic acid is a vitamin that has been greatly investigated in targeted drug and gene delivery, because many malignancies cells including the ovary, brain, kidney, breast, lung, and myeloid cells overexpress folate receptors.<sup>32</sup> Preparation of folate-linked non-viral biocompatible polymeric as gene delivery vectors, such as cationic polymers, cationic lipids, cationic peptides, and so on has already been widely studied.<sup>33-35</sup> Moreover, some folate-conjugated drugs have already entered clinic trials.<sup>36-40</sup>

In addition, structure modification of drug and gene delivery carriers may induce the change of their physical and biological properties. Therefore, the choice of appropriate linker between carriers and delivery enhancing moieties is very important. A covalent disulfide bond is widely used as a linker in drug and gene delivery systems due to the unique properties that cleavage of the redox-sensitive disulfide linker can be adjusted by the large gradient between extracellular and intracellular environment.

Combination therapy can modulate the different signaling pathways in cancer cells, so it is an effective and widely-used approach in cancer therapy. Drug and gene co-delivery has been approved to have the synergistic/combined effects in cancer therapy.<sup>41-46</sup>

The application of CDs in gene delivery thanks to the active hydroxyl groups for further structure modification. Since the first publication of CD-conjugated cationic polymers for gene delivery by Mark E. Davis's group,<sup>47</sup> CD based cationic polymers, especially CD-oligoethylenimine (CD-OEI), have been attracted great interests in gene delivery with combination the advantages of both CD and OEI. Our group reported a series

of cationic star polymers by conjugating oligoethylenimine (OEI) chains to  $\alpha$ -CD as non-viral gene delivery vectors (Scheme 1.1).<sup>48, 49</sup> These  $\alpha$ -CD-OEI star-shaped polymers showed much lower cytotoxicity and excellent gene transfection efficiency that were comparable to or even higher than that of the well-studied branched PEI (25 kDa). However, the synthesized CD-based cationic polymer lacks of target groups which can enhance the gene delivery ability and minimize the dosage and cytotoxicity. Moreover, the hydrophobic CD ring provides possible application in drug delivery, which may further enhance the gene delivery and the synergistic effect of co-delivery.



**Scheme 1.1.** Synthesis procedures of  $\alpha$ -CD-OEI star polymers.

### 1.2. Objective and Scope of Study

This research studied the preparation of novel natural cyclodextrin based cationic polymers and their applications on drug and gene delivery. This study synthesized multi-functional cyclodextrin derivatives according to its interesting physiochemical properties. The inclusion complexes of cyclodextrin with guest molecules and the enhancement of drug properties and synergistic/combined effect on gene delivery were further explored. Specifically, the objectives of this research are:

To prepare series of  $\alpha$ -,  $\beta$ -, and  $\gamma$ -cyclodextrin derivatives conjugated with oligoethylenimine and to evaluate their ability to form inclusion complexes with anticancer drug for potential drug delivery.

To design and synthesis of a new star-shaped cationic polymer containing

a  $\gamma$ -cyclodextrin core and multiple oligoethylenimine arms with folic acid linked by a biodegradable disulfide bond for efficient targeted gene delivery. This study has expanded the strategy of FA-targeted delivery by combining the smart folate receptor-recycling function to achieve the significant enhancement of gene expression.

To synthesize a gene delivery carrier by formation of inclusion complex between a folate-conjugated  $\gamma$ -cyclodextrin-oligoethylenimine with disulfide linker ( $\gamma$ -CD-OEI-SS-FA) and anticancer drug paclitaxel thanks to the hydrophobic cavity of cyclodextrin. Co-delivery of drug and gene shows synergistic/combined effect on gene delivery.

### 1.3. Organization of the Thesis

Encompassing the objectives discussed, the detailed research works about the cyclodextrin-based cationic polymers on drug and gene delivery is organized as the following chapters:

Chapter 2: Literature review on the topic of cancer chemotherapy and gene therapy. The physiochemical and biological properties of cyclodextrin, the application of cyclodextrin (CD) in drug and gene delivery are involved. In addition, the target delivery and methods to improve drug delivery and gene delivery will be discussed.

Chapter 3: Report on the synthesis of  $\alpha$ -,  $\beta$ -, and  $\gamma$ -CD derivatives by conjugation with oligoethylenimine (OEI). These modified CD derivatives can form inclusion complexes with anticancer drug PTX and significantly improve the physiochemical properties, which has potential application as drug delivery carriers.

Chapter 4: Synthesis of a new star-shaped cationic polymer containing a  $\gamma$ -CD core and multiple oligoethylenimine arms. Folic acid (FA) was conjugated for effective target delivery with a biodegradable disulfide bond between the cationic polymer and target group. The new  $\gamma$ -CD-OEI-SS-FA gene

carrier had low cytotoxicity, and possessed capacity to target and deliver DNA to specific tumor cells that overexpress folate receptors, as well as functions to recover and recycle folate receptors onto cellular membranes to facilitate continuous folate receptor mediated endocytosis to achieve very high levels of gene expression.

Chapter 5: Co-delivery of pDNA and Drug by formation of inclusion complex between paclitaxel and folate-grafted  $\gamma$ -CD-OEI with disulfide linker. The drug and gene co-delivery has synergistic effect and it could be an efficient strategy for potential cancer gene therapy.

Chapter 6: Conclusion on the work done with possible future endeavours.

### 1.4. References

- (1) Tamura, M.; De, G.; Ueno, A., *Chemistry* **2001**,7, 1390-1397.
- (2) Michels, J. J.; O'Connell, M. J.; Taylor, P. N.; Wilson, J. S.; Cacialli, F.; Anderson, H. L., *Chemistry* **2003**,9, 6167-6176.
- (3) Cragg, G. M., *Medicinal Research Reviews* **1998**,18, 315-331.
- (4) Manfredi, J. J.; Horwitz, S. B., *Pharmacology & Therapeutics* **1984**,25, 83-125.
- (5) Woods, C. M.; Zhu, J.; Mcquaney, P. A.; Bollag, D.; Lazarides, E., *Mol Med* **1995**,1, 506-526.
- (6) Oliver, A., *Montana Pharmacia* **1993**,17, 17-18.
- (7) Feng, S. S.; Huang, G. F., *Journal of Controlled Release* **2001**,71, 53-69.
- (8) Suffness, M., *Annu Rep Med Chem* **1993**,28, 305-314.
- (9) Mulligan, R. C., *Science* **1993**,260, 926-932.
- (10) Mintzer, M. A.; Simanek, E. E., *Chemical Reviews* **2009**,109, 259-302.
- (11) Boussif, O.; Lezoualch, F.; Zanta, M. A.; Mergny, M. D.; Scherman, D.; Demeneix, B.; Behr, J. P., *P Natl Acad Sci USA* **1995**,92, 7297-7301.
- (12) Suh, J.; Paik, H. J.; Hwang, B. K., *Bioorg Chem* **1994**,22, 318-327.

- (13) Godbey, W. T.; Wu, K. K.; Mikos, A. G., *Journal of Biomedical Materials Research* **1999**, *45*, 268-275.
- (14) Fischer, D.; Li, Y. X.; Ahlemeyer, B.; Krieglstein, J.; Kissel, T., *Biomaterials* **2003**, *24*, 1121-1131.
- (15) Fischer, D.; Bieber, T.; Li, Y. X.; Elsasser, H. P.; Kissel, T., *Pharmaceut Res* **1999**, *16*, 1273-1279.
- (16) Godbey, W. T.; Wu, K. K.; Mikos, A. G., *P Natl Acad Sci USA* **1999**, *96*, 5177-5181.
- (17) Rudolph, C.; Schillinger, U.; Plank, C.; Gessner, A.; Nicklaus, P.; Muller, R. H.; Rosenecker, J., *Bba-Gen Subjects* **2002**, *1573*, 75-83.
- (18) Thomas, M.; Klibanov, A. M., *P Natl Acad Sci USA* **2002**, *99*, 14640-14645.
- (19) Shuai, X. T.; Merdan, T.; Unger, F.; Wittmar, M.; Kissel, T., *Macromolecules* **2003**, *36*, 5751-5759.
- (20) Arote, R.; Kim, T. H.; Kim, Y. K.; Hwang, S. K.; Jiang, H. L.; Song, H. H.; Nah, J. W.; Cho, M. H.; Cho, C. S., *Biomaterials* **2007**, *28*, 735-744.
- (21) Pun, S. H.; Bellocq, N. C.; Liu, A. J.; Jensen, G.; Machemer, T.; Quijano, E.; Schluep, T.; Wen, S. F.; Engler, H.; Heidel, J.; Davis, M. E., *Bioconjugate Chem* **2004**, *15*, 831-840.
- (22) Nosov, D. A.; Esteves, B.; Lipatov, O. N.; Lyulko, A. A.; Anischenko, A. A.; Chacko, R. T.; Doval, D. C.; Strahs, A.; Slichenmyer, W. J.; Bhargava, P., *Journal of clinical oncology : official journal of the American Society of Clinical Oncology* **2012**, *30*, 1678-1685.
- (23) Slichenmyer, W. J.; Von Hoff, D. D., *Anti-cancer drugs* **1991**, *2*, 519-530.
- (24) Slichenmyer, W. J.; Von Hoff, D. D., *Journal of clinical pharmacology* **1990**, *30*, 770-788.
- (25) Cserhati, T.; Forgacs, E.; Hollo, J., *J Pharmaceut Biomed* **1995**, *13*, 533-541.
- (26) Sharma, U. S.; Balasubramanian, S. V.; Straubinger, R. M., *J Pharm Sci* **1995**, *84*, 1223-1230.
- (27) Liu, Y.; Chen, G. S.; Li, L.; Zhang, H. Y.; Cao, D. X.; Yuan, Y. J., *Journal of medicinal chemistry* **2003**, *46*, 4634-4637.
- (28) Liu, Y.; Chen, G. S.; Chen, Y.; Cao, D. X.; Ge, Z. Q.; Yuan, Y. J.,

*Bioorganic & medicinal chemistry* **2004**,12, 5767-5775.

(29)Hamada, H.; Ishihara, K.; Masuoka, N.; Mikuni, K.; Nakajima, N., *Journal of bioscience and bioengineering* **2006**,102, 369-371.

(30)Bouquet, W.; Ceelen, W.; Fritzing, B.; Pattyn, P.; Peeters, M.; Remon, J. P.; Vervaet, C., *Eur J Pharm Biopharm* **2007**,66, 391-397.

(31)Fenyvesi, F.; Kiss, T.; Fenyvesi, E.; Szente, L.; Veszeka, S.; Deli, M. A.; Varadi, J.; Feher, P.; Ujhelyi, Z.; Tosaki, A.; Vecsernyes, M.; Bacska, I., *J Pharm Sci* **2011**,100, 4734-4744.

(32)Lu, Y. J.; Low, P. S., *Adv Drug Deliver Rev* **2002**,54, 675-693.

(33)El-Aneed, A., *Journal of controlled release : official journal of the Controlled Release Society* **2004**,94, 1-14.

(34)Xia, W.; Low, P. S., *Journal of medicinal chemistry* **2010**,53, 6811-6824.

(35)Zhao, X. B. B.; Lee, R. J., *Adv Drug Deliver Rev* **2004**,56, 1193-1204.

(36)Leamon, C. P.; Parker, M. A.; Vlahov, I. R.; Xu, L. C.; Reddy, J. A.; Vetz, M.; Douglas, N., *Bioconjug Chem* **2002**,13, 1200-1210.

(37)Leamon, C. P.; Reddy, J. A.; Vlahov, I. R.; Westrick, E.; Parker, N.; Nicoson, J. S.; Vetz, M., *International journal of cancer. Journal international du cancer* **2007**,121, 1585-1592.

(38)Leamon, C. P.; Reddy, J. A.; Vlahov, I. R.; Westrick, E.; Dawson, A.; Dorton, R.; Vetz, M.; Santhapuram, H. K.; Wang, Y., *Molecular pharmaceutics* **2007**,4, 659-667.

(39)Lu, Y.; Low, P. S., *Cancer immunology, immunotherapy : CII* **2002**,51, 153-162.

(40)Wang, S.; Luo, J.; Lantrip, D. A.; Waters, D. J.; Mathias, C. J.; Green, M. A.; Fuchs, P. L.; Low, P. S., *Bioconjug Chem* **1997**,8, 673-679.

(41)Wiradharma, N.; Tong, Y. W.; Yang, Y. Y., *Biomaterials* **2009**,30, 3100-3109.

(42)Xu, Z. H.; Zhang, Z. W.; Chen, Y.; Chen, L. L.; Lin, L. P.; Li, Y. P., *Biomaterials* **2010**,31, 916-922.

(43)Wang, Y.; Gao, S. J.; Ye, W. H.; Yoon, H. S.; Yang, Y. Y., *Nature Materials* **2006**,5, 791-796.

(44)Yue, X. Y.; Qiao, Y.; Qiao, N.; Guo, S. T.; Xing, J. F.; Deng, L. D.; Xu, J.



Q.; Dong, A. J., *Biomacromolecules* **2010**,*11*, 2306-2312.

(45) Wang, H. J.; Zhao, P. Q.; Su, W. Y.; Wang, S.; Liao, Z. Y.; Niu, R. F.; Chang, J., *Biomaterials* **2010**,*31*, 8741-8748.

(46) Hu, Q. D.; Fan, H.; Ping, Y.; Liang, W. Q.; Tang, G. P.; Li, J., *Chemical Communications* **2011**,*47*, 5572-5574.

(47) Gonzalez, H.; Hwang, S. J.; Davis, M. E., *Bioconjugate Chem* **1999**,*10*, 1068-1074.

(48) Yang, C. A.; Li, H. Z.; Goh, S. H.; Li, J., *Biomaterials* **2007**,*28*, 3245-3254.

(49) Li, J.; Loh, X. J., *Adv Drug Deliver Rev* **2008**,*60*, 1000-1017.

## CHAPTER 2 LITERATURE REVIEW

### 2.1. Cancer and Cancer Therapy

Cancer is defined as a generic term for a large group of diseases that can affect any part of the body (World Health Organization, WHO). WHO reported that cancer is one of the leading causes of death worldwide and 7.6 million people died from cancer (around 13% of all deaths) in 2008. Among of them, lung, stomach, liver, colon and breast cancer cause the most cancer deaths each year (Figure 2.1). In addition, deaths from cancer worldwide are expected to continue rising, with an estimated 13.1 million deaths in 2030 (WHO global cancer statistics). The Singapore Cancer Registry provides information on cancer patterns and trends in Singapore that a total number of 51,657 incident cancer cases were diagnosed among the Resident population during the period 2006-2010.<sup>1</sup> Lung cancer and breast cancer caused the highest mortality rates in males and females respectively.

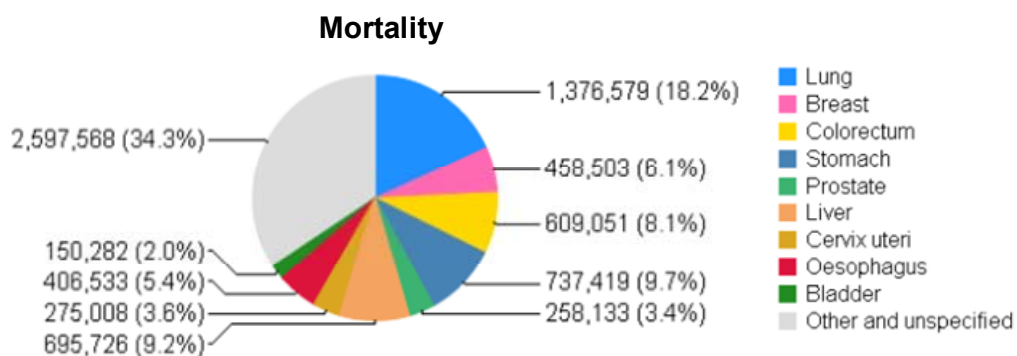


**Figure 2.1.** Illustration of worldwide cancer mortality rates (Referred from WHO GLOBOCAN 2008).

### 2.1.1. Cancer Treatments

Cancer therapy generally includes chemotherapy, radiotherapy, surgery, hormone therapy, and immunotherapy. Complete surgical resection is usually the first consideration for patients and is still the most effective method. However, surgery is often obstructed by several issues, such as potential wound infection, the limitation by the size and location of tumor, and possible tumor relapse. Radiotherapy usually kills both cancer cells and normal cells, resulting in long-term side effects such as fatigue and hair loss. A combination of surgery and radiotherapy is usually used in cancer treatment. But it is still difficult to control the re-growth and metastatic secondary tumor growth.<sup>2,3</sup>

Chemotherapy also faces the selectivity problem that the drugs kill both tumor cells and normal cells. Depending on the properties of different anticancer drugs, the drugs differ in their cytotoxic mechanisms and side effects. Integration of chemotherapy into a combined modality on cancer treatment is often used, such as chemotherapy plus surgery or radiotherapy. Moreover, treatment of cancers with a combination chemotherapy using two or more drugs simultaneously is also widely used in cancer therapy.

### 2.1.2. Anticancer Drugs

There are kinds of drugs commercially available for cancer chemotherapy, including doxorubicin, paclitaxel and docetaxel, fluorouracil, chlorambucil, methotrexate, cisplatin, and so on. These anticancer drugs are categorized into several groups depending on their different mechanism.

Paclitaxel (PTX) is a diterpenoid natural product isolated from *Taxus brevifolia* with potential activity against ovarian, breast, head and neck, and non-small-cell lung cancers.<sup>4,5</sup> The structure of PTX displays in Figure 2.2.

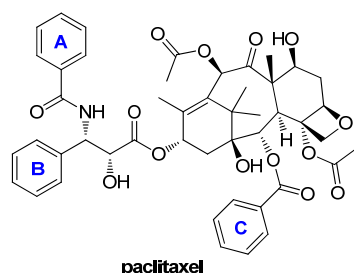


**Figure 2.2.** Structure of paclitaxel.

PTX promotes the polymerization of tubulin. The microtubule formed under PTX are every stable and dysfunctional, causing cell death by disrupting the normal tubule dynamics required for cell division and vital interphase process.<sup>6-10</sup>

One problem for PTX application is the limited source. Around four tree need to be sacrificed to produce 2 g of drug for one patient.<sup>11, 12</sup> Another major problems is its low aqueous solubility.<sup>13</sup> PTX is administrated by an infusion of cremophor EL (polyoxyethylated castor oil) containing 50% absolute ethanol. However, cremophor has been reported to cause severe hypersensitivity reactions and other side effects in animals and humans.<sup>14, 15</sup> Moreover, precipitation may be found on aqueous dilution. Therefore, the development of structure modification or alternate formulation for PTX delivery with good aqueous solubility and less side effects is necessary. There are various studies for PTX delivery include co-solvents, micelles, emulsions, liposomes, microspheres nanoparticles, pastes, implants, cyclodextrins (CDs), and so on. The enhancement ability by CD will be discussed in section 2.3.

### 2.1.3. Gene Therapy

Gene therapy is the treatment of diseases by the transfer of genetic materials into specific cells of a patient.<sup>16</sup> Numerous disease-causing genes can be identified due to the development of molecular biology and the completion of the Human Genome Project.<sup>17</sup> It is promising to treat genetic diseases such as haemophilia,<sup>18</sup> muscular dystrophy,<sup>19</sup> and cystic fibrosis<sup>20</sup> by replacing the errant genes. In addition, gene therapy can also be developed for

cardiovascular, infectious diseases and cancer therapy by adding, correcting, and replacing of genes to amplify naturally occurring proteins, to alter the gene expression, or to produce cytotoxic proteins.<sup>17</sup>

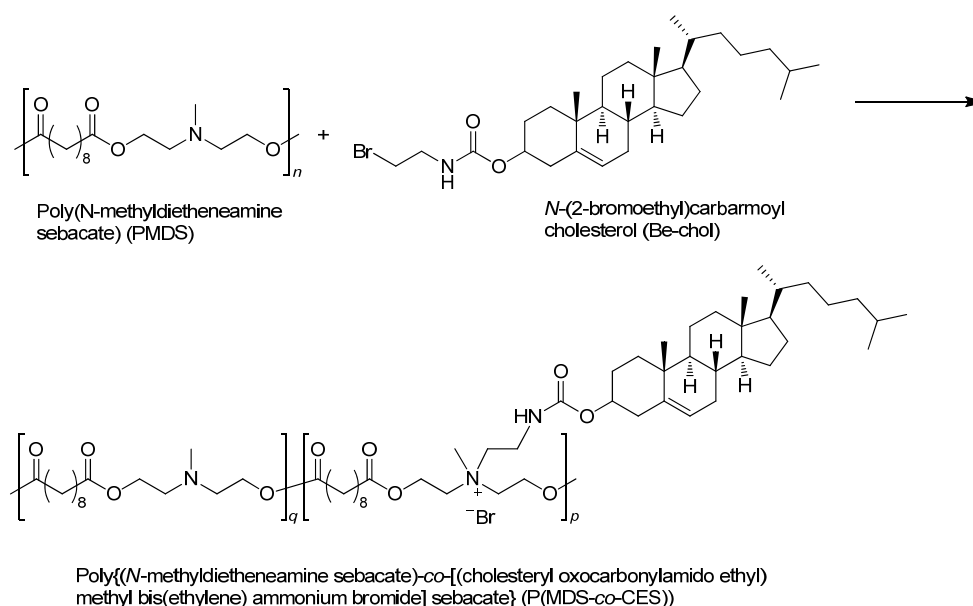
Both the genesis and evolution of cancers can be restrained by various tumor suppressive mechanisms. Effective tumor suppression needs to discriminate the normal and cancer cells. p53 is one of the most frequently delivered genes for effective cancer gene therapy, which plays a role as a prevailing guardian only in damaged or transformed cells, which induces cell growth arrest or apoptosis.<sup>21</sup> The cells cannot control their growth if normal protective function of p53 is lost, resulting in rapid growth and progression toward malignancy.<sup>22, 23</sup> Mover, around 50% of human cancers mutant or loss of p53 gene,<sup>24</sup> and the loss of p53 may also result in resistance to radiotherapy or chemotherapy.<sup>25</sup> Therefore, the reinstatement of wild-type p53 expression is a reasonable method for cancer therapy.

### 2.1.4. Drug and Gene Co-delivery

Combination therapy is an effective tool for cancer therapy due to the modulation of different signaling pathways in cancer cells with reduced toxicity. Moreover, combination therapy possibly overcomes the mechanisms of resistance and avoiding metastasis.<sup>26-28</sup> It would have advantageous to deliver therapeutic genes and drugs in the same vehicle that both of them can be delivered to the same tissues thus maximizing the benefits of the combination.<sup>29</sup>

Co-delivery of DNA and anticancer drug, such as doxorubicin and PTX has shown great promise to achieve the synergistic/combined effects in cancer therapy.<sup>30-35</sup> Yang's group reported the co-delivery of paclitaxel and plasmid DNA by cationic core-shell nanoparticles (Scheme 2.1) that improved gene transfection both *in vitro* and *in vivo*.<sup>32</sup> Moreover, co-delivery of doxorubicin and p53 gene by micelles increased p53 mRNA expression level as well as cytotoxicity towards HepG2 cells.<sup>30</sup> The presence of PTX would enhance gene

expression possibly due to its anti-mitotic function.<sup>36, 37</sup> Although PTX-induced apoptosis is p53-independent,<sup>38, 39</sup> the status of p53 may influence cell-cycle progression following mitotic arrest.<sup>40, 41</sup> Nielsen et al reported adenovirus-mediated p53 gene therapy and PTX have synergistic effect in many cancer cell lines.<sup>42</sup>



**Scheme 2.1.** Synthesis of cationic amphiphilic polymer P(MDS-co-CES).

### 2.1.5. Gene Delivery Vectors

Cancer gene therapy has obtained great attention over the past two decades as an alternative method to traditional chemotherapy.<sup>43, 44</sup> Successful gene therapy needs to solve several problems, such as identification of a therapeutic gene and deliver the gene to specific cells in an efficient and safety method. Free oligonucleotide and DNA are rapidly degraded by nucleases and quick cleared by the mononuclear phagocyte system,<sup>45, 46</sup> so the synthesis of effective gene delivery carriers to compact and protect genetic materials is necessary.

The idea gene delivery vectors should have some specific characteristics: (i) target to specific cells and tissues; (ii) resistance to metabolic degradation and “escape” from the immune system; (iii) safety, the materials especially for

viral vectors should be non-toxic and minimal side effects; (iv) protective effect to keep the activity of genetic materials.

Gene delivery vectors can be generally categorized into viral and non-viral vectors. The application of viral vectors is usually hindered by the toxicity, immunogenicity, and difficulty for large scale preparation.<sup>47</sup> In contrast, non-viral vectors such as cationic lipid, polymers, dendrimers, and peptides, have advantages over viral vectors on the safety, potential for large-scale production, and ability to be readily functionalized, which attract increasing interests in gene delivery.<sup>48</sup> However, non-viral vectors exhibit remarkable decrease of transfection efficiency since they need to overcome extra- and intracellular obstacles. So the synthesis of efficient non-viral vectors for successful gene delivery has attracted great interest. Cationic polymers can form complexes with DNA and avoid both *in vitro* and *in vivo* barriers which have been deeply investigated in the past decade.

Except for the poor stability of free DNA in blood, cellular uptake of free DNA is usually hindered by its size and negative charge. Cationic polymers can carrier DNA by electrostatic interactions between the negative charged DNA and positive charged polymers. Cationic polymers usually compact multiple DNA molecules due to their strong interactions. The sizes of the DNA/polymers complexes mostly depend on the physical properties of the cationic polymers. For non-targeting cationic complexes, they can associate with the cell membrane through electrostatic interactions with the anionic cell surface proteoglycans. Evidence suggests that inhibitory of proteoglycans would inhibit the gene transfection.<sup>49, 50</sup> Many interests have attracted to the target delivery by conjugation of receptor ligands to recognize the specific cells and tissues. The commonly used ligands include asialoglycoprotein, epidermal growth factor (EGF), folate, integrin, lactose, mannose, and transferring.<sup>51</sup> After binding to the cell surface through the ligand/receptor

interactions, the DNA/polymers complexes are usually internalized into cell by clathrin-dependent endocytosis.

Cationic polymers are widely researched as non-viral vectors due to their excellent properties for DNA delivery. Figure 2.3 shows some cationic polymers that have been widely studied as non-viral gene delivery vectors. Polyethylenimine (PEI) is often considered as the gold standard of gene transfection, which will be discussed in the next part.

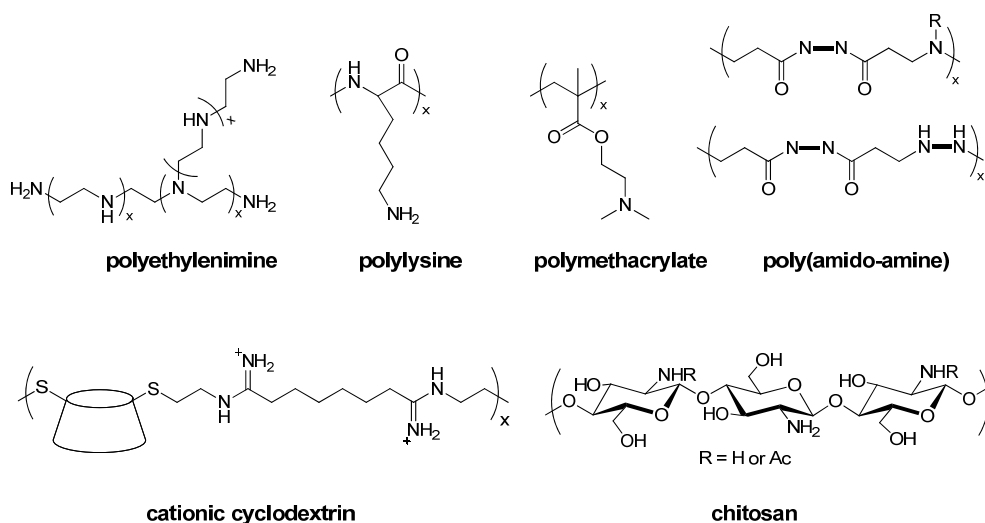


**Figure 2.3.** Selected cationic polymers as non-viral gene delivery vectors.

### ***Polyethylenimine***

Polyethylenimine (PEI) is one of the most prominent examples of cationic polymers.<sup>52</sup> PEI and its derivatives have been extensively studied as non-viral gene carriers. The structures of branched and linear PEI are shown in Figure 2.4. Branched PEI contains many amine groups, resulting in a high charge density. In addition, the high quantity of primary amines help the formation of polyplex, so branched PEI is more suitable for gene delivery compared to linear PEI. The increase of gene delivery ability of PEI was observed as increasing of its molecular weight from 600 to 70,000 Da, but accompanied with high toxicity.<sup>53, 54</sup> The toxicity is induced by the aggregation and adherence on the cell surface, resulting in significant necrosis.<sup>55</sup> Godbey et al reported that PEI forms a stable polyplex with DNA and this PEI/DNA



polyplex can move from endocytosis to nuclear entry.<sup>56</sup> Approximately 80% of nitrogen atoms in PEI is unprotonated at physiological pH compared to less than 50% unprotonated nitrogen atoms at pH of 5.<sup>57</sup> Therefore, the PEI polyplexes can avoid lysosomal trafficking and degradation after internalization into cells because of this buffering capacity.

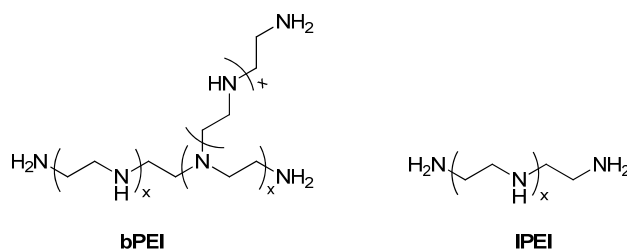


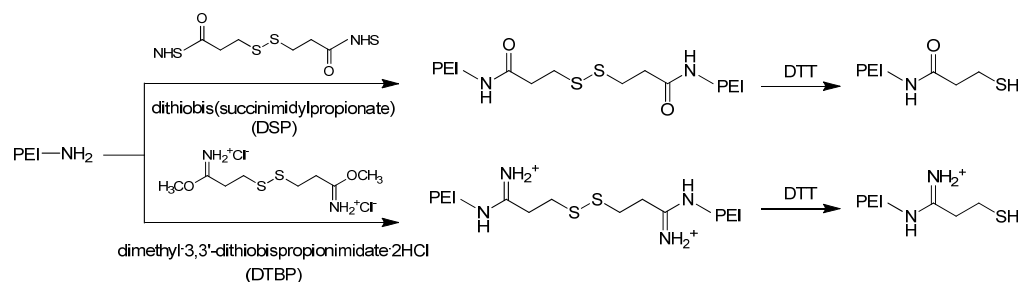
**Figure 2.4.** Structure of branched PEI (bPEI) and linear PEI (IPEI).

### *Polyethylenimine Derivatives*

Significant research has focused on modification of PEI structure to improve the transfection efficiency and reduce the cytotoxicity. One of the most common methods is PEGylation, which reduces salt/serum affects by a hydrophilic poly(ethylene glycol) exterior. However, the reduced gene transfection efficiency is usually obtained because a decreased surface charge of PEG-PEI polymer that decrease the interaction with cell membrane.<sup>58</sup> Moreover, PEI-PEG conjugation with cell-targeting ligands still shows less internalization than unmodified PEI.<sup>59</sup> Therefore, the PEGylation still hinders the gene transfection after cellular uptake. Conjugation of PEI amines with methyl and ethyl groups illustrated reduced gene transfection efficiency in both presence and absence of serum.<sup>60</sup>

PEG-Polycaprolactone (PEG-PCL) is also widely studied. Shuai and co-workers demonstrated the synthesis of biodegradable amphiphilic PEI-g-PCL-b-PEG by grafting PCL-b-PEG onto PEI.<sup>61</sup> These polymers showed low cytotoxicity and the gene transfection efficiency is comparable or even higher than the PEI (25 kDa). In vivo delivery of PCL-PEI conjugates showed that significantly higher transfection efficiency compare to the PEI (25 kDa) through aerosol administration.<sup>62</sup>

Introduction of reducible disulfide bond or ester linkage can reduce the cytotoxicity of PEI.<sup>63</sup> PEI cannot be metabolized by cellular enzymes, so the body clearance of high molecular weight PEI is very slow. Low molecular weight PEI with reducible disulfide linker could assist uncoupling of PEI from DNA to enhance gene delivery (Scheme 2.2), and the cleaved low molecular weight PEI fragments could be easily cleared from the body.<sup>63-67</sup>



**Scheme 2.2.** Conjugation of PEI with crosslinking reagents DSP and DTBP.

Davis's group prepared CD-modified PEI derivatives that the cytotoxicity of both branched and linear PEI was reduced.<sup>68</sup> The CD based modification of PEI will be discussed in section 2.4.

## 2.2. Characteristics of Cyclodextrins

Cyclodextrins (CDs) are a series of natural cyclic oligosaccharides. The most commonly used CD consist of 6, 7, and 8 D(+)-glucose units linked by  $\alpha$ -1,4-linkages, named as  $\alpha$ -,  $\beta$ -, and  $\gamma$ -CD, respectively. Figure 2.5 shows the toroidal structure of CDs with the primary hydroxyl groups at narrow rim and the secondary hydroxyl groups at the wide rim on the outer surface. In contrast, the inner wall of CDs mainly consists of methylene and methane groups.

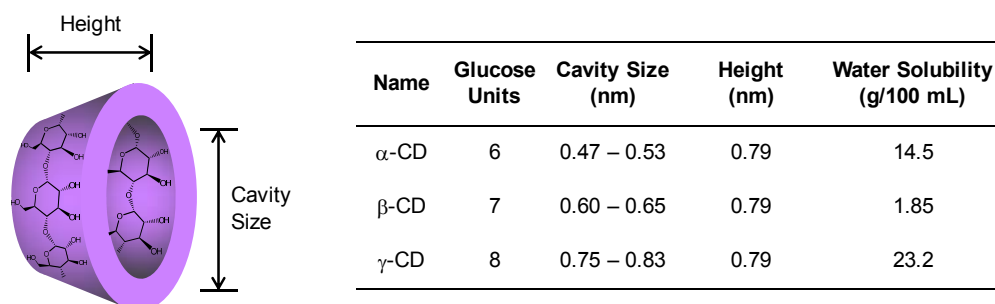


**Figure 2.5.** Illustrated structure of CD and the related profiles.

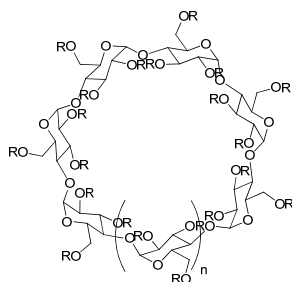
As a result, CDs have a hydrophilic outer surface and a hydrophobic cavity. These properties make CDs form inclusion complexes with some guest molecules by their hydrophobic cavities.<sup>69-71</sup> Therefore, the physical, chemical, and biological properties of guest molecules can be altered. These biocompatible, water-soluble CDs do not have immune responses and show low toxicity in animals and humans.<sup>72</sup> CDs are usually used as solubilization and stabilization reagents for small molecules to improve the solubility, stability, and bioavailability due to their ability to accommodate hydrophobic drugs.<sup>73</sup> CDs can also be applied in gene delivery thanks to the hydroxyl groups on the outer surface that offer opportunity for multiple modifications.

### 2.2.1. The Physiochemical Properties of Cyclodextrins

The superior natural properties of CD make it an excellent drug delivery candidate, which include: (1) many potential sites for chemical modification; (2) different CD has different cavity size suitable for different drug; (3) low toxicity and low pharmacological activity; (4) satisfactory water solubility; (5) protection of included or conjugated drugs from biodegradation.<sup>73</sup> Nowadays, many CD derivatives, such as methylated CDs, hydroxylalkylated CDs, sulfated CDs, glucose conjugated CDs, anionic CDs, et al, have attracted great interest in their pharmaceutical application.<sup>74-78</sup>

The solubility difference may be induced by the aggregation of CDs and the interaction with surrounding water molecules, together with the lattice energy in the solid state.<sup>79</sup> Among of them,  $\beta$ -CD has particularly low water solubility due to the formation of intramolecular hydrogen bond,<sup>80</sup> which inevitably limits its application in drug delivery. Generally, methylation and hydroxyalkylation of the hydroxyl groups of CDs can significantly improve their water solubility. Table 2.1 lists the structure of several CD derivatives and their enhanced solubility and chemical modification.<sup>81</sup>

**Table 2.1.** Structural and physiochemical properties of selected CDs.



Cyclodextrin	n	R	Substance	Solubility in water (mg/mL)
$\alpha$ -cyclodextrin	0	H	0	145
$\beta$ -cyclodextrin	1	H	0	18.5
2-Hydroxypropyl- $\beta$ -cyclodextrin	1	CH <sub>2</sub> CHOHCH <sub>3</sub>	0.65	>600
Sulfobutylether $\beta$ -cyclodextrin sodium salt	1	(CH <sub>2</sub> ) <sub>4</sub> SO <sub>3</sub> <sup>-</sup> Na <sup>+</sup>	0.9	>500
Randomly methylated $\beta$ -cyclodextrin	1	CH <sub>3</sub>	1.8	>500
6-O-Maltosyl- $\beta$ -cyclodextrin	1	Maltosyl	0	>1500
$\gamma$ -Cyclodextrin	2	H	0	232
2-Hydroxypropyl- $\gamma$ -cyclodextrin	2	CH <sub>2</sub> CHOHCH <sub>3</sub>	0.6	>500

The glucopyranose of CD ring has secondary hydroxyl groups at 2- and 3-positions, and primary hydroxyl groups at the 6-positions. Among of them, the 6-OH is the most basic and more easily to be modified than 2- and 3-OH. Under normal conditions, an electrophilic reagent will attack the 6-positions that are most nucleophilic. However, reagents with high reactivity attack not only the primary hydroxyl groups at the 6-positions but also the secondary hydroxyl groups.<sup>82</sup>

### 2.2.2. The Biological Properties of Cyclodextrins

Cyclodextrins are quite stable in alkaline solution. However, they are hydrolyzed by strong acids to give linear oligosaccharides.<sup>71</sup> Moreover,  $\alpha$ - and  $\beta$ -CD are resistant to the metabolism *in vivo*, whereas  $\gamma$ -CD would more easily to be hydrolyzed.<sup>83</sup> On the other hand,  $\beta$ -CD is hardly hydrolyzed<sup>84</sup> and the branched  $\beta$ -CD will be excreted in urine.

Natural CDs shows low toxicity and their oral metabolic fate has already been investigated.<sup>85</sup> 2-Hydroxypropyl- $\beta$ -CD (HP- $\beta$ -CD), 6-O-maltosyl- $\beta$ -CD, and  $\beta$ -CD sulfate can be safely applied via parenteral administration.<sup>86</sup>

Moreover, CDs can induce human erythrocytes to change their shapes. The hemolytic activity of CD derivatives follows the order of methylated  $\beta$ -CDs >  $\beta$ -CD > HP- $\beta$ -CD  $\approx$  G<sub>2</sub>- $\beta$ -CD >  $\alpha$ -CD >  $\gamma$ -CD > HP- $\gamma$ -CD > SBE- $\beta$ -CD.<sup>76, 87-90</sup> The acceptable daily oral intake of CDs is 1.4 g for  $\alpha$ -CD, 0.35 g for  $\beta$ -CD, 10 g for  $\gamma$ -CD, and 0.07 g for RM- $\beta$ -CD.<sup>91</sup>

### 2.3. Cyclodextrin on Drug Delivery

CDs can improve the drug bioavailability due to their enhancement of membrane absorption and protection of biomolecules from non-specific interactions.<sup>92, 93</sup> The reason for their membrane absorption enhancing properties is that the interaction with membrane will release certain membrane components and then destabilization and permeabilization.<sup>94</sup> The ability of CDs to form inclusion complexes with guest molecules in both solution and solid states induces by the hydrophobic environment of the inner cavity (Figure 2.6). The physical, chemical, and biological properties of the guest molecules, such as drugs can be changed due to the interaction and protection of CDs. Since the first CD-based product prostaglandin E<sub>2</sub>/ $\beta$ -CD (Prostarmon E<sup>TM</sup> sublingual tablets) was marketed in 1976, many CD-containing products are marketed as kinds of formulations.<sup>72, 95</sup> Generally, CDs are used to increase the solubility, stability and bioavailability.<sup>96-98</sup> In addition, CDs can also reduce or prevent gastrointestinal and ocular irritation, and unpleasant smells or tastes.<sup>99, 100</sup>

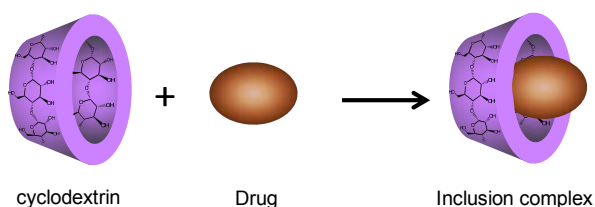


**Figure 2.6.** Illustrated formation of 1:1 CD-drug inclusion complex.

Although  $\alpha$ - and  $\beta$ -CD cannot be hydrolyzed by human salivary and pancreatic amylases,<sup>76</sup> they can be fermented by the intestinal microflora. Oral administration of  $\alpha$ -CD is generally safe without significant adverse effects.<sup>101,</sup>

<sup>102</sup> However, the small cavity size of  $\alpha$ -CD limits its pharmaceutical applications.  $\beta$ -CD is widely used in oral administration with low toxicity, although the low aqueous solubility and adverse effects limit its parenteral administration. Moreover, its derivatives, such as HP- $\beta$ -CD, have low toxicity and much higher water-solubility than  $\beta$ -CD, and it is also well tolerated in humans.<sup>76, 89, 103, 104</sup>

**Table 2.2.** Illustration of CD pharmaceutical products

Drug/cyclodextrin	Trade name	Formulation	Company
<b><math>\alpha</math>-CD</b>			
Alprostadi	Caverject Dual	i.v. solution	Pfizer
Cefotiam-hexetil HCl	Pansporin T	Tablet	Takeda
OP-1206	Opalmon	Tablet	Ono
PGE1	Prostavastin	Parenteral solutions	Ono Schwarz
<b><math>\beta</math>-CD</b>			
Benexate HCl	Ulgut	Capsule	Teikoku
	Lonmiel		Shionogi
Cephalosporin)	Meiact	Tablet	Meiji Seika
Cetirzine	Cetirzin	Chewing tablet	Losan Pharma
Chlordiazepoxide	Transillium	Tablet	Gador
Dexamethasone	Glymesason	Ointment tablet	Fujinaga
Dextromethorphan	Rynathisol		Synthelabo
Diphenhydramin and chlortheophyllin	Stada-Travel	Chewing tablet	Stada
Iodine	Mena-Gargle	Solution	Kyushin
Meloxicam	Mobitil	Tablet and suppository	Medical Union Pharmaceuticals
Nicotine	Nicorette	Sublingual tablets	Pfizer
Nimesulide	Nimedex	Tablets	Novartis
Nitroglycerin	Nitrophen	Sublingual tablet	Nihon Kayaku
Omeprazole	Omebeta	Tablet	Betafarm
PGE2	Prostarmon E	Sublingual tablet	Ono Chiesi
Piroxicam	Brexin, Flogene, Cicladon	Tablet, suppository	Aché
Tiaprofenic acid	Surgamyl	Tablet	Roussel-Maestrelli

Table 2.2. (continued)

Drug/cyclodextrin	Trade name	Formulation	Company
<b>HP-<math>\beta</math>-CD</b>			
Alfaxalone			
Cisapride	Propulsid	Suppository	Janssen
Hydrocortisone	Dexocort	Solution	Actavis
Indomethacin	Indocid	Eye drop	Chauvin
Itraconazole	Sporanox	Oral and i.v.	Janssen
Mitomycin	MitoExtra	i.v. infusion Novartis (Europe)	Novartis
<b>Mitozytrex</b>			
<b>SBE-<math>\beta</math>-CD</b>			
Aripiprazole	Abilify	im solution	Bristol-Myers Squibb; Otsuka Pharm
Maropitant	Cerenia	Parenteral	Pfizer Animal Health
Voriconazole	Vfend	i.v. solution	Pfizer
Ziprasidone	Geodon Zeldox	im solution	Pfizer
<b>RM-<math>\beta</math>-CD</b>			
17 $\beta$ -Estradiol	Aerodiol	Nasal Spray	Servier
Cloramphenicol	Clorocil	Eye drop	Oftalder
Insulin		Nasal spray	Spain
<b>HP-<math>\gamma</math>-CD</b>			
Diclofenac sodium salt	Voltaren	Eye drop solution	Novartis
Tc-99 Teoboroxime	CardioTec	i.v. solution	Bracco

Many drug failures are induced by the poor solubility, poor dissolution or poor permeability.<sup>105, 106</sup> CDs provide a promising solution to improve the physiochemical properties of some drug candidates by formation of inclusion complexes. Table 2.2 illustrates some marketed CD products.<sup>81</sup>

Inclusion complexes between CD derivatives and PTX have already been greatly investigated in the last two decades.<sup>107-113</sup> As the smaller cavity size for  $\alpha$ -CD (0.47 – 0.53 nm), it cannot form stable inclusion complex with PTX.<sup>107</sup> Sharma and co-workers investigated inclusion complexation between PTX and HP- $\beta$ -CD, hydroxyethyl- $\beta$ -CD, DM- $\beta$ -CD, HP- $\gamma$ -CD, and so on, indicating

## Chapter 2. Literature Review

2000-fold or more increase of PTX solubility and maintain its cytostatic properties. However, the solubility of PTX limited by the CD concentration and high viscous was observed at high concentration. Moreover, these inclusion complexes were mostly not stable in aqueous solution and precipitation occurred upon dilution.<sup>108</sup>

**Table 2.3.** Solubility of PTX in aqueous solutions with different CDs.

Sample	Concentration of PTX (mM)	Concentration of CD (mM)	Enhancement Factor
none	0.41 ± 0.05		1
α-CD	0.72 ± 0.06	6	2
β-CD	1.1 ± 0.08	6	3
γ-CD	0.93 ± 0.05	6	2
mono-6-O-maltosyl α-CD	0.74 ± 0.04	6	2
mono-6-O-maltosyl β-CD	1.2 ± 0.08	6	3
mono-6-O-maltosyl γ-CD	0.83 ± 0.07	6	2
heptakis-(2,6-di-O-methyl) α-CD	0.41 ± 0.11	6	1
heptakis-(2,6-di-O-methyl) β-CD	49 ± 0.52	6	120
heptakis-(2,3,6-tri-O-methyl) β-CD	5.5 ± 0.11	6	13
random hydroxyethyl β-CD	4.1 ± 0.14	6	10
random hydroxypropyl β-CD	7.8 ± 0.12	6	19

Lee and coworkers investigated the PTX solubility enhancement by cyclodextrins, DM-β-CD, and HP-β-CD, whereas DM-β-CD has the best effect on the enhancement of solubility. Moreover, the interaction of PTX and DM-β-CD showed increase of fluorescence intensity compared to other molecules, indicating the possible interaction with the hydrophobic cluster site of C-ring in PTX molecule.<sup>114, 115</sup> Alcaro et al. evaluated the interaction of PTX with β-CD, 2,6-DM-β-CD, and 2,3,6-trimethyl-β-CD. The progressive methylation of β-CD modulates the recognition of tumor cells. DM-β-CD is the most stable complex and all the inclusion complexes still have antitumor activity.<sup>116</sup> Hamada et al. investigated the water solubility of PTX inclusion complexes using 11 CD derivatives. The solubility result is shown in Table 2.3,



which DM- $\beta$ -CD has the highest effect. A tubulin assay illustrated that the DM- $\beta$ -CD is 1.23-fold higher polymerization effect than PTX itself.<sup>111</sup> Other studies also found the superior capability of DM- $\beta$ -CD to form inclusion complex with PTX and maintain its antitumor ability.<sup>117-119</sup>

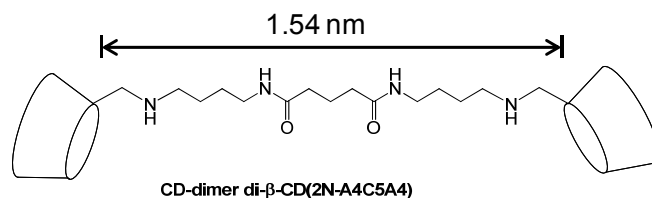


**Figure 2.7.** Illustrated structure of  $\beta$ -CD dimer.

Moser and coworkers demonstrated the synthesis of  $\beta$ -CD dimer by spacers with variant lengths. The length of the dimer in Figure 2.7 matches the distance between two benzoic acid residues of PTX. The affinity constants of the dimer compared to free  $\beta$ -CD are  $10^7$  l/mol. The inclusion complex of  $\beta$ -CD-dimer/PTX has a considerable time delay of incorporation into tumor cell.<sup>120, 121</sup> As shown in Figure 2.8, Liu Yu and coworkers prepared CD dimer with OEI spacer which showed high PTX solubility enhancement (2 mg/mL). Structure with a ratio of 2:1 complex of PTX/CD dimer was confirmed by  $^1\text{H}$  NMR. 2D NMR showed H-3 and H-5 protons of CD cavities are strongly interacted with the ortho and meta protons of PTX A and B rings but weakly correlated with the C ring.<sup>109</sup> Their further studies focused on adjusting the length of OEI linker. However, only long-tethered dimers can form inclusion complexes with PTX with satisfied water solubility, high thermal stability, and high antitumor activity.<sup>110</sup>

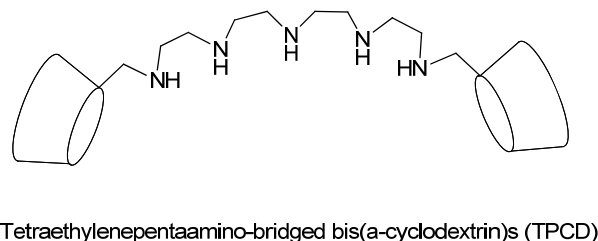


**Figure 2.8.** Illustrated structure of bridged bis( $\beta$ -CD).

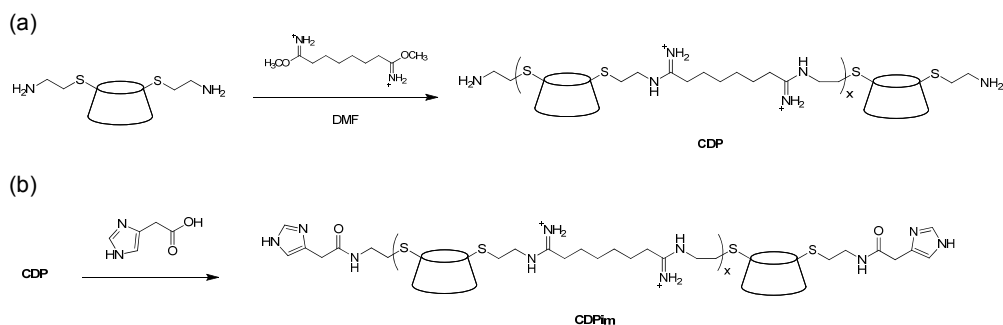
## **2.4. Cyclodextrin on Gene Delivery**

### **2.4.1. Cyclodextrins as Gene Delivery Enhancers**

The gene transfection efficiency can be improved by the addition of CD and its derivatives as formulation excipients. Roessler et al reported that the substituted  $\beta$ -CDs interact with DNA complexes with polyamidoamine (PAMAM) dendrimers.<sup>122</sup> Inclusion of  $\beta$ -CD helps to form smaller and more evenly distributed particles. *In vitro* CAT expression can be enhanced approximately 200-fold when  $\beta$ -CD was added. Pulmonary gene therapy systems with addition of absorption enhancer DM- $\beta$ -CD benefit to the particle morphology and size distribution.<sup>123</sup> The gene transfection is also increased in comparison to the unmodified powder. The application of CDs to enhance stability of DNA/polymer complexes and gene transfection efficiency has also been reported using PLL/hyaluronic acid (HA) system.<sup>124, 125</sup>

### **2.4.2. Cyclodextrin-based Polymers for Gene Delivery**

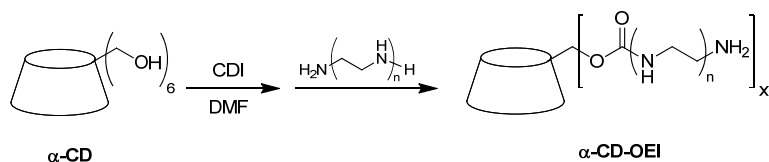
In 1999, Mark E. Davis's group firstly reported the synthesis of CD-conjugated cationic polymers for gene delivery.<sup>126</sup> Scheme 2.3a illustrates the synthetic procedure of CD-conjugated cationic polymer. The synthesized CD-based polymers illustrated lower cytotoxicity and the *in vitro* gene transfection is comparable to the PEI and lipofectamine. Then a series of research work was investigated to discuss the relationship between the gene transfection efficiency and the structure of the CD-based cationic polymers.<sup>68, 72, 127-134</sup> Structure-activity relationship (SAR) studies draw a conclusion that these water-soluble CD-conjugated polymers with low molecular weight (around 10 kDa, degree of polymerization, 5 – 8) are the optimal structures with high gene transfection ability and low cytotoxicity.



**Scheme 2.3.** Synthesis of cyclodextrin-containing polycation (CDP, a) and the imidazole-terminated variant (CDPim, b).

As shown in scheme 2.3b, the imidazole groups were conjugated to the termini of CDP with pH buffering capacity.<sup>135</sup> This buffering capacity may enhance the ability to escape the endocytic pathway. Although the exactly mechanism for the enhancement of gene transfection efficiency of CDPim is not clear, the imidazole-containing variant CDPim showed significant improvement in gene delivery efficiency. In this work, the simple modification of non-viral gene delivery vectors can impart multiple functions.

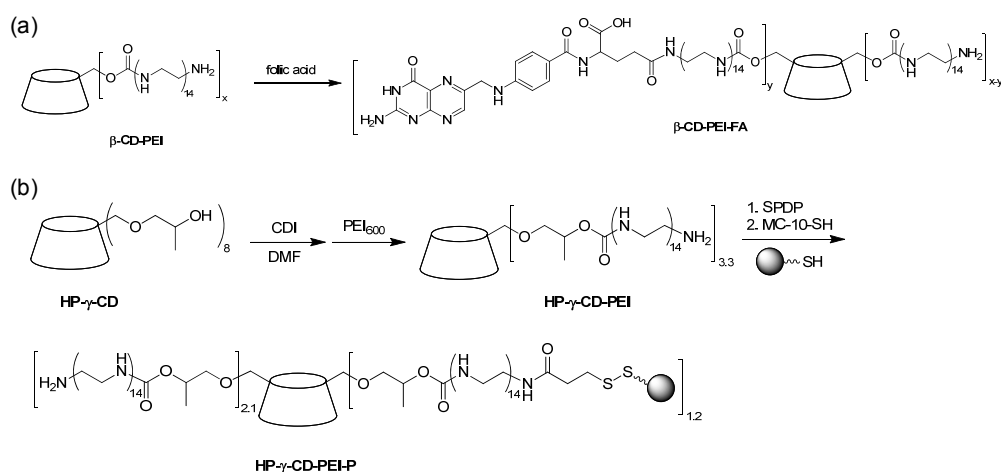
Our group reported a series of cationic star polymers by conjugating oligoethylenimine (OEI) chains to  $\alpha$ -CD as non-viral gene delivery vectors (Scheme 2.4).<sup>136, 137</sup> These  $\alpha$ -CD-OEI star-shaped polymers showed much lower cytotoxicity and excellent gene transfection efficiency that were comparable to or even higher than that of the well-studied branched PEI (25 kDa).



**Scheme 2.4.** Synthesis of  $\alpha$ -CD-OEI star-shaped polymers.

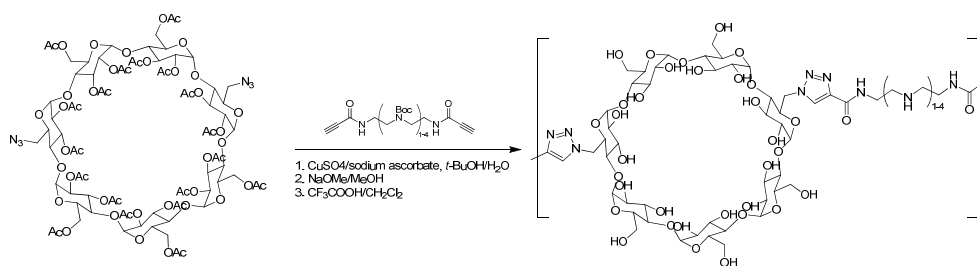
Huang et al synthesized low molecular weight PEI conjugated HP- $\beta$ -CD and HP- $\gamma$ -CD that had low cytotoxicity and 1.5 – 1.7 fold higher gene transfection efficiency than PEI in SKOV-3 cells.<sup>138-140</sup> Improved transfection efficiency can be obtained by grafting target group folic acid, a ligand that

usually over-expresses on the surface of some cancer cells.<sup>141</sup> The synthesized  $\beta$ -CD-PEI-folate polymer has efficient gene transfection in various cancer cell lines with low cytotoxicity, and the effect is higher than folate-free  $\beta$ -CD-PEI polymer (Scheme 2.5a). Similarly, MC-10 oligopeptide with targeting ability to the human epidermal growth factor receptor was conjugated to HP- $\gamma$ -CD, and the polymer HP- $\gamma$ -CD-PEI-P (Scheme 2.5b) expressed low cytotoxicity and high gene transfection efficiency both *in vitro* and *in vivo*.<sup>142</sup> Animal studies using a therapeutic IFN- $\alpha$  gene enhanced the antitumor effect on tumor-bearing mice in comparison with PEI (25 kDa).



**Scheme 2.5.** Synthesis of  $\beta$ -CD-PEI-FA (a) and HP- $\gamma$ -CD-PEI-P (b).

“Click chemistry” has been employed in the synthesis of  $\beta$ -CD-containing cationic polymers in gene delivery.<sup>143-145</sup> Srinivasachari and Reineke synthesized  $\beta$ -CD oligoethyleneamine variants using 1,3-dipolar cycloaddition of a diazido  $\beta$ -CD and  $\alpha,\omega$ -dipropargylated oligoethyleneamine (Scheme 2.6).<sup>143</sup> Polymers with longer oligoethyleneamine have more effective luciferase gene expression. However, the toxicity is quite high for all the polymers.



**Scheme 2.6.** Synthesis of the  $\beta$ -CD-containing cationic polymers by click chemistry.

Taking advantage of the ability of CDs to form inclusion complexes with hydrophobic molecules, the host-guest structure between poly $\beta$ -CDs and amphiphilic connector (DC-Chol or adamantane derivative Ada2) has been prepared.<sup>146</sup> The surface charge of the polymers can be easily adjusted by the addition of connector which the cationic part towards outside. There is 2-fold higher gene transfection efficiency of the poly- $\beta$ CD/DC-Chol inclusion complex than the single DC-Chol. The authors further studied the properties of inclusion complexes between poly $\beta$ -CD and other cationic polymer, such as the cationic surfactant *n*-dodecyltrimethylammonium chloride (DTAC) and other cationic adamantane derivatives.<sup>147, 148</sup>

Davis and coworkers prepared inclusion complex between  $\beta$ CD-containing cationic polymers and adamantane-modified PEG that the PEGylation makes the DNA polyplexes stable in physiological conditions, although their luciferase expression is slightly reduced.<sup>149</sup> In addition, the PEGylation variants show significantly differences in particle morphology and cellular uptake since the PEG moieties prevents particles from aggregation and non-specific interactions with biological component. Targeted delivery was endowed using adamantane-PEG conjugated with ligands.<sup>150</sup> Galactosylated  $\beta$ CD-containing cationic polymers selectively target to hepatocytes through the asialoglycoprotein receptor. Transferrin (Tf) is a well-known ligand for tumor targeted delivery because of the upregulation of transferring receptors in many cancer cells. The Ad-PEG/Ad-PEG-Tf included cationic CD polymers more efficiently deliver pDNA and siRNA than the non-targeted particles.<sup>151,</sup>

<sup>152</sup> The in vivo study demonstrated these transferring-modified, CD-based cationic polymers are able to protect and selectively deliver DNAzyme<sup>153</sup> or small interfering RNA (siRNA)<sup>154-156</sup>. In 2008, a targeted therapeutic agent CALAA-01 (Calando Pharmaceuticals) is on the stage of phase I clinical trials. The agent is designed to inhibit tumor growth and/or reduce tumor size. The active ingredient is a small interfering RNA (siRNA) that inhibits tumor growth through RNA interference to reduce expression of the M2 subunit of ribonucleotide reductase (R2). CALAA-01 consists of four components: (i) siRNA for therapeutic ingredient; (ii) CD-based cationic polymer as carrier; (iii) PEGylation as stabilizing agent; (iv) Ad-PEG-Tf as targeting moiety (<http://www.clinicaltrials.gov/ct2/show/NCT00689065>). The structure has been displayed in Figure 2.9. A specific gene inhibition was induced by systematical administration of siRNA to a human.<sup>157</sup>

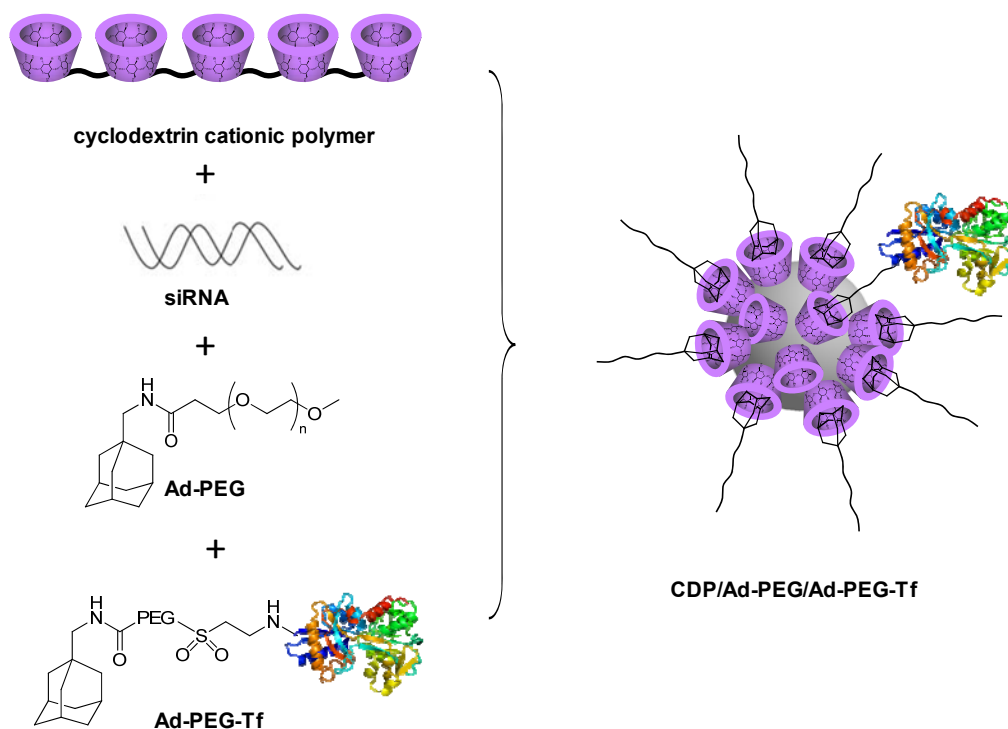


**Figure 2.9.** Schematic representation of the nanoparticles consists of transferrin-targeted siRNA-CDP/Ad-PEG.

## 2.5. Cyclodextrin-based Polyrotaxanes for Drug and Gene

### Delivery

The structure of polyrotaxane includes an appropriate axle, macrocycle wheels threaded on the axle, and bulky end-caps on the end of axle to avoid the slippage of macrocycle wheels. One of the specific features in polyrotaxanes is the absence of covalent bond between cyclic compounds and the polymeric chains. These special structures have attracted tremendous interest because of their unique structures as well as their potential as building blocks for lots of functional nanomaterials. Since the first synthesis of polyrotaxanes with  $\alpha$ -cyclodextrin ( $\alpha$ -CD) rings threaded over a polymer chain (Figure 2.10),<sup>158, 159</sup> supramolecular architectures have greatly intrigued researchers due to their unique structures and promising properties on electronics<sup>160-162</sup> and biomaterials applications, especially in the area of drug and gene delivery.<sup>163-168</sup>

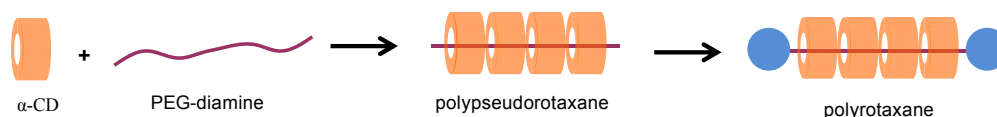


**Figure 2.10.** Demonstration of CD and polyrotaxane: (a) structure of  $\alpha$ -CD, (b) synthesis of polyrotaxane from  $\alpha$ -CD and PEO-diamine.<sup>158</sup>

This kind of polyrotaxane is fascinating and very promising for drug-conjugating delivery due to several unique structural characteristics. Firstly, CDs have many hydroxyl groups that could be easily modified by chemical reactions, allowing the conjugation of bioactive agent onto the CD rings. Secondly, self-assembled polyrotaxanes have highly mobility of CD rings that can rotate around the polymer chain. This flexibility is expected to enhance multivalent ligand-receptor interaction, and is promising for applications on drug/gene delivery and tissue engineering.<sup>168, 169</sup> Thirdly, CDs can dethread through the polymer chain when the bulky end-caps are cleaved, which insures the release of drug into the cell.<sup>170</sup> Furthermore, cationic

polyrotaxanes consist of multiple OEI-grafted CDs threaded on polymer chains were attractive non-viral gene carries due to their low cytotoxicity, strong DNA binding ability, and high gene delivery capability.<sup>168, 171</sup> Generally, thanks to their biocompatibility, flexibility and easily to be modified, polyrotaxanes have attracted much attention as vectors for drug and gene delivery.

**Table 2.4.** List of generally used polymers and corresponding CDs

Polymer	Formula	CD Threaded
Poly(ethylene glycol)	-CH <sub>2</sub> CH <sub>2</sub> O-	$\alpha, \gamma$
Poly(propylene glycol)	-CH <sub>2</sub> CH(CH <sub>3</sub> )O-	$\beta, \gamma$
Poly(methyl vinyl ether)	-CH <sub>2</sub> CH(OCH <sub>3</sub> )-	$\gamma$
Oligoethylene	-CH <sub>2</sub> CH <sub>2</sub> -	$\alpha$
Poly(isobutylene)	-CH <sub>2</sub> C(CH <sub>3</sub> ) <sub>2</sub> -	$\beta, \gamma$
Poly(tetrahydrofuran)	-(CH <sub>2</sub> ) <sub>4</sub> O-	$\alpha, \beta$
Poly(oxytrimethylene)	-(CH <sub>2</sub> ) <sub>3</sub> O-	$\alpha$
Poly(dimethylsiloxane)	-Si(CH <sub>3</sub> ) <sub>2</sub> O-	$\beta, \gamma$
Poly(dimethylsilane)	-Si(CH <sub>3</sub> ) <sub>2</sub> -	$\beta, \gamma$
Nylon 6	-NH(CH <sub>2</sub> ) <sub>5</sub> CO-	$\alpha$
Nylon 11	-NH(CH <sub>2</sub> ) <sub>10</sub> CO-	$\alpha$
Poly(acrylonitrile)	-CH(CN)CH <sub>2</sub> -	$\gamma$
Squalane	-CH <sub>2</sub> CH(CH <sub>3</sub> )CH <sub>2</sub> CH <sub>2</sub> -	$\beta, \gamma$
Poly(1,3-dioxolane)	-OCH <sub>2</sub> O(CH <sub>2</sub> ) <sub>2</sub> -	$\alpha, \beta, \gamma$
Poly(iminooligomethylene)	-NH(CH <sub>2</sub> ) <sub>n</sub> NH-	$\alpha, \beta$
Poly( $\epsilon$ -lysine)	-NH(CH <sub>2</sub> ) <sub>4</sub> CH(NH <sub>2</sub> )CO-	$\alpha$
Polyethyleneimine	-CH <sub>2</sub> CH <sub>2</sub> NH-	$\alpha, \gamma$
Poly(adipate)	-O(CH <sub>2</sub> ) <sub>n</sub> OCO(CH <sub>2</sub> ) <sub>4</sub> CO-	$\alpha, \gamma$
Poly( $\epsilon$ -caprolactone)	-O(CH <sub>2</sub> ) <sub>5</sub> CO-	$\alpha, \gamma$
Poly(L-lactic acid)	-OCH(CH <sub>3</sub> )	$\alpha$
Viologen polymers	-N <sup>+</sup> C <sub>5</sub> H <sub>4</sub> -C <sub>5</sub> H <sub>4</sub> N <sup>+</sup> -	$\alpha, \beta$
Ionene polymers	-N(CH <sub>3</sub> ) <sub>2</sub> (CH <sub>2</sub> ) <sub>n</sub> -	$\gamma$

The cavity size of different CDs and cross-sectional areas of the polymer chains are important factors for the formation of inclusion complexes between



polymers and CDs. Table 2.4 lists the commonly used polymer axles and corresponding CDs for the formation of inclusion complexes.<sup>172</sup>

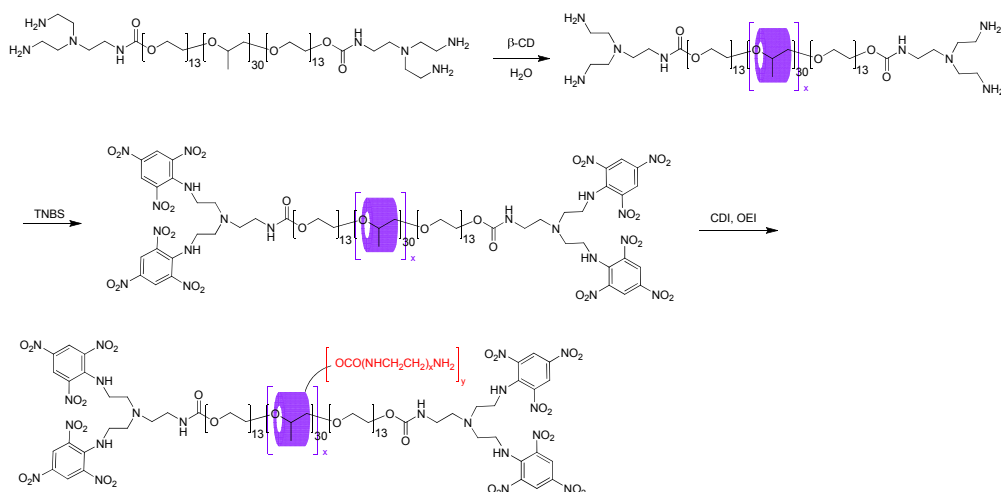
Recently, growing attention has been attracted to the synthesis of inclusion complexes between CDs and block copolymers such as PEO-PPO-PEO triblock copolymers. PEO can form crystalline polypseudorotaxanes with smallest  $\alpha$ -CD, but not with larger  $\beta$ -CD.<sup>173, 174</sup> It is assumed that the PPO chain was too large to penetrate the inner cavity of  $\alpha$ -CD. Larger  $\beta$ -CD would selectively thread the middle PPO block to form a polyrotaxane,<sup>175, 176</sup> whereas  $\alpha$ -CD selectively includes the flanking PEO blocks.<sup>177-179</sup> Our group has already synthesized lots of polyrotaxanes between PEO-PPO-PEO triblock copolymers and  $\alpha$ - or  $\beta$ -CD for application of hydrogels and cationic polyrotaxanes on drug and gene delivery.<sup>168, 177, 180-182</sup>

On the other hand, CD-based polyrotaxanes could be widely applied as drug delivery systems by conjugating drugs or functional proteins onto the CD rings. Because CD rings threaded on polyrotaxane are movable along the polymer chain, this property contribute to the multivalent interaction and targeting delivery.<sup>183</sup> For example, a polyrotaxane consisting of lactoside-CD-polyviologen conjugated polyrotaxane was investigated for its ability to inhibit galectin-1-mediated T-cell agglutination. Due to the rotating properties, the polyrotaxane showed an enhancement for the agglutination.<sup>184</sup> Furthermore, as compared to biodegradable hydrogel matrices for drug release, drug-conjugated biodegradable polyrotaxane can be advantageous in both controlling the drug release by degradation rate of terminal group and the number of CDs threaded onto the biodegradable polymer, and the dethreading of CDs modified with appropriate drugs may enhance drug permeation across biological barriers. The first example of biodegradable polyrotaxanes was reported in 1995.<sup>185</sup> The supramolecular assemblies were formed between  $\alpha$ -CD and PEO chain, capping with L-Phe via biodegradable peptide linkages. The *in vitro* release study shows that HP- $\alpha$ -CD can be released when either of

two terminal peptides was cleaved, and the rate of degradation can be controlled by changing the degree of hydrophobicity of the  $\alpha$ -CDs.<sup>186</sup>

Yang et al demonstrated the application of polyrotaxane-based delivery system for transport of anti-cancer drug doxorubicin (DOX). DOX was chemical conjugated to the polyrotaxane via hydrolysable linkage, which can be hydrolyzed and release DOX for cancer therapy. In addition, a cell-penetrating low molecular weight protamine (LMWP) peptide was further attached to the terminal of polymer chain in order to facilitate the intracellular uptake of tumor cells. The LMWP-PR-DOX conjugates illustrated sustained release of DOX over a period of greater than four days.<sup>187</sup>

Thanks to the advantages of PEO-PPO-PEO triblock copolymer, polyrotaxane between EO<sub>13</sub>PO<sub>30</sub>EO<sub>13</sub> copolymer and  $\beta$ -CD was prepared and capped with TNBS (Scheme 2.7). Then different lengths of OEI chains were linked to the  $\beta$ -CD rings to form cationic polyrotaxanes, which illustrated efficient gene delivery and much lower cytotoxicity than PEI (25 KDa). The spare PEO segment allows efficient link of OEI chains, and the OEI-grafted CD rings can freely move along the polymer chains, resulting flexibility for efficient complexation with DNA. The OEI chains with many primary and secondary amines are also beneficial for interaction with DNA and/or cell membranes.<sup>168</sup> Applications with other systems such as OEI-grafted  $\alpha$ -CD threaded on PEO chains,<sup>188</sup> as OEI-grafted  $\alpha$ -CD threaded on poly[(ethylene oxide)-ran-(propylene oxide)] (P(EO-r-PO)) random copolymer chains,<sup>163</sup> pentaethylenhexamine-grafted  $\alpha$ -CD threaded on PPO-PEO-PPO triblock copolymer,<sup>171</sup> different lengths of OEI-grafted  $\beta$ -CD threaded on PEO-PPO-PEO triblock copolymer<sup>182</sup> all displayed strong DNA binding ability, low cytotoxicity, and high gene delivery capability as a high potential on non-viral gene delivery carriers in cancer therapy.



**Scheme 2.7.** Synthesis procedures and structures of cationic polyrotaxanes with multiple OEI-grafted  $\beta$ -CD rings.<sup>168</sup>

Yui and coworkers synthesized a series of aminoethylcarbamoyl (AEC)-polyrotaxanes between  $\alpha$ -CD and PEG.<sup>189</sup> Further preparation of polyrotaxanes employed dimethylaminoethyl (DMAEC)-modified  $\alpha$ -CD threaded onto PEG chain capped with benzyloxycarboxyl tyrosine via biocleavable disulfide linkages.<sup>190, 191</sup> This system was found to exhibit sufficient cleavage of disulfide linkages, as a result of the rapid endosomal escape and pDNA release. Furthermore, the polyplex with lowest number of DMAEC exhibited a much faster pDNA release in cytoplasm. Thus the transfection activity was related to an appropriate timing for DNA release and high transfection and stability can be achieved by optimizing numbers of DMAEC.<sup>192</sup>

## 2.6. Target Delivery

There are generally two methods to develop tumor-targeted therapies.<sup>193</sup> First is selectively block novel pathways or proteins that emerged or overexpressed in malignant cells but not needed to normal cells. Second strategy is the using of ligands with specific binding ability to receptors that is overexpressed on the malignant cells. The commonly used ligands include monoclonal antibodies<sup>194-196</sup> and receptor-binding molecules such as receptor

antagonists and agonist, peptide hormones, oligosaccharides, oligopeptides, and vitamins.<sup>197-202</sup>

### 2.6.1. Overview of Folic Acid and Folate Receptor

Folic acid is a vitamin essential for biosynthesis of nucleotide bases. Folate receptor (FR) is a glycosylphosphatidylinositol (GPI)-linked membrane glycoprotein with high affinity folate binding ability.<sup>203</sup> Many malignancies cells including of the ovary, brain, kidney, breast, lung, and myeloid cells overexpress folate receptors which rendered folate an attractive candidate for tumor-specific drug delivery.<sup>204</sup> Moreover, the density of FR increases as the cancer worsens. In contrast, FR on the normal cell is not easy to access due to its location on the apical membrane of polarized epithelia.

FRs are significantly upregulated on tumor cells, so the folate-conjugated therapeutic agents can reduce the side effects and enhance the potency against tumor cells in comparison with the non-targeted cells.<sup>205, 206</sup> Several folate-conjugated drugs have already entered clinic trials.<sup>207-211</sup>

### 2.6.2. Folate-targeted Gene Therapy

Great effort has been devoted to prepare folate-linked non-viral biocompatible polymeric gene delivery vectors, such as cationic polymers, cationic lipids, cationic peptides, and so on.<sup>193, 212, 213</sup> PEI has inherent endosomal lytic activity, so PEI can not only condense DNA but also osmotically lyse its entrapping endosomes.<sup>214</sup> The application of PEI usually hinders by its high toxicity from non-specific uptake. Directly conjugation of folate to PEI did not significantly alter the transfection efficiency.<sup>215</sup> However, it can greatly enhance the gene transfection of PEG-modified PEI whereas PEGylation showed reduced cellular uptake and a partial inhibition of gene delivery. Benns et al. reported the synthesis of folate-PEG-folate-grafted-PEI (FPF-g-PEI) for targeted gene delivery.<sup>216</sup> As a result, conjugation of FPF to PEI can reduce the toxicity and enhance gene expression.

### 2.6.3. Factors Affecting Folate-targeted Delivery

Several factors would affect the folate-mediated targeted gene delivery *in vivo*: (i) endogenous folate in systemic circulation potentially blocks FR binding; (ii) the size of folate-conjugated vectors may preclude glomerular filtration; (iii) folate conjugate should escape the vasculature and intratumoral diffusion; (iv) the FR expression on tumor cells might be not sufficient.<sup>213</sup>

### 2.7. Redox-Sensitive Carriers

Introduction of target group, delivery-enhancing molecules, or functional moiety to drug and gene delivery systems has become an efficient approach to enhance the capability of drug and gene delivery systems. Structure modification may result in alternation of its cytotoxicity, pharmacokinetics, dynamics, and metabolism. In addition, the properties of linker between drug and the delivery enhancing entities significantly influence the successful application of drugs. Various redox-sensitive biodegradable cationic polymers have been employed in gene delivery. In comparison to hydrolytically degradable cationic polymers that the hydrolysis rate is proportional to the pH of environment, the redox-sensitive polymers are pretty stable under physiological conditions and rapid degradation occurs in the cytosol due to the thio-disulfide exchange by the high concentration of glutathione. On the one hand, the multi-functional polymers can be degraded into small fragments to alleviate accumulation of high molecular weight cationic polymer and the subsequent cytotoxicity. On the other hand, the degradation helps to efficient intracellular release of DNA or siRNA.<sup>217</sup>

The design of redox-sensitive polymers usually involves incorporation of a covalent disulfide linker (–S–S–). Figure 2.11 lists some disulfide-containing cross-linking agents that are widely used in disulfide chemistry.<sup>217</sup> The unique properties of disulfide bond render it particularly attractive in delivery systems: (i) the covalently bonded disulfides can be synthesized by oxidation of

sulfhydryls and the reversible reduction occur in the presence of reducing agents such as dithiothreitol (DTT),  $\beta$ -mercaptoethanol, and glutathione (GSH); (ii) the large gradient in reducing potential between extracellular (GSH concentration 2 – 20  $\mu$ M) and intracellular (GSH concentration 0.5 – 10 mM) milieu makes disulfide linker intriguing as a smart delivery tool.

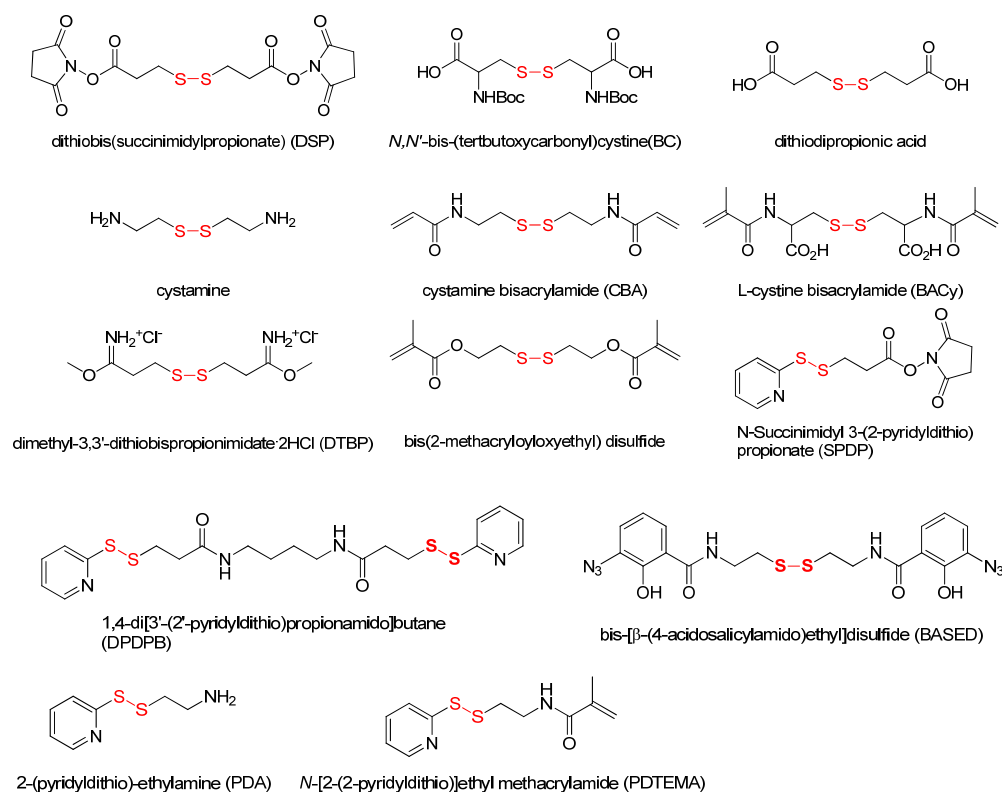


**Figure 2.11.** Selective disulfide cross-linking agents.

The application of disulfide bonds for delivery of macromolecular drugs has been reported *in vitro* and *in vivo*. The first antibody-targeted anticancer drug with disulfide linker Gemtuzumab Ozogamicin (Mylotarg) has been approved by FDA.<sup>218</sup> Recently, more non-viral vectors with disulfide linker to promote DNA or siRNA delivery have been studied.

Many target moieties hinder effect unpacking of gene vector due to their large size. Therefore, the strategy to remove the target groups inside cells is very important. Taking advantage of the redox-sensitive disulfide bond, the application of disulfide linkage between gene delivery vector and target group is a promising tool to solve this problem. Muratovska et al. reported the

attachment of membrane-permeant peptide (MPP) to siRNA with a disulfide linker. The peptide facilitates the transport across the cell membrane, and the bioactive siRNA was released after reduction of disulfide bond in the cytoplasm. The penetratin- or transportan-siRNA conjugates constitutively expressed luciferase and silenced GFP genes in a high proportion of cells of different types.<sup>219</sup> Similarly, a molecular conjugate of asialoglycoprotein (ASGP) and antisense oligonucleotide using disulfide linker were found to significantly increase the effect of antisense oligonucleotides *in vitro*. The number of targeting ligands could be adjusted by the amount of linker.

The reduction-sensitive biodegradable polymers are able to triggered deliver bioactive molecules including DNA, siRNA, antisense oligonucleotide, proteins, anticancer drugs, et al, especially for the systems that required to be stable in circulation and rapid degradation inside cells.

## 2.8. References

- (1) *Singapore Cancer Registry Interim Annual Registry Report 2006-2010.*
- (2) Camphausen, K.; Moses, M. A.; Beecken, W. D.; Khan, M. K.; Folkman, J.; O'Reilly, M. S., *Cancer Res* **2001**, *61*, 2207-2211.
- (3) Chen, W. R.; Huang, Z.; Andrienko, K.; Stefanov, S.; Wolf, R. F.; Liu, H., *P Soc Photo-Opt Ins* **2006**, *6163*, F1630-F1630.
- (4) Wani, M. C.; Taylor, H. L.; Wall, M. E.; Coggon, P.; McPhail, A. T., *Journal of the American Chemical Society* **1971**, *93*, 2325-2327.
- (5) Donehower, R. C.; Rowinsky, E. K.; Grochow, L. B.; Longnecker, S. M.; Ettinger, D. S., *Cancer treatment reports* **1987**, *71*, 1171-1177.
- (6) Schiff, P. B.; Fant, J.; Horwitz, S. B., *Nature* **1979**, *277*, 665-667.
- (7) Hamel, E.; Delcampo, A. A.; Lowe, M. C.; Lin, C. M., *J Biol Chem* **1981**, *256*, 11887-11894.
- (8) Parness, J.; Horwitz, S. B., *J Cell Biol* **1981**, *91*, 479-487.
- (9) Schiff, P. B.; Horwitz, S. B., *Biochemistry* **1981**, *20*, 3247-3252.
- (10) Rowinsky, E. K.; Cazenave, L. A.; Donehower, R. C., *Journal of the National Cancer Institute* **1990**, *82*, 1247-1259.
- (11) Oliver, A., *Montana Pharmacist* **1993**, *17*, 17-18.
- (12) Feng, S. S.; Huang, G. F., *Journal of Controlled Release* **2001**, *71*, 53-69.
- (13) Suffness, M., *Annu Rep Med Chem* **1993**, *28*, 305-314.
- (14) Lorenz, W.; Reimann, H. J.; Schmal, A.; Dormann, P.; Schwarz, B.; Neugebauer, E.; Doenicke, A., *Agents Actions* **1977**, *7*, 63-67.
- (15) Weiss, R. B.; Donehower, R. C.; Wiernik, P. H.; Ohnuma, T.; Gralla, R. J.; Trump, D. L.; Baker, J. R.; Vanecho, D. A.; Vonhoff, D. D.; Leylandjones, B., *Journal of Clinical Oncology* **1990**, *8*, 1263-1268.
- (16) Mulligan, R. C., *Science* **1993**, *260*, 926-932.
- (17) Pack, D. W.; Hoffman, A. S.; Pun, S.; Stayton, P. S., *Nat Rev Drug Discov* **2005**, *4*, 581-593.
- (18) Walsh, C. E., *Gene Ther* **2003**, *10*, 999-1003.
- (19) van Deutekom, J. C. T.; van Ommen, G. J. B., *Nat Rev Genet* **2003**, *4*, 774-783.
- (20) Ferrari, S.; Geddes, D. M.; Alton, E. W. F. W., *Adv Drug Deliver Rev* **2002**, *54*, 1373-1393.
- (21) Junttila, M. R.; Evan, G. I., *Nat Rev Cancer* **2009**, *9*, 821-829.
- (22) Karmakar, A.; Bratton, S. M.; Dervishi, E.; Ghosh, A.; Mahmood, M.; Xu, Y.; Saeed, L. M.; Mustafa, T.; Casciano, D.; Radominska-Pandya, A.; Biris, A. S., *Int J Nanomed* **2011**, *6*, 1045-1055.
- (23) Levine, A. J.; Momand, J.; Finlay, C. A., *Nature* **1991**, *351*, 453-456.
- (24) Evan, G. I.; Vousden, K. H., *Nature* **2001**, *411*, 342-348.
- (25) Li, Y. X.; Lin, Z. B.; Tan, H. R., *Acta Pharmacol Sin* **2004**, *25*, 76-82.
- (26) Greco, F.; Vicent, M. J., *Adv Drug Deliver Rev* **2009**, *61*, 1203-1213.



- (27) Broxterman, H. J.; Georgopapadakou, N. H., *Drug Resist Update* **2005**,*8*, 183-197.
- (28) Georgopapadakou, N.; Broxterman, H.; Arts, E.; Perfect, J.; Ward, S., *Drug Resist Update* **2005**,*8*, 1-2.
- (29) Choudhury, N. N.; He, H. X., *Curr Pharm Biotechno* **2012**,*13*, 1317-1331.
- (30) Wiradharma, N.; Tong, Y. W.; Yang, Y. Y., *Biomaterials* **2009**,*30*, 3100-3109.
- (31) Xu, Z. H.; Zhang, Z. W.; Chen, Y.; Chen, L. L.; Lin, L. P.; Li, Y. P., *Biomaterials* **2010**,*31*, 916-922.
- (32) Wang, Y.; Gao, S. J.; Ye, W. H.; Yoon, H. S.; Yang, Y. Y., *Nature Materials* **2006**,*5*, 791-796.
- (33) Yue, X. Y.; Qiao, Y.; Qiao, N.; Guo, S. T.; Xing, J. F.; Deng, L. D.; Xu, J. Q.; Dong, A. J., *Biomacromolecules* **2010**,*11*, 2306-2312.
- (34) Wang, H. J.; Zhao, P. Q.; Su, W. Y.; Wang, S.; Liao, Z. Y.; Niu, R. F.; Chang, J., *Biomaterials* **2010**,*31*, 8741-8748.
- (35) Hu, Q. D.; Fan, H.; Ping, Y.; Liang, W. Q.; Tang, G. P.; Li, J., *Chemical Communications* **2011**,*47*, 5572-5574.
- (36) Son, K.; Huang, L., *Gene Ther* **1996**,*3*, 630-634.
- (37) Nair, R. R.; Rodgers, J. R.; Schwarz, L. A., *Molecular therapy : the journal of the American Society of Gene Therapy* **2002**,*5*, 455-462.
- (38) Bhalla, K.; Ibrado, A. M.; Tourkina, E.; Tang, C.; Mahoney, M. E.; Huang, Y., *Leukemia : official journal of the Leukemia Society of America, Leukemia Research Fund, U.K* **1993**,*7*, 563-568.
- (39) Woods, C. M.; Zhu, J.; Mcqueney, P. A.; Bollag, D.; Lazarides, E., *Mol Med* **1995**,*1*, 506-526.
- (40) Sorger, P. K.; Dobles, M.; Tournebize, R.; Hyman, A. A., *Current opinion in cell biology* **1997**,*9*, 807-814.
- (41) Blagosklonny, M. V.; Fojo, T., *Int J Cancer* **1999**,*83*, 151-156.
- (42) Nielsen, L. L.; Lipari, P.; Dell, J.; Gurnani, M.; Hajian, G., *Clin Cancer Res* **1998**,*4*, 835-846.
- (43) Culver, K. W.; Blaese, R. M., *Trends Genet* **1994**,*10*, 174-178.
- (44) Yang, Z. R.; Wang, H. F.; Zhao, J.; Peng, Y. Y.; Wang, J.; Guinn, B. A.; Huang, L. Q., *Cancer Gene Ther* **2007**,*14*, 599-615.
- (45) Lechardeur, D.; Sohn, K. J.; Haardt, M.; Joshi, P. B.; Monck, M.; Graham, R. W.; Beatty, B.; Squire, J.; O'Brodovich, H.; Lukacs, G. L., *Gene Ther* **1999**,*6*, 482-497.
- (46) Houk, B. E.; Hochhaus, G.; Hughes, J. A., *Aaps Pharmsci* **1999**,*1*, U1-U9.
- (47) Verma, I. M.; Somia, N., *Nature* **1997**,*389*, 239-242.
- (48) Mintzer, M. A.; Simanek, E. E., *Chemical Reviews* **2009**,*109*, 259-302.
- (49) Mislick, K. A.; Baldeschwieler, J. D., *P Natl Acad Sci USA* **1996**,*93*, 12349-12354.
- (50) Mounkes, L. C.; Zhong, W.; Cipres-Palacin, G.; Heath, T. D.; Debs, R. J., *J Biol Chem* **1998**,*273*, 26164-26170.

- (51) Molas, M.; Gomez-Valades, A. G.; Vidal-Alabro, A.; Miguel-Turu, M.; Bermudez, J.; Bartrons, R.; Perales, J. C., *Current gene therapy* **2003**,*3*, 468-485.
- (52) Boussif, O.; Lezoualch, F.; Zanta, M. A.; Mergny, M. D.; Scherman, D.; Demeneix, B.; Behr, J. P., *P Natl Acad Sci USA* **1995**,*92*, 7297-7301.
- (53) Godbey, W. T.; Wu, K. K.; Mikos, A. G., *Journal of Biomedical Materials Research* **1999**,*45*, 268-275.
- (54) Fischer, D.; Li, Y. X.; Ahlemeyer, B.; Krieglstein, J.; Kissel, T., *Biomaterials* **2003**,*24*, 1121-1131.
- (55) Fischer, D.; Bieber, T.; Li, Y. X.; Elsasser, H. P.; Kissel, T., *Pharmaceut Res* **1999**,*16*, 1273-1279.
- (56) Godbey, W. T.; Barry, M. A.; Saggau, P.; Wu, K. K.; Mikos, A. G., *Journal of Biomedical Materials Research* **2000**,*51*, 321-328.
- (57) Suh, J.; Paik, H. J.; Hwang, B. K., *Bioorg Chem* **1994**,*22*, 318-327.
- (58) Godbey, W. T.; Wu, K. K.; Mikos, A. G., *P Natl Acad Sci USA* **1999**,*96*, 5177-5181.
- (59) Rudolph, C.; Schillinger, U.; Plank, C.; Gessner, A.; Nicklaus, P.; Muller, R. H.; Rosenecker, J., *Bba-Gen Subjects* **2002**,*1573*, 75-83.
- (60) Thomas, M.; Klibanov, A. M., *P Natl Acad Sci USA* **2002**,*99*, 14640-14645.
- (61) Shuai, X. T.; Merdan, T.; Unger, F.; Wittmar, M.; Kissel, T., *Macromolecules* **2003**,*36*, 5751-5759.
- (62) Arote, R.; Kim, T. H.; Kim, Y. K.; Hwang, S. K.; Jiang, H. L.; Song, H. H.; Nah, J. W.; Cho, M. H.; Cho, C. S., *Biomaterials* **2007**,*28*, 735-744.
- (63) Gosselin, M. A.; Guo, W. J.; Lee, R. J., *Bioconjugate Chem* **2001**,*12*, 989-994.
- (64) Oupicky, D.; Parker, A. L.; Seymour, L. W., *Journal of the American Chemical Society* **2002**,*124*, 8-9.
- (65) Neu, M.; Sitterberg, J.; Bakowsky, U.; Kissel, T., *Biomacromolecules* **2006**,*7*, 3428-3438.
- (66) Kloeckner, J.; Wagner, E.; Ogris, M., *Eur J Pharm Sci* **2006**,*29*, 414-425.
- (67) Neu, M.; Germershaus, O.; Mao, S.; Voigt, K. H.; Behe, M.; Kissel, T., *Journal of Controlled Release* **2007**,*118*, 370-380.
- (68) Pun, S. H.; Bellocq, N. C.; Liu, A. J.; Jensen, G.; Machemer, T.; Quijano, E.; Schluep, T.; Wen, S. F.; Engler, H.; Heidel, J.; Davis, M. E., *Bioconjugate Chem* **2004**,*15*, 831-840.
- (69) Nosov, D. A.; Esteves, B.; Lipatov, O. N.; Lyulko, A. A.; Anischenko, A. A.; Chacko, R. T.; Doval, D. C.; Strahs, A.; Slichenmyer, W. J.; Bhargava, P., *Journal of clinical oncology : official journal of the American Society of Clinical Oncology* **2012**,*30*, 1678-1685.
- (70) Slichenmyer, W. J.; Von Hoff, D. D., *Anti-cancer drugs* **1991**,*2*, 519-530.
- (71) Slichenmyer, W. J.; Von Hoff, D. D., *Journal of clinical pharmacology* **1990**,*30*, 770-788.
- (72) Davis, M. E.; Brewster, M. E., *Nat Rev Drug Discov* **2004**,*3*, 1023-1035.

- (73) Uekama, K.; Hirayama, F.; Irie, T., *Chemical Reviews* **1998**, *98*, 2045-2076.
- (74) Loftsson, T.; Brewster, M. E., *J Pharm Sci* **1996**, *85*, 1017-1025.
- (75) Rajewski, R. A.; Stella, V. J., *J Pharm Sci* **1996**, *85*, 1142-1169.
- (76) Irie, T.; Uekama, K., *J Pharm Sci* **1997**, *86*, 147-162.
- (77) Stella, V. J.; Rajewski, R. A., *Pharmaceut Res* **1997**, *14*, 556-567.
- (78) Connors, K. A., *Chem Rev* **1997**, *97*, 1325-1358.
- (79) Coleman, A. W.; Nicolis, I.; Keller, N.; Dalbiez, J. P., *J Inclus Phenom Mol* **1992**, *13*, 139-143.
- (80) Szejtli, J., *Chemical Reviews* **1998**, *98*, 1743-1753.
- (81) Brewster, M. E.; Loftsson, T., *Adv Drug Deliver Rev* **2007**, *59*, 645-666.
- (82) Khan, A. R.; Forgo, P.; Stine, K. J.; D'Souza, V. T., *Chemical Reviews* **1998**, *98*, 1977-1996.
- (83) Marshall, J. J.; Miwa, I., *Biochim Biophys Acta* **1981**, *661*, 142-147.
- (84) Yamamoto, M. A., H.; Irie, T.; Hirayama, F.; Uekama, K., *S.T.P. Pharma Sci.* **1991**, *1*, 397.
- (85) Szejtli, J.; Sebestyen, G., *Starke* **1979**, *31*, 385-389.
- (86) Uekama, K. H., F.; Irie, T., *In Drug Targeting Delivery; Boer, A. G., Ed.; Harwood Publishers: Amsterdam*, **1993**, *3*, 411.
- (87) Irie, T.; Otagiri, M.; Sunada, M.; Uekama, K.; Ohtani, Y.; Yamada, Y.; Sugiyama, Y., *J Pharmacobio-Dynam* **1982**, *5*, 741-744.
- (88) Ohtani, Y.; Irie, T.; Uekama, K.; Fukunaga, K.; Pitha, J., *Eur J Biochem* **1989**, *186*, 17-22.
- (89) Thompson, D. O., *Crit Rev Ther Drug* **1997**, *14*, 1-104.
- (90) Uekama, K., *Chem Pharm Bull* **2004**, *52*, 900-915.
- (91) G. Antlsperger, G. S., J. Szejtli, L. Szenté (Eds.), *Proceedings of the eighth international symposium on cyclodextrins. Budapest, Hungary, March 32 – April 2 1996*, 149–155.
- (92) Challa, R.; Ahuja, A.; Ali, J.; Khar, R. K., *Aaps Pharmscitech* **2005**, *6*, E329–E357.
- (93) Villalonga, R.; Cao, R.; Frago, A., *Chemical Reviews* **2007**, *107*, 3088-3116.
- (94) Zidovetzki, R.; Levitan, I., *Bba-Biomembranes* **2007**, *1768*, 1311-1324.
- (95) T. Loftsson, M. B., M. Masson, *Am. J. Drug Deliv.* **2004**, *2*, 261–275.
- (96) Avdeef, A.; Bendels, S.; Tsinman, O.; Tsinman, K.; Kansy, M., *Pharmaceut Res* **2007**, *24*, 530-545.
- (97) C. Kim, J. P., *Am. J. Drug Deliv.* **2004**, *2*, 113-130.
- (98) Loftsson, T.; Jarho, P.; Masson, M.; Jarvinen, T., *Expert opinion on drug delivery* **2005**, *2*, 335-351.
- (99) Szejtli, J.; Szenté, L., *Eur J Pharm Biopharm* **2005**, *61*, 115-125.
- (100) Lantz, A. W.; Rodriguez, M. A.; Wetterer, S. M.; Armstrong, D. W., *Anal Chim Acta* **2006**, *557*, 184-190.
- (101) Lina, B. A. R.; Bar, A., *Regul Toxicol Pharm* **2004**, *39*, S14-S26.
- (102) Lina, B. A. R.; Bar, A., *Regul Toxicol Pharm* **2004**, *39*, S27-S33.

- (103) Gould, S.; Scott, R. C., *Food Chem Toxicol* **2005**,*43*, 1451-1459.
- (104) M.E. Brewster, C. M., A. Lampo, M. Noppe, T. Loftsson, *Solvent systems and their selection in pharmaceuticals and biopharmaceutics, American Association of Pharmaceutical Scientists and Springer: New York* **2007**,*VI*, 221-256.
- (105) Prentis, R. A.; Lis, Y.; Walker, S. R., *British journal of clinical pharmacology* **1988**,*25*, 387-96.
- (106) Kola, I.; Landis, J., *Nat Rev Drug Discov* **2004**,*3*, 711-715.
- (107) Cserhati, T.; Forgacs, E.; Hollo, J., *J Pharmaceut Biomed* **1995**,*13*, 533-541.
- (108) Sharma, U. S.; Balasubramanian, S. V.; Straubinger, R. M., *J Pharm Sci* **1995**,*84*, 1223-1230.
- (109) Liu, Y.; Chen, G. S.; Li, L.; Zhang, H. Y.; Cao, D. X.; Yuan, Y. J., *Journal of medicinal chemistry* **2003**,*46*, 4634-4637.
- (110) Liu, Y.; Chen, G. S.; Chen, Y.; Cao, D. X.; Ge, Z. Q.; Yuan, Y. J., *Bioorganic & medicinal chemistry* **2004**,*12*, 5767-5775.
- (111) Hamada, H.; Ishihara, K.; Masuoka, N.; Mikuni, K.; Nakajima, N., *Journal of bioscience and bioengineering* **2006**,*102*, 369-371.
- (112) Bouquet, W.; Ceelen, W.; Fritzing, B.; Pattyn, P.; Peeters, M.; Remon, J. P.; Vervaet, C., *Eur J Pharm Biopharm* **2007**,*66*, 391-397.
- (113) Fenyvesi, F.; Kiss, T.; Fenyvesi, E.; Szente, L.; Veszeka, S.; Deli, M. A.; Varadi, J.; Feher, P.; Ujhelyi, Z.; Tosaki, A.; Vecsernyes, M.; Bacska, I., *J Pharm Sci* **2011**,*100*, 4734-4744.
- (114) Lee, S.; Seo, D. H.; Kim, H. W.; Jung, S. H., *Carbohydr Res* **2001**,*334*, 119-126.
- (115) Kim, H.; Choi, J.; Kim, H. W.; Jung, S., *Carbohydr Res* **2002**,*337*, 549-555.
- (116) Alcaro, S.; Ventura, C. A.; Paolino, D.; Battaglia, D.; Ortuso, F.; Cattel, L.; Puglisi, G.; Fresta, M., *Bioorganic & medicinal chemistry letters* **2002**,*12*, 1637-1641.
- (117) Bouquet, W.; Ceelen, W.; Fritzing, B.; Pattyn, P.; Peeters, M.; Remon, J. P.; Vervaet, C., *Eur J Pharm Biopharm* **2007**,*66*, 391-397.
- (118) Bouquet, W.; Boterberg, T.; Ceelen, W.; Pattyn, P.; Peeters, M.; Bracke, M.; Remon, J. P.; Vervaet, C., *International journal of pharmaceuticals* **2009**,*367*, 148-154.
- (119) Bouquet, W.; Ceelen, W.; Adriaens, E.; Almeida, A.; Quinten, T.; De Vos, F.; Pattyn, P.; Peeters, M.; Remon, J. P.; Vervaet, C., *Annals of surgical oncology* **2010**,*17*, 2510-2517.
- (120) Ruebner, A.; Kirsch, D.; Andrees, S.; Decker, W.; Roeder, B.; Spengler, B.; Kaufmann, R.; Moser, J. G., *J Incl Phenom Mol* **1997**,*27*, 69-84.
- (121) Moser, J. C.; Rose, I.; Wagner, B.; Wieneke, T.; Vervoorts, A., *J Incl Phenom Macro* **2001**,*39*, 13-18.

- (122) Roessler, B. J.; Bielinska, A. U.; Janczak, K.; Lee, I.; Baker, J. R., *Biochem Bioph Res Co* **2001**,283, 124-129.
- (123) Li, H. Y.; Seville, P. C.; Williamson, I. J.; Birchall, J. C., *J Gene Med* **2005**,7, 1035-1043.
- (124) Jessel, N.; Oulad-Abdeighani, M.; Meyer, F.; Lavalle, P.; Haikel, Y.; Schaaf, P.; Voegel, J. C., *P Natl Acad Sci USA* **2006**,103, 8618-8621.
- (125) Zhang, X.; Sharma, K. K.; Boeglin, M.; Ogier, J.; Mainard, D.; Voegel, J. C.; Mely, Y.; Benkirane-Jessel, N., *Nano Lett* **2008**,8, 2432-2436.
- (126) Gonzalez, H.; Hwang, S. J.; Davis, M. E., *Bioconjugate Chem* **1999**,10, 1068-1074.
- (127) Hwang, S. J.; Bellocq, N. C.; Davis, M. E., *Bioconjugate Chem* **2001**,12, 280-290.
- (128) Cheng, J. J.; Khin, K. T.; Jensen, G. S.; Liu, A. J.; Davis, M. E., *Bioconjugate Chem* **2003**,14, 1007-1017.
- (129) Davis, M. E., *Molecular pharmaceutics* **2009**,6, 659-668.
- (130) Hwang, S. J.; Bellocq, N. C.; Davis, M. E., *Bioconjug Chem* **2001**,12, 280-290.
- (131) Reineke, T. M.; Davis, M. E., *Bioconjug Chem* **2003**,14, 247-254.
- (132) Reineke, T. M.; Davis, M. E., *Bioconjug Chem* **2003**,14, 255-261.
- (133) Popielarski, S. R.; Mishra, S.; Davis, M. E., *Bioconjug Chem* **2003**,14, 672-678.
- (134) Davis, M. E.; Pun, S. H.; Bellocq, N. C.; Reineke, T. M.; Popielarski, S. R.; Mishra, S.; Heidel, J. D., *Curr Med Chem* **2004**,11, 179-197.
- (135) Mishra, S.; Heidel, J. D.; Webster, P.; Davis, M. E., *Journal of Controlled Release* **2006**,116, 179-191.
- (136) Yang, C. A.; Li, H. Z.; Goh, S. H.; Li, J., *Biomaterials* **2007**,28, 3245-3254.
- (137) Li, J.; Loh, X. J., *Adv Drug Deliver Rev* **2008**,60, 1000-1017.
- (138) Huang, H. L.; Tang, G. P.; Wang, Q. Q.; Li, D.; Shen, F. P.; Zhou, J.; Yu, H., *Chemical Communications* **2006**, 2382-2384.
- (139) Huang, H. L.; Yu, H.; Li, D.; Liu, Y.; Shen, F.; Zhou, J.; Wang, Q. Q.; Tang, G. P., *Int J Mol Sci* **2008**,9, 2278-2289.
- (140) Tang, G. P.; Guo, H. Y.; Alexis, F.; Wang, X.; Zeng, S.; Lim, T. M.; Ding, J.; Yang, Y. Y.; Wang, S., *J Gene Med* **2006**,8, 736-744.
- (141) Yao, H.; Ng, S. S.; Tucker, W. O.; Tsang, Y. K. T.; Man, K.; Wang, X. M.; Chow, B. K. C.; Kung, H. F.; Tang, G. P.; Lin, M. C., *Biomaterials* **2009**,30, 5793-5803.
- (142) Huang, H. L.; Yu, H.; Tang, G. P.; Wang, Q. Q.; Li, J., *Biomaterials* **2010**,31, 1830-1838.
- (143) Srinivasachari, S.; Reineke, T. M., *Biomaterials* **2009**,30, 928-938.
- (144) Mendez-Ardoy, A.; Gomez-Garcia, M.; Mellet, C. O.; Sevillano, N.; Giron, M. D.; Salto, R.; Santoyo-Gonzalez, F.; Fernandez, J. M. G., *Org Biomol Chem* **2009**,7, 2681-2684.

- (145) O'Mahony, A. M.; Ogier, J.; Desgranges, S.; Cryan, J. F.; Darcy, R.; O'Driscoll, C. M., *Org Biomol Chem* **2012**,*10*, 4954-4960.
- (146) Burckbuchler, V.; Wintgens, V.; Lecomte, S.; Percot, A.; Leborgne, C.; Danos, O.; Kichler, A.; Amiel, C., *Biopolymers* **2006**,*81*, 360-370.
- (147) Galant, C.; Amiel, C.; Loic, A., *Macromol Biosci* **2005**,*5*, 1057-1065.
- (148) Burckbuchler, V.; Wintgens, V.; Leborgne, C.; Lecomte, S.; Leygue, N.; Scherman, D.; Kichler, A.; Amiel, C., *Bioconjugate Chem* **2008**,*19*, 2311-2320.
- (149) Mishra, S.; Webster, P.; Davis, M. E., *Eur J Cell Biol* **2004**,*83*, 97-111.
- (150) Pun, S. H.; Davis, M. E., *Bioconjugate Chem* **2002**,*13*, 630-639.
- (151) Bellocq, N. C.; Pun, S. H.; Jensen, G. S.; Davis, M. E., *Bioconjugate Chem* **2003**,*14*, 1122-1132.
- (152) Bartlett, D. W.; Davis, M. E., *Bioconjugate Chem* **2007**,*18*, 456-468.
- (153) Pun, S. H.; Tack, F.; Bellocq, N. C.; Cheng, J. J.; Grubbs, B. H.; Jensen, G. S.; Davis, M. E.; Brewster, M.; Janicot, M.; Janssens, B.; Floren, W.; Bakker, A., *Cancer Biol Ther* **2004**,*3*, 641-650.
- (154) Hu-Lieskovan, S.; Heidel, J. D.; Bartlett, D. W.; Davis, M. E.; Triche, T. J., *Cancer Res* **2005**,*65*, 8984-8992.
- (155) Bartlett, D. W.; Davis, M. E., *Biotechnol Bioeng* **2008**,*99*, 975-985.
- (156) Heidel, J. D.; Yu, Z. P.; Liu, J. Y. C.; Rele, S. M.; Liang, Y. C.; Zeidan, R. K.; Kornbrust, D. J.; Davis, M. E., *P Natl Acad Sci USA* **2007**,*104*, 5715-5721.
- (157) Davis, M. E.; Zuckerman, J. E.; Choi, C. H. J.; Seligson, D.; Tolcher, A.; Alabi, C. A.; Yen, Y.; Heidel, J. D.; Ribas, A., *Nature* **2010**,*464*, 1067-1070.
- (158) Harada, A.; Li, J.; Kamachi, M., *Nature* **1992**,*356*, 325-327.
- (159) Wenz, G.; Keller, B., *Angew. Chem.-Int. Edit. Engl.* **1992**,*31*, 197-199.
- (160) Tamura, M.; De, G.; Ueno, A., *Chemistry* **2001**,*7*, 1390-1397.
- (161) Cacialli, F.; Wilson, J. S.; Michels, J. J.; Daniel, C.; Silva, C.; Friend, R. H.; Severin, N.; Samori, P.; Rabe, J. P.; O'Connell, M. J.; Taylor, P. N.; Anderson, H. L., *Nat Mater* **2002**,*1*, 160-164.
- (162) Michels, J. J.; O'Connell, M. J.; Taylor, P. N.; Wilson, J. S.; Cacialli, F.; Anderson, H. L., *Chemistry* **2003**,*9*, 6167-6176.
- (163) Yang, C.; Wang, X.; Li, H. Z.; Goh, S. H.; Li, J., *Biomacromolecules* **2007**,*8*, 3365-3374.
- (164) Li, J.; Ni, X.; Leong, K. W., *J Biomed Mater Res A* **2003**,*65*, 196-202.
- (165) Li, J.; Li, X.; Ni, X.; Wang, X.; Li, H.; Leong, K. W., *Biomaterials* **2006**,*27*, 4132-40.
- (166) Yui, N.; Ooya, T.; Kumeno, T., *Bioconjug Chem* **1998**,*9*, 118-125.
- (167) Liu, Y.; Wang, H.; Chen, Y.; Ke, C. F.; Liu, M., *Journal of the American Chemical Society* **2005**,*127*, 657-666.

- (168) Li, J.; Yang, C.; Li, H. Z.; Wang, X.; Goh, S. H.; Ding, J. L.; Wang, D. Y.; Leong, K. W., *Advanced Materials* **2006**,*18*, 2969-2974.
- (169) Yui, N.; Katoono, R.; Yamashita, A., Functional Cyclodextrin Polyrotaxanes for Drug Delivery. In *Inclusion Polymers*, 2009; Vol. 222, pp 55-77.
- (170) Ooya, T.; Yui, N., *Crit Rev Ther Drug* **1999**,*16*, 289-330.
- (171) Yang, C.; Li, J., *Journal of Physical Chemistry B* **2009**,*113*, 682-690.
- (172) Loethen, S.; Kim, J. M.; Thompson, D. H., *Polym. Rev.* **2007**,*47*, 383-418.
- (173) Li, J.; Harada, A.; Kamachi, M., *Bull. Chem. Soc. Jpn.* **1994**,*67*, 2808-2818.
- (174) Harada, A.; Li, J.; Kamachi, M., *Macromolecules* **1993**,*26*, 5698-5703.
- (175) Fujita, H.; Ooya, T.; Yui, N., *Macromol. Chem. Phys.* **1999**,*200*, 706-713.
- (176) Fujita, H.; Ooya, T.; Yui, N., *Macromolecules* **1999**,*32*, 2534-2541.
- (177) Li, J.; Li, X.; Zhou, Z. H.; Ni, X. P.; Leong, K. W., *Macromolecules* **2001**,*34*, 7236-7237.
- (178) Mayer, B.; Klein, C. T.; Topchieva, I. N.; Kohler, G., *J. Comput.-Aided Mol. Des.* **1999**,*13*, 373-383.
- (179) Olson, K.; Chen, Y. Y.; Baker, G. L., *J. Polym. Sci. Pol. Chem.* **2001**,*39*, 2731-2739.
- (180) Ni, X. P.; Cheng, A.; Li, J., *Journal of Biomedical Materials Research Part A* **2009**,*88A*, 1031-1036.
- (181) Yang, C.; Yang, J. S.; Ni, X. P.; Li, J., *Macromolecules* **2009**,*42*, 3856-3859.
- (182) Yang, C.; Wang, X.; Li, H. Z.; Tan, E.; Lim, C. T.; Li, J., *Journal of Physical Chemistry B* **2009**,*113*, 7903-7911.
- (183) Cairo, C. W.; Gestwicki, J. E.; Kanai, M.; Kiessling, L. L., *Journal of the American Chemical Society* **2002**,*124*, 1615-1619.
- (184) Nelson, A.; Belitsky, J. M.; Vidal, S.; Joiner, C. S.; Baum, L. G.; Stoddart, J. F., *Journal of the American Chemical Society* **2004**,*126*, 11914-11922.
- (185) Ooya, T.; Mori, H.; Terano, M.; Yui, N., *Macromolecular Rapid Communications* **1995**,*16*, 259-263.
- (186) Watanabe, J.; Ooya, T.; Yui, N., *Journal of Biomaterials Science-Polymer Edition* **1999**,*10*, 1275-1288.
- (187) Moon, C.; Kwon, Y. M.; Lee, W. K.; Park, Y. J.; Yang, V. C., *Journal of Controlled Release* **2007**,*124*, 43-50.
- (188) Yang, C. A.; Li, H. Z.; Wang, X.; Li, J., *Journal of Biomedical Materials Research Part A* **2009**,*89A*, 13-23.
- (189) Ooya, T.; Yamashita, A.; Kurisawa, M.; Sugaya, Y.; Maruyama, A.; Yui, N., *Science and Technology of Advanced Materials* **2004**,*5*, 363-369.

- (190) Ooya, T.; Choi, H. S.; Yamashita, A.; Yui, N.; Sugaya, Y.; Kano, A.; Maruyama, A.; Akita, H.; Ito, R.; Kogure, K.; Harashima, H., *Journal of the American Chemical Society* **2006**,*128*, 3852-3853.
- (191) Yamashita, A.; Yui, N.; Ooya, T.; Kano, A.; Maruyama, A.; Akita, H.; Kogure, K.; Harashima, H., *Nature Protocols* **2006**,*1*, 2861-2869.
- (192) Yamashita, A.; Kanda, D.; Katoono, R.; Yui, N.; Ooya, T.; Maruyama, A.; Akita, H.; Kogure, K.; Harashima, H., *Journal of Controlled Release* **2008**,*131*, 137-144.
- (193) Xia, W.; Low, P. S., *Journal of medicinal chemistry* **2010**,*53*, 6811-6824.
- (194) Lambert, J. M., *Curr Opin Pharmacol* **2005**,*5*, 543-549.
- (195) Rao, A. V.; Schmader, K., *The American journal of geriatric pharmacotherapy* **2007**,*5*, 247-262.
- (196) Modjtahedi, H.; Essapen, S., *Anti-cancer drugs* **2009**,*20*, 851-855.
- (197) Garanger, E.; Boturyn, D.; Dumy, P., *Anti-cancer agents in medicinal chemistry* **2007**,*7*, 552-558.
- (198) Irache, J. M.; Salman, H. H.; Gamazo, C.; Espuelas, S., *Expert opinion on drug delivery* **2008**,*5*, 703-724.
- (199) Gupta, Y.; Kohli, D. V.; Jain, S. K., *Crit Rev Ther Drug Carrier Syst* **2008**,*25*, 347-379.
- (200) Low, P. S.; Kularatne, S. A., *Current opinion in chemical biology* **2009**,*13*, 256-262.
- (201) Carpenter, R. D.; Andrei, M.; Aina, O. H.; Lau, E. Y.; Lightstone, F. C.; Liu, R.; Lam, K. S.; Kurth, M. J., *Journal of medicinal chemistry* **2009**,*52*, 14-19.
- (202) Kularatne, S. A.; Wang, K.; Santhapuram, H. K.; Low, P. S., *Molecular pharmaceutics* **2009**,*6*, 780-789.
- (203) Antony, A. C., *Annual review of nutrition* **1996**,*16*, 501-521.
- (204) Lu, Y. J.; Low, P. S., *Adv Drug Deliver Rev* **2002**,*54*, 675-693.
- (205) Low, P. S.; Henne, W. A.; Doorneweerd, D. D., *Accounts of chemical research* **2008**,*41*, 120-129.
- (206) Parker, N.; Turk, M. J.; Westrick, E.; Lewis, J. D.; Low, P. S.; Leamon, C. P., *Analytical biochemistry* **2005**,*338*, 284-293.
- (207) Leamon, C. P.; Parker, M. A.; Vlahov, I. R.; Xu, L. C.; Reddy, J. A.; Vetzal, M.; Douglas, N., *Bioconjug Chem* **2002**,*13*, 1200-1210.
- (208) Leamon, C. P.; Reddy, J. A.; Vlahov, I. R.; Westrick, E.; Parker, N.; Nicoson, J. S.; Vetzal, M., *International journal of cancer. Journal international du cancer* **2007**,*121*, 1585-1592.
- (209) Leamon, C. P.; Reddy, J. A.; Vlahov, I. R.; Westrick, E.; Dawson, A.; Dorton, R.; Vetzal, M.; Santhapuram, H. K.; Wang, Y., *Molecular pharmaceutics* **2007**,*4*, 659-667.
- (210) Lu, Y.; Low, P. S., *Cancer immunology, immunotherapy : CII* **2002**,*51*, 153-162.



## Chapter 2. Literature Review

---

- (211) Wang, S.; Luo, J.; Lantrip, D. A.; Waters, D. J.; Mathias, C. J.; Green, M. A.; Fuchs, P. L.; Low, P. S., *Bioconjug Chem* **1997**,8, 673-679.
- (212) El-Aneed, A., *Journal of controlled release : official journal of the Controlled Release Society* **2004**,94, 1-14.
- (213) Zhao, X. B. B.; Lee, R. J., *Adv Drug Deliver Rev* **2004**,56, 1193-1204.
- (214) Lungwitz, U.; Breunig, M.; Blunk, T.; Gopferich, A., *Eur J Pharm Biopharm* **2005**,60, 247-266.
- (215) Guo, W. J.; Lee, R. J., *Aaps Pharmsci* **1999**,1, 20-26.
- (216) Bennis, J. M.; Maheshwari, A.; Furgeson, D. Y.; Mahato, R. I.; Kim, S. W., *J Drug Target* **2001**,9, 123-136.
- (217) Meng, F.; Hennink, W. E.; Zhong, Z., *Biomaterials* **2009**,30, 2180-2198.
- (218) Niculescu-Duvaz, I., *Curr Opin Mol Ther* **2000**,2, 691-696.
- (219) Muratovska, A.; Eccles, M. R., *Febs Lett* **2004**,566, 317-317.

## **CHAPTER 3 SOLUBILITY AND ANTITUMOR ACTIVITY OF INCLUSION COMPLEXES OF CYCLODEXTRIN-OLIGOETHYLENIMINES AND PACLITAXEL**

### **3.1. Introduction**

Paclitaxel (PTX) is a diterpenoid natural product isolated from *Taxus brevifolia* with potential activity against ovarian, breast, head and neck, and non-small-cell lung cancers.<sup>1,2</sup> PTX is an antimicrotubule agent that promotes the polymerization of tubulin. The formed microtubules under treatment of PTX are every stable and dysfunctional, resulting in cell death by disrupting the normal tubule dynamics that is required for cell division and vital interphase process.<sup>3-7</sup>

One of the major problems for PTX application is its low aqueous solubility.<sup>8</sup> PTX is administrated by injection or infusion with cremophor EL (polyoxyethylated castor oil) containing 50% absolute ethanol for clinical application. However, cremophor has been reported to cause severe hypersensitivity reactions and other side effects in animals and humans.<sup>9,10</sup> To circumvent the application of cremophor, many approaches include micelles,

emulsions, liposomes, microsphere nanoparticles, and cyclodextrins (CDs), etc. have been investigated.<sup>11, 12</sup>

CDs are a series of natural cyclic oligosaccharides composed of 6, 7, and 8 D(+)-glucose units connected by  $\alpha$ -1,4-linkages, named  $\alpha$ -,  $\beta$ -, and  $\gamma$ -CD, respectively. The hydrophobic cavity of CDs allows formation of inclusion complexes with poorly water soluble drugs to increase their solubility, dissolution, and bioavailability.<sup>13</sup> CDs can improve the drug bioavailability through the enhancement of membrane absorption and protection of biomolecules from non-specific interactions.<sup>14, 15</sup> For a variety of reasons, CDs can be chemically or enzymatically modified their hydroxyl groups to further improve their aqueous solubility and other physical properties.<sup>16, 17</sup> Some CD derivatives, such as (2-hydroxypropyl)- $\beta$ -CD (HP- $\beta$ -CD) can be administrated to humans with high dose.<sup>18, 19</sup>

Since the first CD-based product prostaglandin E<sub>2</sub>/ $\beta$ -CD (Prostarmon E<sup>TM</sup> sublingual tablets) was marketed in 1976, many CD-containing products are marketed as kinds of formulations.<sup>20, 21</sup> Inclusion complexes between cyclodextrin derivatives and PTX have already been greatly investigated in the last two decades. As the smaller cavity size for  $\alpha$ -CD (0.47 – 0.53 nm), it cannot form stable inclusion complex with PTX.<sup>22</sup> The naturally  $\beta$ - and  $\gamma$ -CD showed 12-fold and 50-fold increase of PTX solubility, which was too low for administration. Sharma and co-workers investigated inclusion complexation between PTX and HP- $\beta$ -CD, hydroxyethyl- $\beta$ -CD (HE- $\beta$ -CD), dimethyl- $\beta$ -CD (DM- $\beta$ -CD), HP- $\gamma$ -CD, and so on, indicating 2000-fold or more increase of PTX solubility and maintain its cytostatic properties. However, the solubility of PTX was determined by the concentration of CD and high viscous was observed at high concentration. Moreover, these inclusion complexes were mostly not stable in aqueous solution and precipitation occurred upon dilution.<sup>23</sup> DM- $\beta$ -CD has also been proved to be one of the most effect solubilizers for PTX delivery with satisfactory antitumor activity by other

researchers.<sup>24-30</sup> Uncomplexed DM- $\beta$ -CD and HP- $\beta$ -CD had a maximum tolerated dose (MTD) at doses of 2 g and 5 g CD/kg body weight respectively, and studies showed that the applications of taxane formulation need to reduce the toxicity of the CD carriers.<sup>23</sup> Moser and Liu's groups investigated  $\beta$ -CD dimers for delivery of PTX that illustrated high water solubility, high thermal stability, and high antitumor activity.<sup>31-34</sup> However, the synthesis and purification of the  $\beta$ -CD dimers is difficult which may limit their applications.

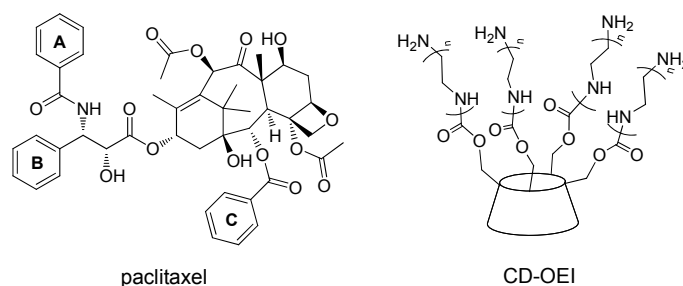


**Figure 3.1.** Illustrated structure of paclitaxel and OEI-grafted cyclodextrins.

Herein, we report the convenient structure modification of  $\alpha$ -,  $\beta$ -, and  $\gamma$ -CD by different lengths of oligoethylenimine (abbreviated as CD-OEI, Figure 3.1) to further improve their water solubility and encapsulation ability. Moreover, the antitumor activity of the CD-OEI/PTX inclusion complexes was studied.

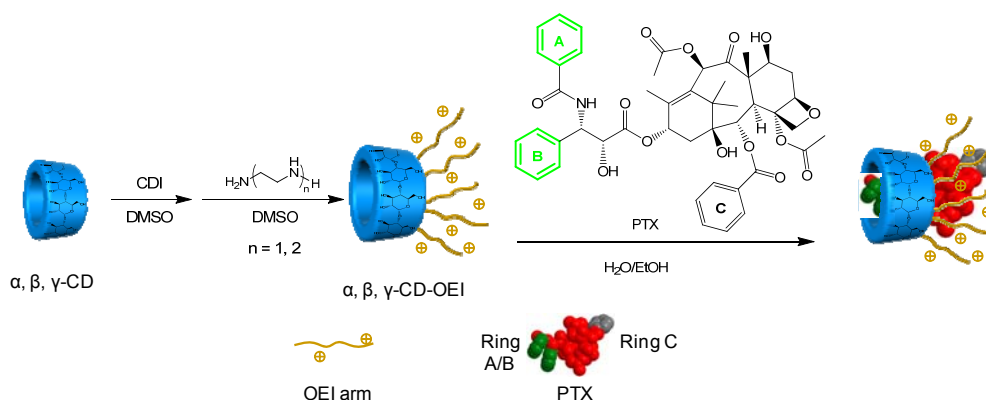
## 3.2. Experimental Section

### 3.2.1. Materials

$\alpha$ -,  $\beta$ -,  $\gamma$ -CD, and 1,1'-carbonyldiimidazole (CDI) were purchased from Tokyo Chemical Industry Co. Ltd (Tokyo, Japan). Paclitaxel (PTX) was purchased from LC Laboratories Ltd (MA, USA). Ethylenediamine (OEI-1), bis(2-aminoethyl)amine (OEI-2), and dimethyl sulfoxide (DMSO) were purchased from Sigma-Aldrich. D<sub>2</sub>O used as solvents in the NMR measurement was obtained from Cambridge Isotope Laboratories, Inc. (Andover, U.S.A.). 3-(4,5-Dimethyl-thiazol-2-yl)-2,5-diphenyl tetrazodium bromide (MTT) was obtained from Alfa Aesar (MA, U.S.A.).

## 3.2.2. Synthesis

The synthesis procedures of  $\alpha$ -,  $\beta$ -, and  $\gamma$ -CD-OEI derivatives and their inclusion complexes with PTX are shown in Scheme 3.1. The following describes the detailed synthesis of  $\gamma$ -CD-OEI-2 and  $\gamma$ -CD-OEI-2/PTX as typical examples.



**Scheme 3.1.** Synthesis of  $\alpha$ -,  $\beta$ -, and  $\gamma$ -CD-OEI/PTX inclusion complexes

*N*-(2-aminoethyl)-2-aminoethyl-carbamoyl- $\gamma$ -cyclodextrin ( $\gamma$ -CD-OEI-2):

To a solution of CDI (1.3 g, 8.0 mmol) in anhydrous DMSO (15 mL) was added dropwise a solution of  $\gamma$ -CD (650 mg, 0.5 mmol) in anhydrous DMSO (10 mL) during 30 min. After stirring for 4 hours, the solution was added dropwise into a mixture of THF/Et<sub>2</sub>O (100 mL/200 mL). The white precipitate was collected by centrifuge and dissolved into 20 mL of fresh anhydrous DMSO. Then the solution was added immediately by dropwise into a solution of ethylenediamine (960 mg, 16 mmol) in DMSO (10 mL) during 30 min. The mixture was then stirred at room temperature for an additional 1 day. The mixture was added into Et<sub>2</sub>O (160 mL) and the white precipitate was collected. Further purification by sephadex G50 column with water as eluent, freeze dried for 2 days at  $-87^{\circ}\text{C}$  and 0.25 mbar to yield a white solid (yield, 88%). <sup>1</sup>H NMR: (400 MHz, D<sub>2</sub>O):  $\delta$  5.03 (brs, 8 H, H-1 of  $\gamma$ -CD), 2.98 – 4.56 (m, 61 H, H2-6 of  $\gamma$ -CD, -OCONHCH<sub>2</sub>-), 2.34 – 2.98 (m, 40 H, -CH<sub>2</sub>CH<sub>2</sub>N-).

2-Aminoethyl-carbamoyl- $\alpha$ -CD ( $\alpha$ -CD-OEI-1): white solid (yield, 85%).

<sup>1</sup>H NMR: (400 MHz, D<sub>2</sub>O):  $\delta$  4.98 (s, 6 H, H-1 of  $\alpha$ -CD), 2.85 – 4.55 (m, 46

H, H2-6 of  $\alpha$ -CD, -OCONHCH<sub>2</sub>- of amine), 2.50 – 2.85 (m, 10.4 H, -CH<sub>2</sub>CH<sub>2</sub>NH-).

*N*-(2-aminoethyl)-2-aminoethyl-carbamoyl- $\alpha$ -cyclodextrin ( $\alpha$ -CD-OEI-2): white solid (yield, 81%). <sup>1</sup>H NMR: (400 MHz, D<sub>2</sub>O):  $\delta$  5.15 (s, 6 H, H-1 of  $\alpha$ -CD), 2.87 – 4.52 (m, 46 H, H2-6 of  $\alpha$ -CD, -OCONHCH<sub>2</sub>- of amine), 2.40 – 2.87 (m, 31 H, -CH<sub>2</sub>CH<sub>2</sub>NH-).

2-Aminoethyl-carbamoyl- $\beta$ -CD ( $\beta$ -CD-OEI-1): white solid (yield, 90%). <sup>1</sup>H NMR: (400 MHz, D<sub>2</sub>O):  $\delta$  4.99 (brs, 7 H, H-1 of  $\beta$ -CD), 2.90 – 4.57 (m, 52 H, H2-6 of  $\beta$ -CD, -OCONHCH<sub>2</sub>-), 2.64 – 2.85 (m, 10 H, -CH<sub>2</sub>NH<sub>2</sub>).

*N*-(2-aminoethyl)-2-aminoethyl-carbamoyl- $\beta$ -cyclodextrin ( $\beta$ -CD-OEI-2): white solid. (yield, 82%) <sup>1</sup>H NMR: (400 MHz, D<sub>2</sub>O):  $\delta$  4.99 (brs, 7 H, H-1 of  $\beta$ -CD), 2.87 – 4.57 (m, 54 H, H2-6 of  $\beta$ -CD, -OCONHCH<sub>2</sub>-), 2.30 – 2.87 (m, 38 H, -CH<sub>2</sub>CH<sub>2</sub>NH-).

2-Aminoethyl-carbamoyl- $\gamma$ -CD ( $\gamma$ -CD-OEI-1): white solid (yield, 84%). <sup>1</sup>H NMR: (400 MHz, D<sub>2</sub>O):  $\delta$  5.02 (brs, 8 H, H-1 of  $\gamma$ -CD), 2.87 – 4.55 (m, 64 H, H2-6 of  $\gamma$ -CD, -OCONHCH<sub>2</sub>-), 2.69 (brs, 16 H, -CH<sub>2</sub>CH<sub>2</sub>N-).

$\gamma$ -CD-OEI-2/PTX: To a solution of  $\gamma$ -CD-OEI-2 (22 mg, 0.01 mmol) in H<sub>2</sub>O (0.5 mL) was added a solution of PTX (8.5 mg, 0.01 mmol) in ethanol (0.5 mL). The mixture was stirred at room temperature for 5 days under dark, and then centrifuged to remove the insoluble PTX. After evaporating the solvent to around 0.5 mL under vacuum by a rotary evaporator, the residue was centrifuged again to remove the precipitate and freeze dried for 2 d at –87 °C and 0.25 mbar to yield 25 mg of white solid (yield, 94%). <sup>1</sup>H NMR: (400 MHz, D<sub>2</sub>O):  $\delta$  7.20 – 8.15 (m, 9 H, ArH of PTX), 4.85 – 5.65 (m, 12 H, H-1 of  $\gamma$ -CD, H of PTX), 3.05 – 4.50 (m, 65 H, H2-6 of  $\gamma$ -CD, -CONHCH<sub>2</sub>- of OEI, H of PTX), 2.42 – 3.05 (s, 40 H, -CH<sub>2</sub>CH<sub>2</sub>NH- of OEI), 1.20 – 2.40 (m, 9 H, H of PTX).

$\alpha$ -CD-OEI-1/PTX, white solid (yield, 97%).  $^1\text{H}$  NMR: (400 MHz,  $\text{D}_2\text{O}$ ):  $\delta$  7.20 – 8.13 (m, 0.7 H, ArH of PTX), 4.86 – 5.42 (m, 7.5 H, H-1 of  $\alpha$ -CD, H of PTX), 2.98 – 4.53 (m, 48 H, H2-6 of  $\alpha$ -CD, -CONHCH<sub>2</sub>- of OEI, H of PTX), 2.56 – 2.98 (s, 10.4 H, -CH<sub>2</sub>CH<sub>2</sub>NH- of OEI), 1.12 – 2.40 (m, 1 H, H of PTX).

$\alpha$ -CD-OEI-2/PTX, white solid (yield, 95%).  $^1\text{H}$  NMR: (400 MHz,  $\text{D}_2\text{O}$ ):  $\delta$  7.15 – 8.11 (m, 1.4 H, ArH of PTX), 4.82 – 5.64 (m, 8.6 H, H-1 of  $\alpha$ -CD, H of PTX), 2.98 – 4.55 (m, 52 H, H2-6 of  $\alpha$ -CD, -CONHCH<sub>2</sub>- of OEI, H of PTX), 2.40 – 2.98 (s, 31 H, -CH<sub>2</sub>CH<sub>2</sub>NH- of OEI), 1.12 – 2.40 (m, 2.5 H, H of PTX).

$\beta$ -CD-OEI-1/PTX, white solid (yield, 97%).  $^1\text{H}$  NMR: (400 MHz,  $\text{D}_2\text{O}$ ):  $\delta$  7.19 – 8.15 (m, 4.9 H, ArH of PTX), 4.81 – 5.68 (m, 11 H, H-1 of  $\beta$ -CD, H of PTX), 2.97 – 4.52 (m, 56 H, H2-6 of  $\beta$ -CD, -CONHCH<sub>2</sub>- of OEI, H of PTX), 2.66 – 2.97 (s, 10 H, -CH<sub>2</sub>CH<sub>2</sub>NH- of OEI), 1.12 – 2.40 (m, 4 H, H of PTX).

$\beta$ -CD-OEI-2/PTX, white solid. (yield, 94%)  $^1\text{H}$  NMR: (400 MHz,  $\text{D}_2\text{O}$ ):  $\delta$  7.20 – 8.15 (m, 7 H, ArH of PTX), 4.83 – 5.68 (m, 12 H, H-1 of  $\beta$ -CD, H of PTX), 2.92 – 4.52 (m, 58 H, H2-6 of  $\beta$ -CD, -CONHCH<sub>2</sub>- of OEI, H of PTX), 2.46 – 2.92 (s, 40 H, -CH<sub>2</sub>CH<sub>2</sub>NH- of OEI), 1.12 – 2.40 (m, 7 H, H of PTX).

$\gamma$ -CD-OEI-1/PTX, white solid (yield, 96%).  $^1\text{H}$  NMR: (400 MHz,  $\text{D}_2\text{O}$ ):  $\delta$  7.20 – 8.20 (m, 5 H, ArH of PTX), 4.88 – 5.67 (m, 12 H, H-1 of  $\gamma$ -CD, H of PTX), 3.08 – 4.50 (m, 68 H, H2-6 of  $\gamma$ -CD, -CONHCH<sub>2</sub>- of OEI, H of PTX), 2.40 – 3.07 (s, 16 H, -CH<sub>2</sub>CH<sub>2</sub>NH- of OEI), 1.20 – 2.40 (m, 6 H, H of PTX).

**Fluorescence Labeling:** The general synthesis procedure of rhodamine-grafted  $\gamma$ -CD-OEI-2 ( $\gamma$ -CD-OEI-2-rhd) is as follows. To a solution of  $\gamma$ -CD-OEI-2 (22 mg, 10  $\mu\text{mol}$ ) in anhydrous DMSO (1 mL) was added rhodamine B (7 mg, 15  $\mu\text{mol}$ ), DCC (4 mg, 20  $\mu\text{mol}$ ), and DMAP (5%). The mixture was then stirred at room temperature for 1 day under dark. Purification by dialysis (MWCO, 1000) against water under dark for 5 days until no pink dye was observed. The mixture was freeze dried to yield a red solid as product.

*PTX Labeling:* The detailed synthetic method for PTX-FITC was followed previous report.<sup>35</sup> The synthesized fluorescent PTX is bioactive and modification of 7-position will not influence the formation of inclusion complex with CD ring.

#### 3.2.3. NMR Spectroscopy.

The <sup>1</sup>H and <sup>13</sup>C NMR spectra were recorded on a Bruker AV-400 NMR spectrometer at 400.1 and 100.6 MHz at room temperature, respectively. The <sup>1</sup>H NMR measurements were carried out with an acquisition time of 3.2 s, a pulse repetition time of 2.0 s, a 30° pulse width, 5208 Hz spectral width, and 32 K data points. Chemical shifts were referenced to the solvent peak ( $\delta = 4.70$  ppm for D<sub>2</sub>O,  $\delta = 2.50$  ppm for DMSO-*d*<sub>6</sub>).

The encapsulated PTX in the inclusion complex was calculated by <sup>1</sup>H NMR by comparing the integration of PTX aromatic signal and OEI ethylene peaks. The PTX loading efficiency was calculated using the following equation:

$$PTX\text{ loading efficiency} = \frac{\text{Amount of PTX}}{\text{Amount of PTX} + \text{Polymer}} \times 100\% \quad (1)$$

#### 3.2.4. UV-Vis Spectroscopy

All absorption spectra were recorded on a Shimadzu UV 2501 spectrophotometer. 1 mL of aqueous solution containing  $\alpha$ -,  $\beta$ -,  $\gamma$ -CD-OEI-2 and  $\alpha$ -,  $\beta$ -,  $\gamma$ -CD-OEI-2/PTX on a concentration of 0.2 mg/mL were transferred into quartz cuvettes for the measurement.

#### 3.2.5. Fourier Transform Infrared Spectroscopy

Fourier transform infrared (FTIR) spectra of the  $\gamma$ -CD-OEI-2, PTX, and  $\gamma$ -CD-OEI-2/PTX inclusion complex in potassium bromide (KBr) were measured on a Perkin-Elmer FTIR 2000 spectrometer in the region of 4000 – 400 cm<sup>-1</sup>.



### 3.2.6. Solubility Test

The general procedure for solubility test is as follows. To a 100  $\mu$ L of DI water was added the CD-OEI polymer or CD-OEI/PTX inclusion complex to prepare over-saturated solution. The mixture was centrifuged to precipitate the insoluble solid. Then 50  $\mu$ L of supernatant was extracted, freeze dried, and the maximum solubility was calculated by weight.

### 3.2.7. Stability Test

The physical stability of CD-OEI/PTX inclusion complexes was evaluated as follows. A solution of 1 mL (3 mg/mL) CD-OEI/PTX inclusion complex was distributed into sealed glass tube and incubated at 25 °C. At suitable intervals, 100  $\mu$ L of solution was extracted and diluted into 1 mL solution with DI water. The absorptions of CD-OEI/PTX were measured by UV spectroscopy at 230 nm.

In order to determine the concentrations of CD-OEI/PTX, a linear correlation of concentration – absorbance standard curve was drawn by measuring the absorption of  $\beta$ -CD-OEI-2/PTX (11.6% PTX according to  $^1\text{H}$  NMR) at 230 nm which the concentration changes from 0.01 to 0.8 mg/mL. Therefore, the concentrations of CD-OEI/PTX can be calculated according to the PTX absorbance at 230 nm and the drug loading efficiency obtained by  $^1\text{H}$  NMR and equation 1.

### 3.2.8. Confocal Microscopy

Confocal microscopy was used to evaluate the cellular uptake of PTX-7-FITC,  $\gamma$ -CD-OEI-2-rhd, and  $\gamma$ -CD-OEI-2-rhd/PTX-7-FITC in HeLa cells. In brief, a density of  $1.2 \times 10^4$ /well HeLa cells in 0.3 mL of DMEM medium were seeded onto a Lab-Tekfour-chambered coverglass system (Nalge-Nane International, Naperville, IL). After 24 h, fresh medium with 2  $\mu$ M of polymer was replaced. After incubation for 2 h, the medium was replaced with 0.3 mL of DMEM medium and imaged using an Olympus

Fluoview FV500 confocal laser scanning microscope (Olympus, Japan). Green fluorescence was excited by 488 nm laser line and detected using a 515 nm filter. The excitation wavelength for red fluorescence was set at 559 nm with an emission at 575 to 675 nm.

#### 3.2.9. Cell Viability Assay

All cell lines were purchased from ATCC (Rockville, MD). HeLa and MCF-7 cells were cultured in Dulbecco's Modified Eagle's Medium (DMEM) supplemented with 10% heat-inactivated fetal bovine serum, 100 units/mg penicillin, 100 µg/mL streptomycin at 37 °C and 5% CO<sub>2</sub>. DMEM medium was purchased from Gibco BRL (Gaithersburg, MD).

HeLa and MCF-7 cells were cultured in DMEM medium supplemented with 10% FBS. 100 µL of medium with a density of  $1 \times 10^5$  cells/mL were seeded into 96-well plates (NUNC, Wiesbaden, Germany). After 24 hours, culture media were replaced with fresh DMEM medium containing serial dilutions of polymers, in which the cells were cultured for an additional 20 hours or 44 hours. Then 10 µL of sterile filtered MTT (5 mg/mL) stock solution in PBS was added to each well, reaching a final MTT concentration of 0.5 mg/mL. After 4 h, unreacted dye was removed by aspiration. The formazan crystals were dissolved in 100 µL/well DMSO and the absorbance was measured using a microplate reader (Spectra Plus, TECAN) at a wavelength of 570 nm. Four wells were treated together as a group. The relative cell growth (%) related to control cells cultured in media without polymer was calculated by  $[A]_{\text{test}}/[A]_{\text{control}} \times 100\%$ . The IC<sub>50</sub> value represents the concentration of polymer at which 50% reduction of cell growth was calculated.

### 3.3. Results and Discussions

The application of natural CDs usually limits by their low aqueous solubility and thus the formation of inclusion complexes with hydrophobic

molecules would be influenced, especially for  $\beta$ -CD. Generally, CD derivatives for pharmaceutical usage mainly include introduction of hydroxypropyl groups, methyl groups, and maltosyl groups.

In our research, OEI chains with different lengths were linked into cyclodextrin rings, which illustrated significantly increase of water solubility and their capability to form inclusion complexes with anticancer drug PTX.

### 3.3.1. Synthesis of CD-OEI/PTX Inclusion Complexes

Scheme 3.1 shows the synthesis procedure of CD-OEI/PTX inclusion complexes. The 6-hydroxyl group from glucose units of CD exhibits high reactivity, which can be activated by CDI and then substituted by OEI with different ethylenediamine units to prepare OEI-grafted CD. Two methods were used to avoid the cross-linking between CDs. First, the CDI-activated intermediates were purified by precipitation under THF/Et<sub>2</sub>O. Second, slowly addition of CDI-modified CD derivatives into large excess of OEI solutions can reduce the cross-linking reaction.

**Table 3.1.** Solubility of  $\alpha$ -,  $\beta$ -,  $\gamma$ -CD-OEIs at 25 °C

Sample	Glucose Units	NHCH <sub>2</sub> CH <sub>2</sub> . repeat units	OEI arms	Solubility		Enhancement Factor*
				(mg/mL)	(mM)	
$\alpha$ -CD-OEI-1	6	1	5.2	468	329	3
$\alpha$ -CD-OEI-2	6	2	5.2	586	356	4
$\beta$ -CD-OEI-1	7	1	5.0	410	261	22
$\beta$ -CD-OEI-2	7	2	6.3	460	235	25
$\gamma$ -CD-OEI-1	8	1	11.0	500	222	2
$\gamma$ -CD-OEI-2	8	2	7.0	580	263	3

\* Solubility of  $\alpha$ -,  $\beta$ -,  $\gamma$ -CD is 145, 18.5, and 232 mg/mL, respectively.

PTX formed inclusion complexes with the CD-OEIs *via* physical interaction in a mixture of water/ethanol for several days under dark. Table 3.1 illustrates the detailed structure and included PTX for each molecule. The

encapsulation ability followed the order of  $\alpha$ -CD <  $\beta$ -CD <  $\gamma$ -CD corresponding to their cavity size. Moreover, longer OEI chain and more substituted arms benefit to the formation of inclusion complex.

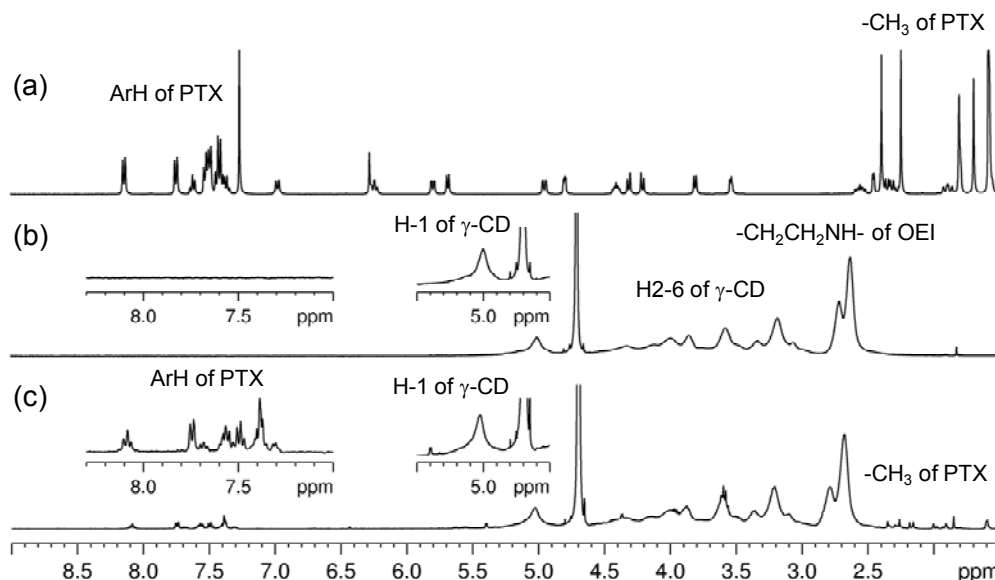


**Figure 3.2.**  $^1\text{H}$  NMR spectra of PTX in  $\text{CDCl}_3$  (a),  $\gamma$ -CD-OEI-2 (b), and  $\gamma$ -CD-OEI-2/PTX (c) in  $\text{D}_2\text{O}$ .

As shown in Figure 3.2,  $^1\text{H}$  NMR provides direct evidence for the formation of inclusion complexes between  $\gamma$ -CD-OEI-2 and PTX. Generally, PTX has no signal in  $^1\text{H}$  NMR using  $\text{D}_2\text{O}$  as solvent due to its extremely low water solubility. Therefore, the aryl signal in the spectra derived from PTX provided strong support for the formation of inclusion complex. The stoichiometry information can also be obtained according to integration between aryl area ( $\delta$  7.2 – 8.2 ppm) derived from PTX and ethylene signal ( $\delta$  2.42 – 3.05 ppm) derived from  $\gamma$ -CD-OEI. Similarly, the number of included PTX with other CD-OEI carriers was also calculated according to their  $^1\text{H}$  NMR data. We found that even  $\alpha$ -CD-OEI can help to solubilize PTX with satisfactory enhancement that is rarely reported, because the general opinion is that the  $\alpha$ -CD ring is too small to form inclusion complex with PTX.

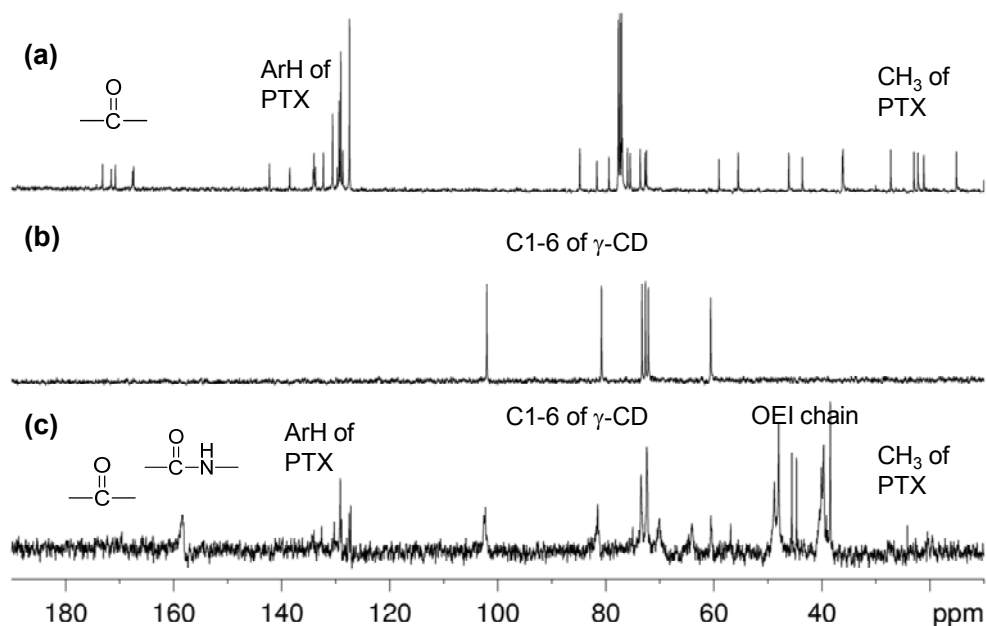


**Figure 3.3.**  $^{13}\text{C}$  NMR spectra of PTX in  $\text{CDCl}_3$  (a),  $\gamma\text{-CD}$  (b), and  $\gamma\text{-CD-OEI-2/PTX}$  (c) in  $\text{D}_2\text{O}$ .

$^{13}\text{C}$  NMR spectrum of  $\gamma\text{-CD-OEI-2/PTX}$  was shown in Figure 3.3. The peak at  $\delta$  158.3 ppm is the urethane groups linked to the OEI chains, and the peaks at 37.5 – 50.0 ppm correspond to the OEI chains. Signals of  $\gamma\text{-CD}$  core can be found at chemical shift 102.5, 81.5, 73.5, 72.4, and 60.5. Furthermore, the peaks at  $\delta$  125.0 – 140.0 demonstrate the aromatic rings from PTX. The  $^{13}\text{C}$  NMR data further proved the successful formation of inclusion complex.

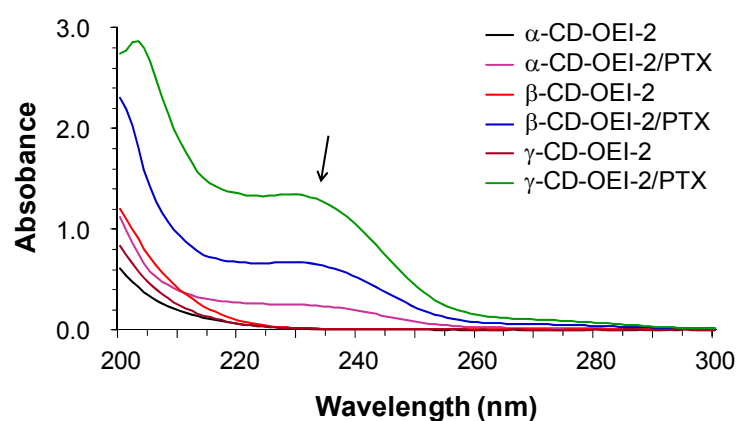


**Figure 3.4.** UV-Visible spectra of  $\alpha$ -,  $\beta$ -,  $\gamma\text{-CD-OEI-2}$  and  $\alpha$ -,  $\beta$ -,  $\gamma\text{-CD-OEI-2/PTX}$  on a concentration of 0.2 mg/mL in  $\text{H}_2\text{O}$ . The arrow indicates UV absorption of PTX at 230 nm.

UV-Vis spectroscopy was used to further confirm the formation of inclusion complexes. PTX aqueous solution also showed almost no absorption signal in UV-Vis spectroscopy because of its low solubility in water. In contrast, the inclusion complex of  $\alpha$ -,  $\beta$ -, and  $\gamma$ -CD-OEI-2/PTX illustrated strong absorption at  $\lambda = 230$  nm (Figure 3.4), indicating the typical signal of PTX. As shown in Figure 3.5, FT-IR spectroscopy illustrated that the C=O stretching vibration is shifted from  $1732\text{ cm}^{-1}$  in PTX to  $1704\text{ cm}^{-1}$  in the  $\gamma$ -CD-OEI-2/PTX inclusion complexes. The IR result is similar as previous reported data.<sup>33</sup>

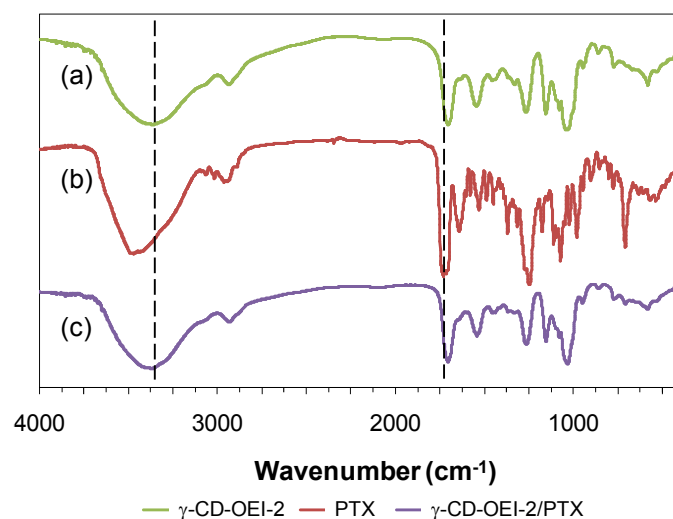


**Figure 3.5.** FT-IR spectra of  $\gamma$ -CD-OEI-2 (a), PTX (b), and  $\gamma$ -CD-OEI-2/PTX inclusion complex (c).

### 3.3.2. Water Solubility and Stability

$\beta$ -CD has lower water solubility (18.5 g/L) than  $\alpha$ -, and  $\gamma$ -CD (145 and 232 g/L), which also influence the solubility of CD/drug inclusion complexes. As shown in Table 3.1, structure modification with OEIs significantly increased the water solubility of  $\beta$ -CD to more than 20 folds, and longer OEI chain will further increase the solubility. After conjugation with OEI arms with  $\alpha$ -, and  $\gamma$ -CD, the solubility was increased as 2 – 4 folds.

**Table 3.2.** Water solubility of CD-OEI/PTX inclusion complexes at 25 °C

Samples	Solubility (mg/mL)	PTX Included*	PTX (mM)	CDs (mM)	Enhancement Factor	References
PTX	$3.5 \times 10^{-4}$	-	$4.1 \times 10^{-4}$	-	1.0	23
$\alpha$ -CD-OEI-1/PTX	208	$4.0 \times 10^{-2}$	5.7	123.3	$1.4 \times 10^4$	
$\alpha$ -CD-OEI-2/PTX	220	0.1	12.7	126.9	$3.1 \times 10^4$	
$\beta$ -CD-OEI-1/PTX	86	0.2	9.9	49.4	$2.4 \times 10^4$	
$\beta$ -CD-OEI-2/PTX	104	0.3	14.1	47.1	$3.4 \times 10^4$	
$\gamma$ -CD-OEI-1/PTX	220	0.3	26.3	87.6	$6.4 \times 10^4$	
$\gamma$ -CD-OEI-2/PTX	230	0.6	50.7	84.6	$1.2 \times 10^5$	
HP- $\beta$ -CD/PTX	-	$1.3 \times 10^{-3}$	$7.8 \times 10^{-3}$	6.0	19.5	25
DM- $\beta$ -CD/PTX	-	$8.2 \times 10^{-3}$	$4.9 \times 10^{-2}$	6.0	$1.2 \times 10^2$	25

\* The included PTX means number of PTX in one CD-OEI/PTX inclusion complex that is calculated by  $^1\text{H}$  NMR.

Table 3.2 illustrated the enhanced solubility of PTX by CD-OEIs. The recommended administrated concentration of PTX is 0.7 – 1.4 mM.<sup>36</sup> Our CD-OEI carriers can easily come up to the standard.  $\alpha$ -CD-OEI-1 and  $\alpha$ -CD-OEI-2 can also encapsulate up to 6 and 13 mM of PTX, respectively. In addition, the maximum PTX concentration in the formulation of  $\beta$ -CD-OEI-1/PTX and  $\beta$ -CD-OEI-2/PTX was 10 and 14 mM, respectively, which showed 24099-fold and 34430-fold higher than the pure PTX. Among of them,  $\gamma$ -CD-OEI-2 has the largest drug loading capacity that encapsulates 51 mM PTX (123772-fold higher water solubility than pure PTX). In comparison, these synthesized CD-OEI derivatives illustrated significantly higher encapsulation of PTX than previous reported CD derivatives, such as random HP- $\beta$ -CD (19-fold), DM- $\beta$ -CD (120-fold), and so on.<sup>25</sup>

A standard curve was drawn by determining the absorbance values of the difference concentrations of  $\beta$ -CD-OEI-2/PTX at 230 nm. It was calculated the following equation, where  $y$  is the absorbance values, and  $x$  is the concentration of  $\beta$ -CD-OEI-2/PTX. The calibration curve was linear under the concentration ranging from 0.01 to 0.8 mg/mL with a correlation coefficient of

$R^2 = 0.0098$ . Moreover, the concentrations of CD-OEI/PTX can be calculated using equation 1 and 2.

$$y = 3.2767x + 0.0085 \quad (2)$$

The stability test showed that the CD-OEI/PTX inclusion complexes were stable in aqueous solution. As displayed in Figure 3.6, after storage at 25 °C from 2 h to 72 h, no PTX precipitate was observed in the tube for all the inclusion complexes and their PTX content had almost no change.

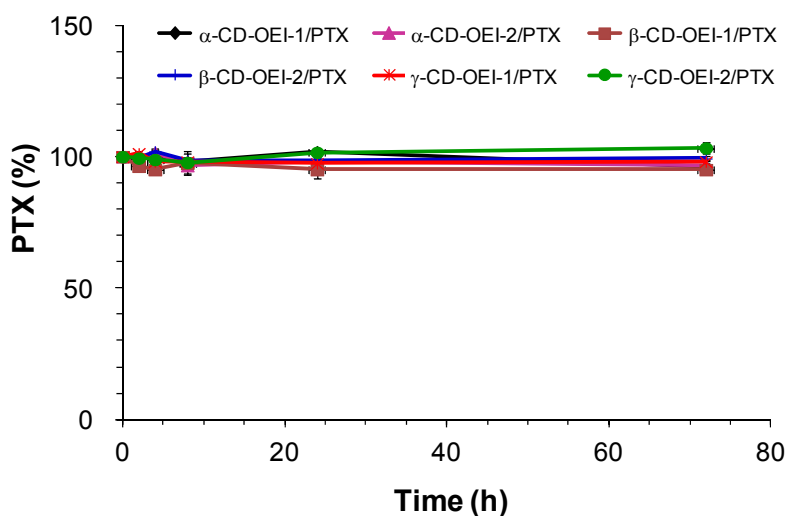


**Figure 3.6.** Stability of  $\alpha$ -,  $\beta$ -,  $\gamma$ -CD-OEI-1/PTX and  $\alpha$ -,  $\beta$ -,  $\gamma$ -CD-OEI-2/PTX in aqueous solution with a concentration of 3 mg/mL from 2 to 72 hours at 25 °C.

### 3.3.3. Cellular Uptake Test

Figure 3.7 shows the cellular uptake of PTX-7-FITC,  $\gamma$ -CD-OEI-2-rhd, and  $\gamma$ -CD-OEI-2-rhd/PTX-7-FITC in Hela cells after treating polymers for 2 h. Directly administration of FITC-conjugated PTX showed relative low cellular uptake. In contrast, the red fluorescence stained  $\gamma$ -CD-OEI-2 showed very strong signals that illustrated very high cellular uptake, which renders these CD-OEIs to be potential drug delivery carriers. Moreover, green fluorescence was found in the whole cell including nucleus area when the cells were treated



with the inclusion complexes  $\gamma$ -CD-OEI-2-rhd/PTX-7-FITC for 2 h that indicated obvious drug release (Figure 3.7c, merged image).

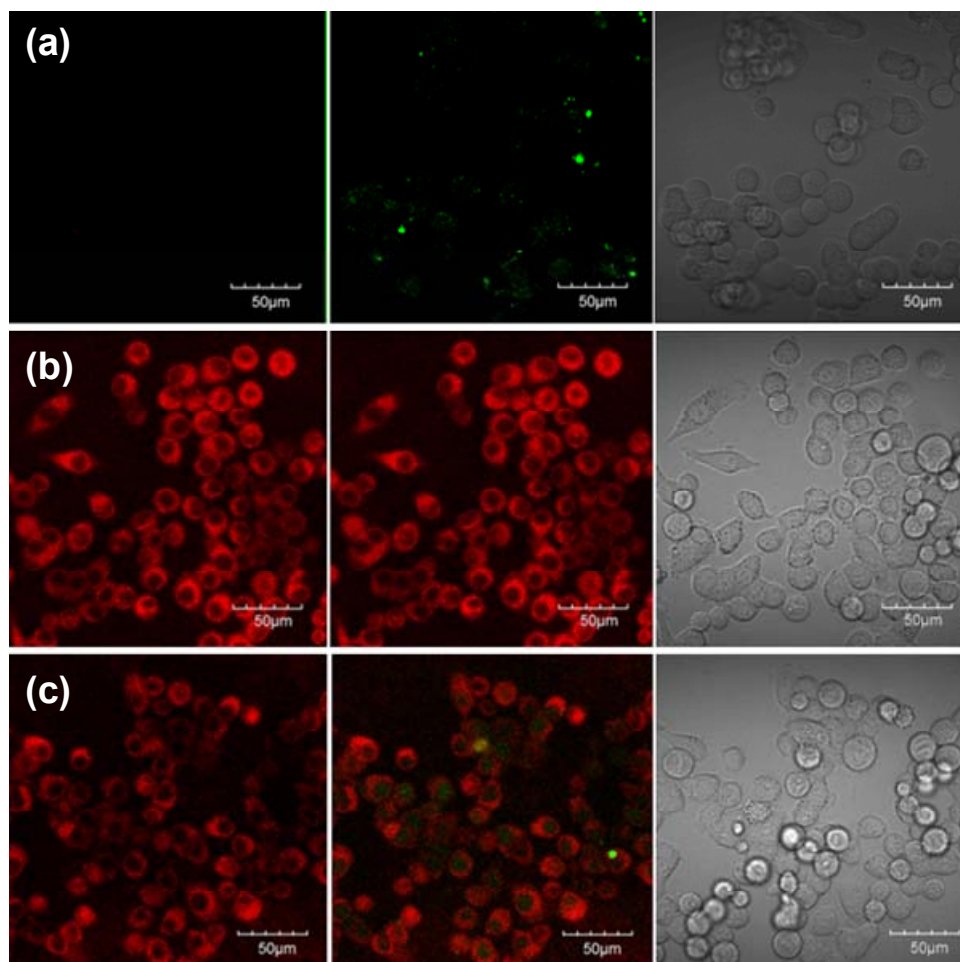


**Figure 3.7.** Confocal microscopy images of PTX-7-FITC (a),  $\gamma$ -CD-OEI-2-rhodamine (b), and  $\gamma$ -CD-OEI-2-rhodamine/PTX-7-FITC (c) in HeLa cells. The same field of cells was observed by red fluorescent image (left), red and green merged image (middle), and bright field (right).

#### 3.3.4. Cell Viability Test

The antitumor assay for the CD-OEI/PTX inclusion complexes was tested *in vitro* by the MTT assay using CD-OEI carriers and free PTX as reference compounds. As shown in Figure 3.8a and 3.8c, there is almost no cytotoxicity for all the CD-OEI derivatives when the concentration is 100 – 800  $\mu\text{g/mL}$  in HeLa and MCF-7 cells. Generally,  $\gamma$ -CD-OEI/PTX illustrated higher cytotoxicity activity in comparison with  $\alpha$ -, and  $\beta$ -CD-OEI/PTX under the

same concentration due to their high drug loading efficiency (Figure 3.8b and 3.8d). Although all the inclusion complexes illustrated PTX-induced cytotoxicity, their  $IC_{50}$  are still lower than the PTX in cremophor ( $IC_{50} = 5.1$  and  $17.6 \mu\text{g/mL}$  in Hela and MCF-7 cells) in Hela and MCF-7 cells after treatment of 48 hours.

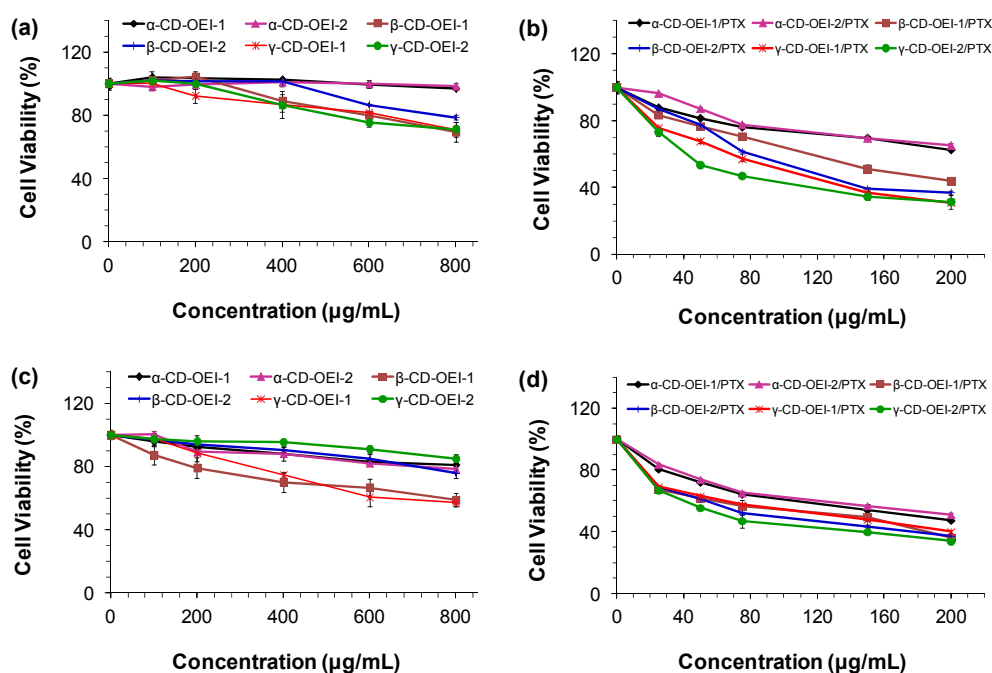


**Figure 3.8.** Cell viability assay of  $\alpha$ -CD-OEI-1,  $\alpha$ -CD-OEI-2,  $\beta$ -CD-OEI-1,  $\beta$ -CD-OEI-2,  $\gamma$ -CD-OEI-1,  $\gamma$ -CD-OEI-2 in Hela (a) and MCF-7 cells (c), and  $\alpha$ -CD-OEI-1/PTX,  $\alpha$ -CD-OEI-2/PTX,  $\beta$ -CD-OEI-1/PTX,  $\beta$ -CD-OEI-2/PTX,  $\gamma$ -CD-OEI-1/PTX,  $\gamma$ -CD-OEI-2/PTX in Hela (b) and MCF-7 cells (d) at various concentrations for 48 hours in DMEM medium. Data represent mean  $\pm$  standard deviation ( $n = 4$ ).

### 3.4. Conclusions

In this study, a series of short chain OEI grafted  $\alpha$ -,  $\beta$ -, and  $\gamma$ -CDs were synthesized. The structures were confirmed by  $^1\text{H}$  NMR,  $^{13}\text{C}$  NMR, UV, and FT-IR spectroscopy. Modification of CD ring with OEI chains has significantly higher water solubility than the pure CD and higher encapsulation ability to solubilize the anticancer drug PTX. The  $\gamma$ -CD-OEI-2

polymer can solubilize PTX up to 51 mM, which is much higher than most of the CD derivatives reported. Moreover, the CD-OEI/PTX inclusion complexes illustrated satisfactory stability in aqueous solution. Although the antitumor activity is lower than PTX/cremophor formulations, the absence of cremophor may expand their applications in clinical trials. Generally, the synthesized CD-OEI polymers are promising carriers for potentially drug delivery.

### 3.5. References

- (1) Wani, M. C.; Taylor, H. L.; Wall, M. E.; Coggon, P.; McPhail, A. T., *Journal of the American Chemical Society* **1971**,*93*, 2325-2327.
- (2) Donehower, R. C.; Rowinsky, E. K.; Grochow, L. B.; Longnecker, S. M.; Ettinger, D. S., *Cancer treatment reports* **1987**,*71*, 1171-1177.
- (3) Schiff, P. B.; Fant, J.; Horwitz, S. B., *Nature* **1979**,*277*, 665-667.
- (4) Hamel, E.; Delcampo, A. A.; Lowe, M. C.; Lin, C. M., *J Biol Chem* **1981**,*256*, 11887-11894.
- (5) Parness, J.; Horwitz, S. B., *J Cell Biol* **1981**,*91*, 479-487.
- (6) Schiff, P. B.; Horwitz, S. B., *Biochemistry* **1981**,*20*, 3247-3252.
- (7) Rowinsky, E. K.; Cazenave, L. A.; Donehower, R. C., *Journal of the National Cancer Institute* **1990**,*82*, 1247-1259.
- (8) Suffness, M., *Annu Rep Med Chem* **1993**,*28*, 305-314.
- (9) Lorenz, W.; Reimann, H. J.; Schmal, A.; Dormann, P.; Schwarz, B.; Neugebauer, E.; Doenicke, A., *Agents Actions* **1977**,*7*, 63-67.
- (10) Weiss, R. B.; Donehower, R. C.; Wiernik, P. H.; Ohnuma, T.; Gralla, R. J.; Trump, D. L.; Baker, J. R.; Vanecho, D. A.; Vonhoff, D. D.; Leylandjones, B., *Journal of Clinical Oncology* **1990**,*8*, 1263-1268.
- (11) Ceruti, M.; Crosasso, P.; Brusa, P.; Arpicco, S.; Dosio, F.; Cattel, L., *Journal of Controlled Release* **2000**,*63*, 141-153.
- (12) Singla, A. K.; Garg, A.; Aggarwal, D., *International journal of pharmaceutics* **2002**,*235*, 179-192.
- (13) Uekama, K.; Hirayama, F.; Irie, T., *Chemical Reviews* **1998**,*98*, 2045-2076.
- (14) Challa, R.; Ahuja, A.; Ali, J.; Khar, R. K., *Aaps Pharmscitech* **2005**,*6*, E329-E357.
- (15) Villalonga, R.; Cao, R.; Fragoso, A., *Chemical Reviews* **2007**,*107*, 3088-3116.
- (16) Khan, A. R.; Forgo, P.; Stine, K. J.; D'Souza, V. T., *Chemical Reviews* **1998**,*98*, 1977-1996.
- (17) Szejtli, J., *Chemical Reviews* **1998**,*98*, 1743-1753.
- (18) Brewster, M. E.; Estes, K. S.; Bodor, N., *International journal of pharmaceutics* **1990**,*59*, 231-243.
- (19) Pitha, J.; Irie, T.; Sklar, P. B.; Nye, J. S., *Life Sci* **1988**,*43*, 493-502.
- (20) T. Loftsson, M. B., M. Masson, *Am. J. Drug Deliv.* **2004**,*2*, 261-275.
- (21) Davis, M. E.; Brewster, M. E., *Nat Rev Drug Discov* **2004**,*3*, 1023-1035.
- (22) Cserhati, T.; Forgacs, E.; Hollo, J., *J Pharmaceut Biomed* **1995**,*13*, 533-541.
- (23) Sharma, U. S.; Balasubramanian, S. V.; Straubinger, R. M., *J Pharm Sci* **1995**,*84*, 1223-1230.

- (24) Alcaro, S.; Ventura, C. A.; Paolino, D.; Battaglia, D.; Ortuso, F.; Cattel, L.; Puglisi, G.; Fresta, M., *Bioorganic & medicinal chemistry letters* **2002**,*12*, 1637-1641.
- (25) Hamada, H.; Ishihara, K.; Masuoka, N.; Mikuni, K.; Nakajima, N., *Journal of bioscience and bioengineering* **2006**,*102*, 369-371.
- (26) Bouquet, W.; Ceelen, W.; Fritzing, B.; Pattyn, P.; Peeters, M.; Remon, J. P.; Vervaet, C., *Eur J Pharm Biopharm* **2007**,*66*, 391-397.
- (27) Bouquet, W.; Boterberg, T.; Ceelen, W.; Pattyn, P.; Peeters, M.; Bracke, M.; Remon, J. P.; Vervaet, C., *International journal of pharmaceutics* **2009**,*367*, 148-154.
- (28) Bouquet, W.; Ceelen, W.; Adriaens, E.; Almeida, A.; Quinten, T.; De Vos, F.; Pattyn, P.; Peeters, M.; Remon, J. P.; Vervaet, C., *Annals of surgical oncology* **2010**,*17*, 2510-2517.
- (29) Lee, S.; Seo, D.; Kim, H. W.; Jung, S., *Carbohydr Res* **2001**,*334*, 119-126.
- (30) Kim, H.; Choi, J.; Kim, H. W.; Jung, S., *Carbohydr Res* **2002**,*337*, 549-555.
- (31) Ruebner, A.; Kirsch, D.; Andrees, S.; Decker, W.; Roeder, B.; Spengler, B.; Kaufmann, R.; Moser, J. G., *J Inclusion Phenom Mol* **1997**,*27*, 69-84.
- (32) Moser, J. C.; Rose, I.; Wagner, B.; Wieneke, T.; Vervoorts, A., *J Incl Phenom Macro* **2001**,*39*, 13-18.
- (33) Liu, Y.; Chen, G. S.; Li, L.; Zhang, H. Y.; Cao, D. X.; Yuan, Y. J., *Journal of medicinal chemistry* **2003**,*46*, 4634-4637.
- (34) Liu, Y.; Chen, G. S.; Chen, Y.; Cao, D. X.; Ge, Z. Q.; Yuan, Y. J., *Bioorganic & medicinal chemistry* **2004**,*12*, 5767-5775.
- (35) Rao, C. S.; Chu, J. J.; Liu, R. S.; Lai, Y. K., *Bioorganic & medicinal chemistry* **1998**,*6*, 2193-2204.
- (36) Slichenmyer, W. J.; Vonhoff, D. D., *Anti-cancer drugs* **1991**,*2*, 519-530.

## **CHAPTER 4 FOLIC ACID MODIFIED CATIONIC $\gamma$ -CYCLODEXTRIN-OLIGOETHYLENIMINE STAR POLYMER WITH BIOREDUCIBLE DISULFIDE LINKER FOR EFFICIENT TARGETED GENE DELIVERY**

### **4.1. Introduction**

In recent years, great interest has been focused on design and synthesis of safe and effective non-viral vectors to carry and protect oligonucleotides for gene therapy. Non-viral vectors, including cationic lipids, polymers, and dendrimers are promising due to their advantages over viral vectors, such as the safety, low cytotoxicity, easy manipulation, and ability to be readily functionalized.<sup>1</sup> Polyethylenimine (PEI) is one of the most prominent examples of cationic polymers that have been extensively studied for non-viral gene delivery.<sup>2</sup> The increase of gene delivery ability of PEI was observed as increasing of its molecular weight from 600 to 70,000 Da, but accompanied with high toxicity.<sup>3, 4</sup>

Cyclodextrins (CDs) are a series of natural cyclic oligosaccharides composed of 6, 7, and 8 D(+)-glucose units linked by  $\alpha$ -1,4-linkages, named

$\alpha$ -,  $\beta$ -, and  $\gamma$ -CD, respectively. These water-soluble, biocompatible oligosaccharides do not have immune responses and show low toxicity in animals and humans.<sup>5</sup> CDs are usually used as solubilization and stabilization reagents for small molecules.<sup>6</sup> Their application for oligonucleotide delivery thanks to the property that the hydroxyl groups of CD rings offer opportunity for multiple modifications. In 1999, Davis' group reported the first synthesis of CD-conjugated cationic polymers for gene delivery.<sup>7</sup> These CD-based polymers illustrated lower cytotoxicity and improved transfection efficiency as non-viral gene delivery vectors.<sup>8-10</sup> Considering the good gene transfection efficiency of PEI, CD-modified PEI may have great potential as a promising gene delivery vector. Our group reported a series of cationic star polymers by conjugating PEI or oligoethylenimine (OEI) chains to  $\alpha$ -CD as non-viral gene delivery vectors.<sup>11, 12</sup> These CD-OEI star-shaped polymers showed much lower cytotoxicity and excellent gene transfection efficiency that were comparable to or even higher than that of the well-studied branched PEI (25 kDa).

The strategy to employ proper targeting groups is often used to develop gene delivery vectors which can target to specific cells or tissues. Folic acid (FA) is essential for the biosynthesis of nucleotide bases. Many malignant cells overexpress folate receptors (FRs) that is a high affinity folate-binding protein in cellular membrane,<sup>13</sup> which renders FA an attractive candidate ligand for tumor-specific targeted gene delivery. Therefore, vectors conjugated with FA can be efficiently taken up by malignant cells which overexpress FRs via receptor-mediated endocytosis.<sup>14, 15</sup> The total amount of folate-conjugated vectors internalized into a cell is roughly proportional to the overall number of FRs expressed on the cell.<sup>13</sup> However, after the FRs on the cell surface are consumed during the internalization of the folate-conjugated vectors, the cells can no longer recognize the folate ligand, and the folate-conjugated vectors lose the ability of tumor-specific targeted delivery. Only if the cellular

membranes can readily recover the consumed FRs, the folate-conjugated vectors can be efficiently and continuously internalized by the target tumor cells.<sup>16</sup> Therefore, the continuous recycling of FRs after cellular endocytosis is essential.

Disulfide bond (-S-S-) is a covalent linkage which can be easily synthesized by oxidation of sulfhydryl, and can be cleaved in the presence of reducing agents. The oxidizing extracellular milieu and reducing intracellular space renders disulfide bond a delivery tool, which allows the vector to be degraded and to release the carried gene within the cells. In non-viral gene delivery systems, disulfide-based conjugates have been demonstrated to have higher gene transfection efficiency in comparison with disulfide-free precursors.<sup>17, 18</sup> Low molecular weight PEI linked with reducible disulfide bond could assist uncoupling of PEI from DNA to enhance gene delivery, and the cleaved low molecular weight PEI could be easily cleared from the body.<sup>18-22</sup> Disulfide bond was also incorporated in some folate-mediated targeted gene delivery systems, where disulfide linker was used to trigger cleavage of polymers followed by enhanced DNA release.<sup>23-25</sup> Moreover, folate-drug conjugates with cleavable linkers (such as disulfide bond) were reported to ensure the release of drugs after endocytosis in the target cells.<sup>26-30</sup>

Herein we design a folate-conjugated  $\gamma$ -CD-OEI star-shaped cationic polymer with disulfide bond as the linker between folate and  $\gamma$ -CD-OEI as a new multi-functional gene carrier. We have demonstrated that the newly designed  $\gamma$ -CD-OEI-SS-FA gene carrier had low cytotoxicity, and possessed capacity to target and deliver DNA to specific tumor cells that overexpress FRs, as well as function to recover and recycle FRs onto cellular membranes to facilitate continuous FR-mediated endocytosis to achieve very high levels of gene expression.



## 4.2. Experimental Section

### 4.2.1. Materials

Branched PEI (MW, 600 and 25,000), *N,N'*-dicyclohexylcarbodiimide (DCC), 4-dimethylaminopyridine (DMAP), folic acid (FA), buthionine sulphoximine (BSO), pyridine, and anhydrous dimethyl sulfoxide (DMSO) were purchased from Sigma-Aldrich. Cystamine dihydrochloride, succinic anhydride, 3-(4,5-Dimethyl-thiazol-2-yl)-2,5-diphenyl tetrazodium bromide (MTT), and DL-dithiothreitol (DTT) were obtained from Alfa Aesar (MA, U.S.A.). 1,1'-Carbonyldiimidazole (CDI),  $\alpha$ -,  $\beta$ -, and  $\gamma$ -CD, were purchased from Tokyo Chemical Industry Co. Ltd (Tokyo, Japan). D<sub>2</sub>O and DMSO-*d*<sub>6</sub> used as solvents in the NMR measurement were obtained from Cambridge Isotope Laboratories, Inc. (Andover, U.S.A.).

### 4.2.2. Synthesis Procedure

The intermediates and the final cationic gene carriers were synthesized as follows.

*FA-SS-NH<sub>2</sub>*: To a suspension of FA (265 mg, 0.6 mmol) and cystamine dihydrochloride (180 mg, 0.8 mmol) in a mixture of DMSO (4 mL) and pyridine (4 mL) was added DCC (144 mg, 0.7 mmol) and DMAP (cat.). The mixture was stirred at room temperature for 18 hours under dark, and then poured into acetone (80 mL). The yellow precipitate was collected and washed with acetone (40 mL) twice, and dried under vacuum to yield 330 mg of yellow solid (yield, 96%). The crude was used in the next step without further purification.

*FA-SS-COOH*: To a solution of FA-SS-NH<sub>2</sub> crude (330 mg, 0.6 mmol) in pyridine (5 mL) was added succinic anhydride (100 mg, 1.0 mmol), and then the mixture was stirred at room temperature for 18 hours under dark. The reaction mixture was then poured into acetone (80 mL). The yellow precipitate was collected, washed with acetone (40 mL) twice, and dried under vacuum to

yield 348 mg of yellow solid (yield, 90%).  $^1\text{H}$  NMR: (400 MHz,  $\text{DMSO}-d_6$ ):  $\delta$  8.62 (s, 1 H, -CH- of pyrazine), 8.01 (brs, 2 H, -NH-), 7.63 (d, 2 H,  $J = 8.4$  Hz, -CH- of benzyl ring), 6.90 (brs, 2H, -NH-), 6.62 (d, 2 H,  $J = 8.4$  Hz, -CH- of phenyl ring), 4.47 (s, 2 H, -CH<sub>2</sub>-), 4.32 (m, 1 H, -CH-), 2.72 (t, 4 H,  $J = 6.8$  Hz, -CH<sub>2</sub>S-), 2.20 – 2.45 (m, 4 H, -CH<sub>2</sub>CO- of succinic anhydride), 1.80 – 2.20 (m, 4 H, -CH<sub>2</sub> of FA).

$\gamma$ -CD-OEI: To a solution of CDI (4.9 g, 30.0 mmol) in DMSO (30 mL) was added dropwise a solution of  $\gamma$ -CD (1.3 g, 1.0 mol) in DMSO (20 mL) during 1 h. After stirring for 20 h, the solution was added dropwise into a mixture of Et<sub>2</sub>O/THF (400 mL/200 mL). The white precipitate was collected by centrifuge and washed with Et<sub>2</sub>O/THF (20 mL/10 mL) twice, then dissolved into anhydrous DMSO (20 mL). The previous solution was added dropwise into a solution of PEI-600 (12.6 g, 21 mmol) in DMSO (40 mL) during 30 min, and then stirred at room temperature for an additional 24 h. Purification by dialysis (MWCO, 2000) against water for 5 d, freeze dried to yield 2.1 g of colorless solid (yield, 56.0%).  $^1\text{H}$  NMR: (400 MHz, D<sub>2</sub>O):  $\delta$  5.05 (brs, 8 H, H-1 of  $\gamma$ -CD), 2.95 – 4.57 (m, 62 H, H-2-6 of  $\gamma$ -CD, -CONHCH<sub>2</sub>- of OEI), 1.87 – 2.95 (m, 395 H, -CH<sub>2</sub>CH<sub>2</sub>NH- of OEI).

$\gamma$ -CD-OEI-FA<sub>1,2</sub>: To a solution of  $\gamma$ -CD-OEI (110 mg, 20.9  $\mu\text{mol}$ ) and FA (9.2 mg, 20.8  $\mu\text{mol}$ ) in DMSO/Pyridine (1 mL/1 mL) was added DCC (4.3 mg, 20.8  $\mu\text{mol}$ ) and DMAP (cat.). The mixture was stirred at room temperature for 18 hours under dark. Purification by dialysis (MWCO, 2000) against water under dark for 5 d, freeze dried to yield 95 mg of yellow solid (73.4%).  $^1\text{H}$  NMR: (400 MHz, D<sub>2</sub>O):  $\delta$  8.57 (s, 1.2 H, -CH- of pyrazine on FA), 7.65 (d, 2.4 H, -CH- of phenyl ring on FA), 6.77 (d, 2.4 H, -CH- of phenyl ring on FA), 4.98 (brs, 8 H, H-1 of  $\gamma$ -CD), 4.52 (2.4 H, -CH<sub>2</sub>NHPh- of FA), 4.25 (1.2 H, -CHCOOH- of FA), 3.00 – 4.50 (m, 63 H, H-2-6 of  $\gamma$ -CD, -CONHCH<sub>2</sub>- of OEI), 2.10 – 2.92 (m, 395 H, -CH<sub>2</sub>CH<sub>2</sub>NH- of OEI).

*$\gamma$ -CD-OEI-SS-FA<sub>0.8</sub>*: To a solution of  $\gamma$ -CD-OEI (57 mg, 10  $\mu$ mol) and FA-SS-COOH (7 mg, 10  $\mu$ mol) in DMSO (1 mL) and pyridine (1 mL) was added DCC (2 mg, 10  $\mu$ mol) and DMAP (cat.). The reaction mixture was stirred at room temperature for 18 hours under dark. Purification by dialysis (MWCO, 2000) against water under dark for 5 d, freeze dried to yield 42 mg of yellow solid (68%). <sup>1</sup>H NMR (400 MHz, D<sub>2</sub>O):  $\delta$  8.45 – 8.61 (m, 0.8 H, -CH- of pyrazine on FA), 7.53 – 7.74 (m, 1.6 H, -CH- of phenyl ring on FA), 6.57 – 6.81 (m, 1.6 H, -CH- of phenyl ring on FA), 5.02 (brs, 8 H, H-1 of  $\gamma$ -CD), 2.95 – 4.57 (m, 64 H, -CH<sub>2</sub>NHPh and -CHCOOH- of FA, H-2-6 of  $\gamma$ -CD, and -CONHCH<sub>2</sub>- of OEI), 1.88 – 2.95 (m, 395 H, -CH<sub>2</sub>CH<sub>2</sub>NH- of OEI).

*$\gamma$ -CD-OEI-SS-FA<sub>1.3</sub>*: To a solution of  $\gamma$ -CD-OEI (57 mg, 10  $\mu$ mol) and FA-SS-COOH (10 mg, 15  $\mu$ mol) in DMSO (1 mL) and pyridine (1 mL) was added DCC (3 mg, 15  $\mu$ mol) and DMAP (cat.). The reaction mixture was stirred at room temperature for 18 hours under dark. Purification by dialysis (MWCO, 2000) against water under dark for 5 d, freeze dried to yield 54 mg of yellow solid (83%). <sup>1</sup>H NMR (400 MHz, D<sub>2</sub>O):  $\delta$  8.42 – 8.69 (m, 1.3 H, -CH- of pyrazine on FA), 7.48 – 7.77 (m, 2.6 H, -CH- of phenyl ring on FA), 6.54 – 6.84 (m, 2.6 H, -CH- of phenyl ring on FA), 5.00 (brs, 8 H, H-1 of  $\gamma$ -CD), 2.95 – 4.57 (m, 65 H, -CH<sub>2</sub>NHPh and -CHCOOH- of FA, H-2-6 of  $\gamma$ -CD, and -CONHCH<sub>2</sub>- of OEI), 1.91 – 2.96 (m, 395 H, -CH<sub>2</sub>CH<sub>2</sub>NH- of OEI).

*$\gamma$ -CD-OEI-SS-FA<sub>1.7</sub>*: To a solution of  $\gamma$ -CD-OEI (57 mg, 10  $\mu$ mol) and FA-SS-COOH (16 mg, 25  $\mu$ mol) in DMSO (1 mL) and pyridine (1 mL) was added DCC (5 mg, 25  $\mu$ mol) and DMAP (cat.). The reaction mixture was stirred at room temperature for 18 hours under dark. Purification by dialysis (MWCO, 2000) against water under dark for 5 d, freeze dried to yield 57 mg of yellow solid (84%). <sup>1</sup>H NMR (400 MHz, D<sub>2</sub>O):  $\delta$  8.42 – 8.70 (m, 1.7 H, -CH- of pyrazine on FA), 7.47 – 7.79 (m, 3.4 H, -CH- of phenyl ring on FA),

6.51 – 6.92 (m, 3.4 H, -CH- of phenyl ring on FA), 5.00 (brs, 8 H, H-1 of  $\gamma$ -CD), 2.98 – 4.57 (m, 66 H, -CH<sub>2</sub>NHPh and -CHCOOH- of FA, H-2-6 of  $\gamma$ -CD, and -CONHCH<sub>2</sub>- of OEI), 1.91 – 2.98 (m, 395 H, -CH<sub>2</sub>CH<sub>2</sub>NH- of OEI).

#### **4.2.3. Characterization Methods**

##### ***NMR Spectroscopy***

The <sup>1</sup>H and <sup>13</sup>C NMR spectra were recorded on a Bruker AV-400 NMR spectrometer at 400.1 and 100.6 MHz at room temperature, respectively. The <sup>1</sup>H NMR measurements were carried out with an acquisition time of 3.2 s, a pulse repetition time of 2.0 s, a 30° pulse width, 5208 Hz spectral width, and 32 K data points. Chemical shifts were referenced to the solvent peak ( $\delta$  = 4.70 ppm for D<sub>2</sub>O,  $\delta$  = 2.50 ppm for DMSO-*d*<sub>6</sub>).

##### ***UV-Vis Spectroscopy***

All absorption spectra were recorded on a Shimadzu UV 2501 spectrophotometer against a solvent blank. Absorption was measured in quartz cuvettes (frosted wall, 0.7 mL). Samples were dilute to 0.01 mg/mL for FA, and 0.1 mg/mL for cationic polymer  $\gamma$ -CD-OEI,  $\gamma$ -CD-OEI-FA<sub>1,2</sub>, and  $\gamma$ -CD-OEI-SS-FA<sub>1,3</sub> before measurement.

##### ***Release Test***

The concentrations of released FA by cleavage of disulfide linker from  $\gamma$ -CD-OEI-SS-FA using DTT were measured by UV-Vis spectroscopy. In Brief, 1.0 mL of  $\gamma$ -CD-OEI-SS-FA<sub>1,3</sub> (5 mg/mL with DTT concentrations at 0  $\mu$ M, 10  $\mu$ M, and 10 mM in PBS buffer) was loaded into dialysis tubes (MWCO 2000, Spectrum Laboratories Inc., USA). These dialysis tubes were put into centrifuge tubes immersed 50 mL of PBS solution with corresponding DTT concentrations. Then the centrifuge tubes were placed in a shaker agitated at 200 rpm and maintained the temperature at 37 °C. At appropriate intervals, 1 mL of the dissolution medium was withdrawn and analyzed by

UV-Vis spectroscopy (Shimadzu UV 2501) at wavelength of 284 nm. Meanwhile, 1 mL of fresh medium was added to replace the medium that was withdrawn.

#### ***Dynamic Light Scattering and Zeta-potential Measurements***

Particle size and zeta potential of the polymer/pDNA complexes were assessed using a Zetasizer Nano ZS (Malvern Instruments, Southborough, MA, USA) with a laser light wavelength of 633 nm at a 173° scattering angle. Briefly, 100 µL of appropriate polymers mixed with 3 µg of pDNA to prepare various solutions with N/P ratios ranging from 10 to 100. The mixture was vortexed for 30 s and incubated for 30 min at room temperature, and then diluted into 1 mL of distilled water and vortexed for 30 s before test by the Zetasizer. The particle size measurement was carried out at 25 °C in triplicate.

The deconvolution of the measured correlation curve to an intensity size distribution was accomplished using a nonnegative least squares algorithm. The Z-average hydrodynamic diameters of the particles were provided by the instrument. The Z-average size is the intensity weighted mean diameter derived from a Cumulants or single-exponential fit of the intensity autocorrelation function. The zeta potential measurements were carried using a capillary zeta potential cell in automatic mode with same samples measured for particle size.

#### **4.2.4. Biological Characterization Methods**

##### ***Plasmids***

The pRL-CMV (Promega, USA) plasmid, encoding Renilla luciferase, originally cloned from the marine organism *Renilla reniformis* was used. This plasmid DNA (pDNA) was amplified in *Escherichia coli* and purified following the protocol of supplier (Qiagen, Hilden, Germany). The concentration of the purified plasmid DNA was measured by optical density at 260 and 280 nm. The quality was detected by electrophoresis in 1% agarose

gel. The purified pDNA was resuspended in TE buffer (10 mM Tris-Cl, pH 7.5, 1 mM EDTA) and kept at a concentration of 1.0 mg/mL.

#### ***Cells and Media***

All cell lines were purchased from ATCC (Rockville, MD). KB cells are FR-positive human nasopharyngeal cells, cultured in Minimum Essential Medium (MEM) supplemented with 10% heat-inactivated fetal bovine serum (FBS), 0.3 g/L of L-glutamine, 0.1 g/L of sodium pyruvate, 100 units/mg of penicillin, and 100 µg/mL of streptomycin at 37 °C and 5% CO<sub>2</sub>. The A549 human lung epithelial carcinoma cell line was cultured in Ham's F-12 Nutrient Mixture (F-12) supplemented with 10% FBS, 100 units/mg of penicillin, and 100 µg/mL of streptomycin at 37 °C and 5% CO<sub>2</sub>. Roswell Park Memorial Institute (RPMI) 1640 medium (FA free) supplemented with 10% FBS, 100 units/mg of penicillin, and 100 µg/mL of streptomycin was used during cell viability and gene transfection test. MEM, F-12, and RPMI-1640 medium was purchased from Gibco BRL (Gaithersburg, MD).

#### ***Gel Retardation Assay***

The binding ability of the all cationic polymers with pRL-CMV was tested by gel electrophoresis experiments. The sample solutions were diluted as various nitrogen concentrations by distilled water. Then pRL-CMV (0.1 mg/mL of TE buffer) was mixed with an equal volume of previous polymer solution to prepare DNA/polymer complex at various nitrogen/phosphate (N/P) ratio solutions from 0 to 4. Each sample was vortexed and incubated for 30 min at room temperature before loading to 1% agarose gel containing 0.5 µg/mL ethidium bromide (EtBr). Gel electrophoresis was done in TAE buffer (40 mM Tris-acetate, 1 mM EDTA) at 100 V for 40 min in a Sub-Cell system (Bio-Rad Laboratories, CA). DNA bands were visualized by a UV lamp by a GelDoc system (Synoptics Ltd., UK).

### *Cell Viability Assay*

Human KB carcinoma cell line was cultured in FA free RPMI 1640 medium supplemented with 10% FBS at 37 °C, 5% CO<sub>2</sub>, and 95% relative humidity. 100 µL of medium with a density of  $1.5 \times 10^5$  cells/mL were seeded into 96-well plates (NUNC, Wiesbaden, Germany). After 24 h, culture media were replaced with fresh culture media containing serial dilutions of polymers, in which the cells were cultured for 20 h. Then 10 µL of sterile filtered MTT (5 mg/mL) stock solution in PBS was added to each well, reaching a final MTT concentration of 0.5 mg/mL. After 4 h, unreacted dye was discarded by aspiration. The formazan crystals were dissolved in 100 µL/well DMSO and the absorbance was measured using a microplate reader (Spectra Plus, TECAN) at a wavelength of 570 nm. Five wells were treated together as a group. The relative cell growth (%) related to control cells cultured in media without polymer was calculated by  $[A]_{\text{test}}/[A]_{\text{control}} \times 100\%$ .

### *In vitro Transfection and Luciferase Assay*

Gene transfection efficiency studies were carried out in KB and A549 cell lines using pRL-CMV as reporter gene. In brief, 24-well plates were seeded with cells at a density of  $8 \times 10^4$ /well (KB cells) or  $6 \times 10^4$ /well (A549 cells) for 24 hours before transfection. The sample/DNA complexes at various N/P ratios were prepared by adding the samples into DNA solutions, followed by vortexing for 20 s and incubation for 30 min at room temperature before the transfection. Each well was first replaced with 400 µL of fresh RPMI 1640 medium (FA free) for gene transfection efficiency test, or RPMI 1640 medium with FA at different concentrations (0.000, 0.001, 0.010, and 0.100 g/L) for FA competition test, or RPMI 1640 medium (FA free) with BSO at different concentrations (0, 50, 250, and 500 µM) for disulfide inhibition assay. Then the sample/DNA complexes were added into previous medium and incubated for 4 hours under standard incubator conditions. After 4 h, the medium was replaced with 500 µL of fresh RPMI 1640 medium (FA free), and the cells

were further incubated for an additional 20 hours under the same conditions. Cells were washed with PBS twice and added 100  $\mu$ L of cell culture lysis reagent (Promega, Cergy Pontoise, France), then shook at 1000 rpm for 2 hours at room temperature before test. Luciferase gene expression was quantified using a commercial kit (Promega, Cergy Pontoise, France) and a luminometer (Berthold Lumat LB 9507, Germany). Protein concentration in the samples was analyzed using a bicinchoninic acid assay (Biorad, CA, USA). Absorption was measured on a microplate reader (Spectra Plus, TECAN) at 570 nm and compared to a standard curve calibrated with BSA samples of known concentration. Results are expressed as relative light units per milligram of cell protein lysate (RLU/mg protein).

#### ***Confocal Microscopy***

Confocal microscopy was used to evaluate the expression of the plasmid pEGFP-N1 (Clontech Laboratories, Inc., Mountain View, CA), encoding a red-shifted variant of wild-type green fluorescence protein (GFP) by a KB cell line. In brief, a density of  $1.2 \times 10^4$ /well KB cells in 0.3 ml of RPMI 1640 medium (FA free) were seeded onto a Lab-Tekfour-chambered coverglass system (Nalge-Nane International, Naperville, IL). After 24 h, EGFP polyplexes with PEI (25 kDa) at N/P ratio of 10, and the EGFP polyplexes with  $\gamma$ -CD-OEI,  $\gamma$ -CD-OEI-FA<sub>1,2</sub>, and  $\gamma$ -CD-OEI-SS-FA<sub>1,3</sub> at N/P ratio of 50 were added into the transfection medium. After incubation for 4 h, the medium was replaced with 0.3 mL of fresh RPMI 1640 medium (FA free) and further incubated for an additional 20 hours under same conditions. The cells were imaged using an Olympus Fluoview FV500 confocal laser scanning microscope (Olympus, Japan). EGFP fluorescence was excited by 488 nm laser line and detected using a 515 nm filter.

#### ***Statistical Analysis***

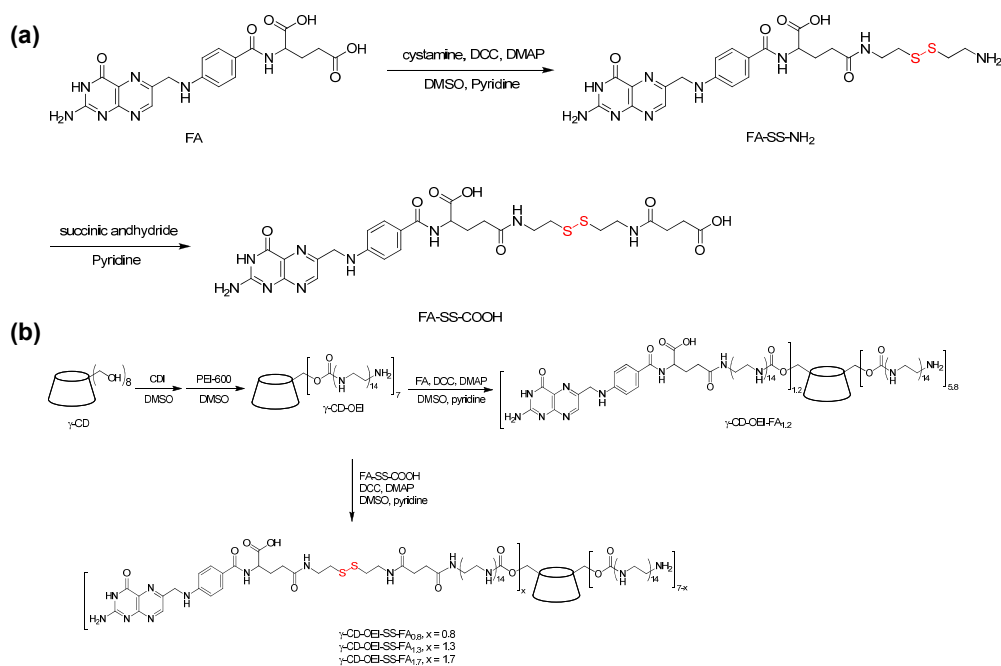


Statistical analysis was carried out by a standard Student's *t*-test with a minimum confidence level of 0.05 as significant statistical difference. All the data are reported as mean  $\pm$  standard deviation.

### **4.3. Results and Discussion**

#### **4.3.1. Synthesis of $\gamma$ -CD-OEI-SS-FA**

$\gamma$ -CD has 8 primary hydroxyl groups that can be easily modified. Scheme 1 shows the synthesis procedures of FA-SS-COOH and  $\gamma$ -CD-OEI-SS-FA.  $\gamma$ -CD-OEI-FA was also synthesized as a control compound. Firstly, coupling reaction between FA and cystamine dihydrochloride was carried out by DCC and DMAP to introduce disulfide bond. Secondly, the amino-terminated FA was allowed to react with succinic anhydride to give FA-SS-COOH. The feeding ratio of DCC and cystamine was less than 1:1 to make sure that only the  $\gamma$ -carboxyl group of FA was conjugated with disulfide bond because over-modification of  $\alpha$ -carboxyl group of FA may result in loss of binding ability to FR. Thirdly, the primary hydroxyl groups of  $\gamma$ -CD were activated by CDI, and then allowed to react with large excess of PEI-600 to give a  $\gamma$ -CD-OEI star-shaped cationic polymer (this step is similar to our previous report on the synthesis of cationic star-shaped  $\alpha$ -CD-OEI polymers).<sup>11</sup> To ensure there was no intra- or intermolecular crosslinking, the CDI-activated intermediate was purified by precipitation in Et<sub>2</sub>O/THF and large excess of PEI was used. Finally, unmodified FA and the FA-SS-COOH were allowed to react with  $\gamma$ -CD-OEI to produce  $\gamma$ -CD-OEI-FA and  $\gamma$ -CD-OEI-SS-FA, respectively. By varying the feeding ratio of FA-SS-COOH to  $\gamma$ -CD-OEI, three samples of  $\gamma$ -CD-OEI-SS-FA were obtained with different amounts of FA grafted onto  $\gamma$ -CD-OEI (Scheme 4.1b).



**Scheme 4.1.** Synthesis of FA with disulfide linker FA-SS-COOH (a) and  $\gamma$ -CD-OEI-FA and  $\gamma$ -CD-OEI-SS-FA (b).

The successful synthesis of these samples was confirmed by  $^1\text{H}$  NMR,  $^{13}\text{C}$  NMR and UV-Vis spectroscopy. Figure 4.1 shows the  $^1\text{H}$  NMR spectra of  $\gamma$ -CD-OEI-SS-FA<sub>0.8</sub>,  $\gamma$ -CD-OEI-SS-FA<sub>1.3</sub>,  $\gamma$ -CD-OEI-SS-FA<sub>1.7</sub> in comparison with  $\gamma$ -CD-OEI and  $\gamma$ -CD-OEI-FA<sub>1.2</sub>. The typical signals from H-1 of  $\gamma$ -CD and OEI ethylene protons appeared at 5.0 and 1.9 – 3.0 ppm, respectively. The numbers of grafted OEI arms were calculated based on the integral ratios of these peaks. Successful linkage of FA to  $\gamma$ -CD-OEI was confirmed by their aromatic proton signals with chemical shifts at 6.8, 7.7, and 8.6 ppm. Meanwhile, the number of grafted FA was determined to be 1.2 for  $\gamma$ -CD-OEI-FA<sub>1.2</sub>, 0.8 for  $\gamma$ -CD-OEI-SS-FA<sub>0.8</sub>, 1.3 for  $\gamma$ -CD-OEI-SS-FA<sub>1.3</sub>, and 1.7 for  $\gamma$ -CD-OEI-SS-FA<sub>1.7</sub> according to the peak integrals of FA aromatic proton signals and OEI ethylene proton signals.

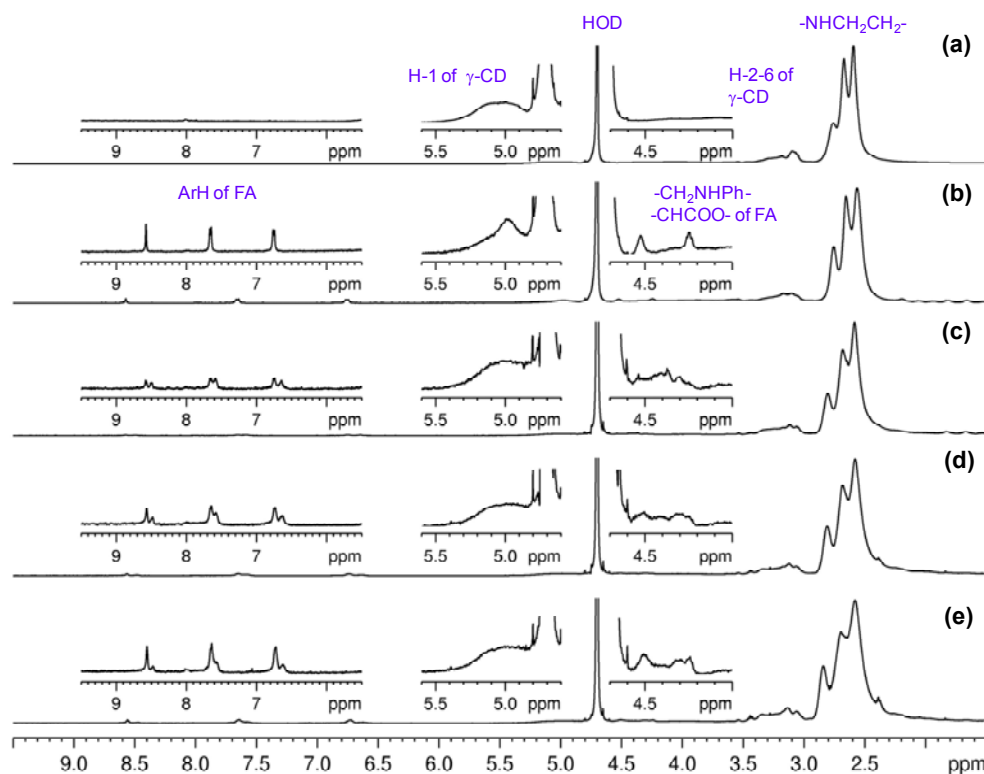


**Figure 4.1.**  $^1\text{H}$  NMR spectra of  $\gamma$ -CD-OEI (a),  $\gamma$ -CD-OEI-FA<sub>1.2</sub> (b),  $\gamma$ -CD-OEI-SS-FA<sub>0.8</sub> (c),  $\gamma$ -CD-OEI-SS-FA<sub>1.3</sub> (d), and  $\gamma$ -CD-OEI-SS-FA<sub>1.7</sub> (e) in  $\text{D}_2\text{O}$ .

$^{13}\text{C}$  NMR spectrum of  $\gamma$ -CD-OEI-SS-FA<sub>1.3</sub> was shown in Figure 4.2. The peak at  $\delta$  158.0 ppm is the urethane groups linked to the OEI chains. In addition, the other carbonyl groups from FA can also be found at  $\delta$  160 – 180. Signals at chemical shift 101.7, 69.7, and 64.1 correspond to the  $\beta$ -CD core. Moreover, the peaks at  $\delta$  32.9 and 24.9 demonstrate the methylene groups derived from disulfide linker. The typical aromatic signals of FA were observed at  $\delta$  112.7, 128.8, 129.8, 147.8, and 151.8. The  $^{13}\text{C}$  NMR spectrum further demonstrates the successful conjugation of FA with disulfide linker.

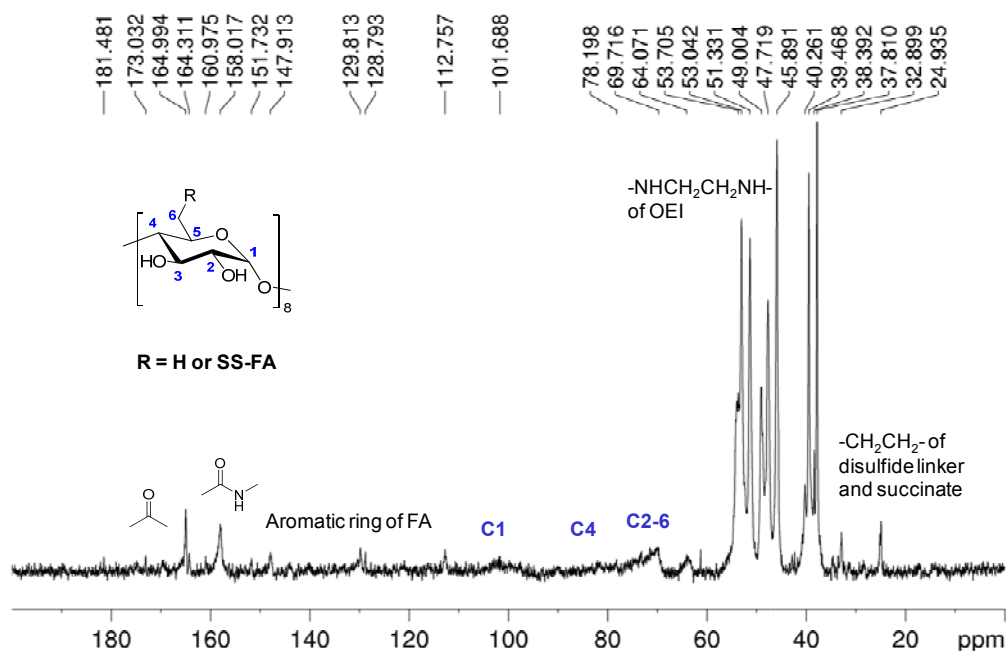


**Figure 4.2.**  $^{13}\text{C}$  NMR spectra of  $\gamma\text{-CD-OEI-SS-FA}_{1.3}$  in  $\text{D}_2\text{O}$ .

UV-Vis spectroscopy was used to further confirm the structure of the synthesized  $\gamma\text{-CD-OEI-FA}$  and  $\gamma\text{-CD-OEI-SS-FA}$ . As shown in Figure 4.3, both  $\gamma\text{-CD-OEI-FA}_{1.2}$  and  $\gamma\text{-CD-OEI-SS-FA}_{1.3}$  have three absorption peaks at 260, 291, and 369 nm, due to the conjugation of FA, while FA shows peaks at 282 nm, and 362 nm. In contrast,  $\gamma\text{-CD-OEI}$  has no UV-Vis absorption. The positively charged  $\gamma\text{-CD-OEI}$  withdraws electrons of unsaturated aryl rings, causing red shifts of FA absorption bands from 282 nm to 291 nm, and 362 nm to 369 nm.

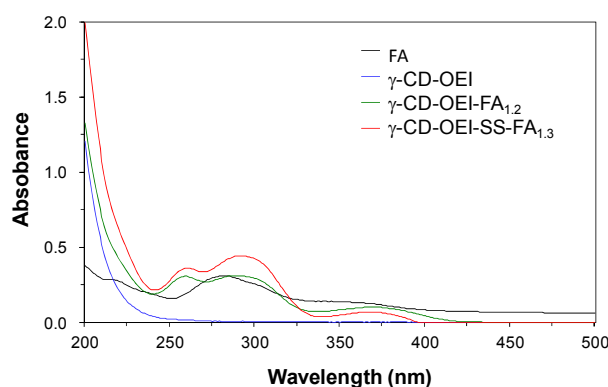


**Figure 4.3.** UV-Visible spectra of FA (0.01 mg/mL),  $\gamma\text{-CD-OEI}$  (0.1 mg/mL),  $\gamma\text{-CD-OEI-FA}_{1.2}$  (0.1 mg/mL), and  $\gamma\text{-CD-OEI-SS-FA}_{1.3}$  (0.1 mg/mL) in  $\text{H}_2\text{O}$ .

FA release test was used to demonstrate the cleavage of disulfide bond in the presence of DTT.  $\gamma$ -CD-OEI-SS-FA<sub>1.3</sub> was incubated with 10  $\mu$ M and 10 mM of DTT in PBS at 37 °C to mimic the different extracellular and intracellular environments, where glutathione (GSH) concentrations should be *ca.* 10  $\mu$ M and *ca.* 1 – 10 mM, respectively. As shown in Figure 4.4, the degradation of disulfide bond was very slow at low DTT concentrations (0 and 10  $\mu$ M) and only 10% of FA derived from  $\gamma$ -CD-OEI-SS-FA<sub>1.3</sub> was detected after 120 h. However, increasing DTT concentration to 10 mM significantly increased the reduction and cleavage rate of the disulfide bond in  $\gamma$ -CD-OEI-SS-FA<sub>1.3</sub>. As the result, more than 80% of FA released within 48 hours, and nearly 100% of FA released at 120 hours.

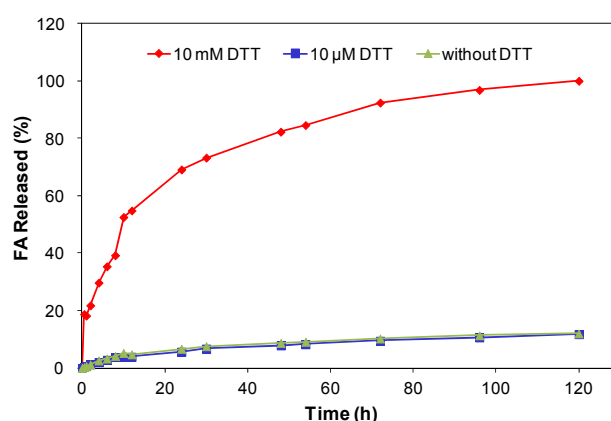


**Figure 4.4.** Release profiles of  $\gamma$ -CD-OEI-SS-FA<sub>1.3</sub> in the absence and presence of DTT at 10  $\mu$ M and 10 mM in PBS buffer (pH 7.4, 1.0 mL) at 37 °C.

#### 4.3.2. Formation of $\gamma$ -CD-OEI-SS-FA/DNA Complexes

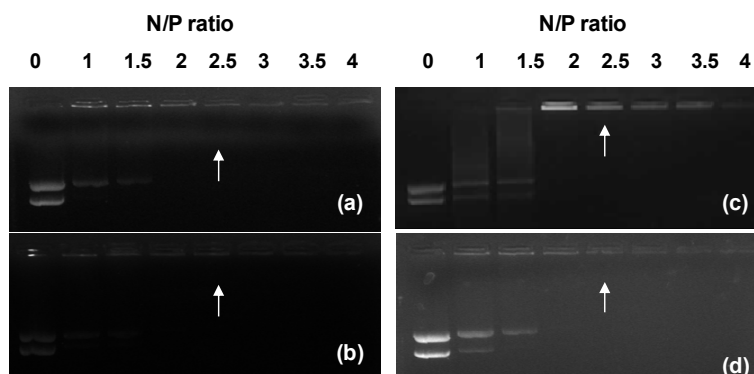


**Figure 4.5.** Electrophoretic mobility of pDNA in the polyplexes formed with PEI (a),  $\gamma$ -CD-OEI (b),  $\gamma$ -CD-OEI-FA<sub>1,2</sub> (c), and  $\gamma$ -CD-OEI-SS-FA<sub>1,3</sub> (d). The arrows indicate the N/P ratios where the DNA mobility is completely retarded.

It is a prerequisite for a gene delivery vector to effectively condense DNA to form nanoparticles. When negatively charged DNA encounters positively charged cationic polymer in an aqueous solution, the electrostatic interaction will cause the phase separation of DNA and the polymer, which induces the formation of condensed DNA/polymer complexes (polyplexes) as colloidal nanoparticles suitable for cellular internalization through endocytosis and/or other pathways. The ability of cationic  $\gamma$ -CD-OEI-SS-FA<sub>1,3</sub> to condense pDNA was analyzed by agarose gel electrophoresis in comparison with PEI (25 kDa),  $\gamma$ -CD-OEI, and  $\gamma$ -CD-OEI-FA<sub>1,2</sub> (Figure 4.5). All the cationic polymers could entirely compact pDNA at N/P ratios of 2.5, which is same as the standard PEI.

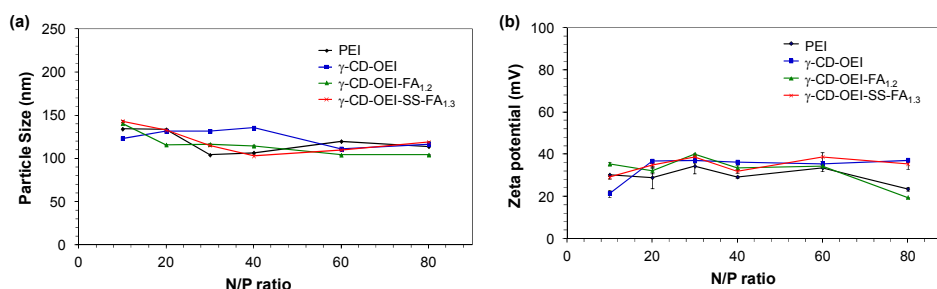


**Figure 4.6.** Particle size (a) and zeta potential (b) of the pDNA polyplexes with PEI (25 kDa),  $\gamma$ -CD-OEI,  $\gamma$ -CD-OEI-FA<sub>1,2</sub>, and  $\gamma$ -CD-OEI-SS-FA<sub>1,3</sub>, respectively, at various N/P ratios.

The surface charge and particle size of the OEI-grafted polymers are important parameters for their biological application, which might be related to their blood circulation, cell encapsulation mechanism, and bioavailability.<sup>31, 32</sup> Figure 4.6 displays the results of zeta potential and particle size measurements of the pDNA complexes with PEI,  $\gamma$ -CD-OEI,  $\gamma$ -CD-OEI-FA<sub>1,2</sub>, and  $\gamma$ -CD-OEI-SS-FA<sub>1,3</sub> at various N/P ratios. Figure 4.6a shows that all the

three cationic polymers efficiently compact pDNA into small nanoparticles with particle sizes around 100 – 150 nm, which is suitable for cellular uptake through endocytosis for gene delivery application.<sup>1</sup> The surface charge of these complexes is around 20 – 40 mV in Figure 4.6b. Unlike the negative DNA, positive charged polymer/DNA complexes are easier to bind to cell membrane and endocytosis would be one of the possible mechanisms of cellular uptake.

### 4.3.3. Cytotoxicity

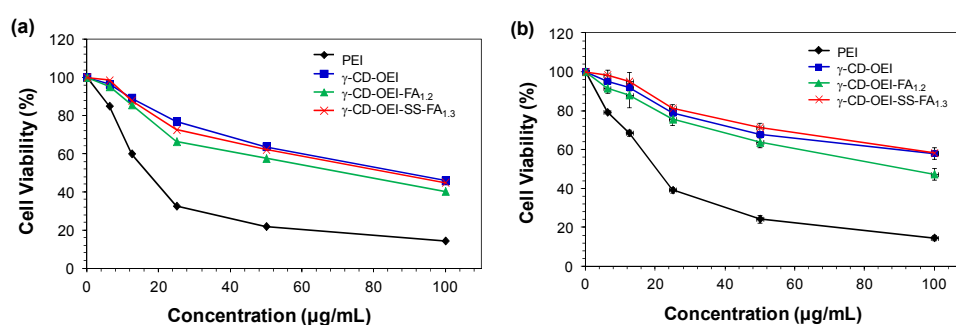


**Figure 4.7.** Cell viability assay in KB cell line. The cells were treated with PEI (25 kDa),  $\gamma$ -CD-OEI,  $\gamma$ -CD-OEI-FA<sub>1,2</sub>, and  $\gamma$ -CD-OEI-SS-FA<sub>1,3</sub> at various concentrations for 24 hours in the absence (a) and presence (b) of FA (0.001 g/L) in RPMI 1640 medium. Data represent mean  $\pm$  standard deviation (n = 5).

Cytotoxicity is an important factor that must be considered for gene delivery materials. Kissel et al. reported that the aggregation and adherence on the cell surface is the reason for the increased toxicity of PEI.<sup>33</sup> Our previous studies showed that the introduction of CDs can reduce the toxicity of PEI or OEI.<sup>10, 11</sup> Figure 6 shows the cell cytotoxicity of  $\gamma$ -CD-OEI,  $\gamma$ -CD-OEI-FA<sub>1,2</sub>, and  $\gamma$ -CD-OEI-SS-FA<sub>1,3</sub> compared to PEI (25 kDa) in the absence (Figure 6a) and presence (Figure 6b) of FA in the culture medium. All the synthesized cationic polymers showed lower cytotoxicity than PEI (25 kDa). Since the cytotoxicity is mostly derived from the OEI chains, modification of  $\gamma$ -CD-OEI by FA and disulfide bond does not significantly change the cytotoxicity. In both absence and presence of FA in the culture medium, the introduction of

disulfide linker resulted in slight decrease of cytotoxicity (Figure 6a and 6b). The addition of FA in the cell culture medium slightly decreased the cytotoxicity of all the samples (Figure 6b). The possible reason is that FA benefits cell growth of the control group (cells without polymers).<sup>34</sup>

#### 4.3.4. *In vitro* gene transfection

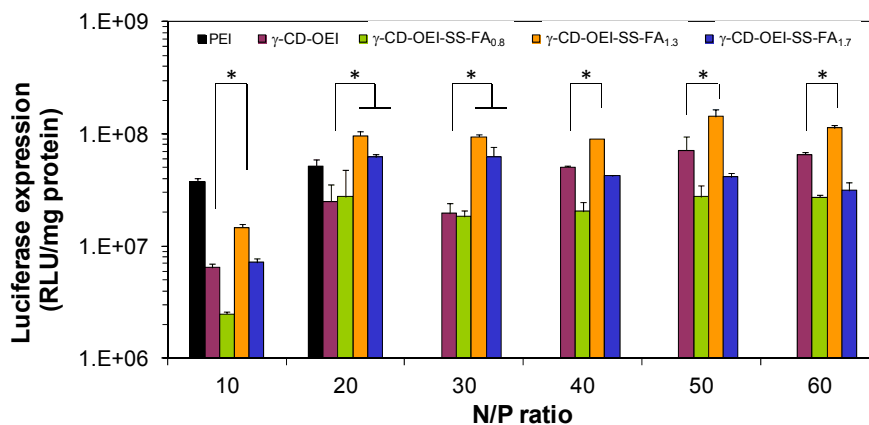


**Figure 4.8.** *In vitro* gene transfection efficiency of the pDNA polyplexes with PEI (25 kDa),  $\gamma$ -CD-OEI,  $\gamma$ -CD-OEI-SS-FA<sub>0.8</sub>,  $\gamma$ -CD-OEI-SS-FA<sub>1.3</sub>, and  $\gamma$ -CD-OEI-SS-FA<sub>1.7</sub> in KB cells in RPMI 1640 medium in the absence of FA. Data represent mean  $\pm$  standard deviation (\* $P$  < 0.05,  $n$  = 4).

*In vitro* gene transfection efficiency was assessed using luciferase as a marker gene in FR-positive KB cells and FR-negative A549 cells. We first investigated the influence of the grafting amount of the targeting group FA on the gene delivery ability of  $\gamma$ -CD-OEI-SS-FA in FR-positive KB cells in RPMI 1640 medium (Figure 4.8). The RPMI 1640 medium does not contain free FA, so the FA ligand attached to  $\gamma$ -CD-OEI-SS-FA can facilitate the FR-mediated endocytosis.  $\gamma$ -CD-OEI-SS-FA<sub>1.3</sub> showed the highest gene transfection ability among all three  $\gamma$ -CD-OEI-SS-FA samples, namely,  $\gamma$ -CD-OEI-SS-FA<sub>0.8</sub>,  $\gamma$ -CD-OEI-SS-FA<sub>1.3</sub>, and  $\gamma$ -CD-OEI-SS-FA<sub>1.7</sub>. The gene transfection efficiency of  $\gamma$ -CD-OEI-SS-FA<sub>1.3</sub> was also higher than that of PEI (25 kDa) and  $\gamma$ -CD-OEI. Therefore, the grafting ratio of FA in



$\gamma$ -CD-OEI-SS-FA<sub>1.3</sub> is considered optimized, and  $\gamma$ -CD-OEI-SS-FA<sub>1.3</sub> was used in all the other experiments in this work.

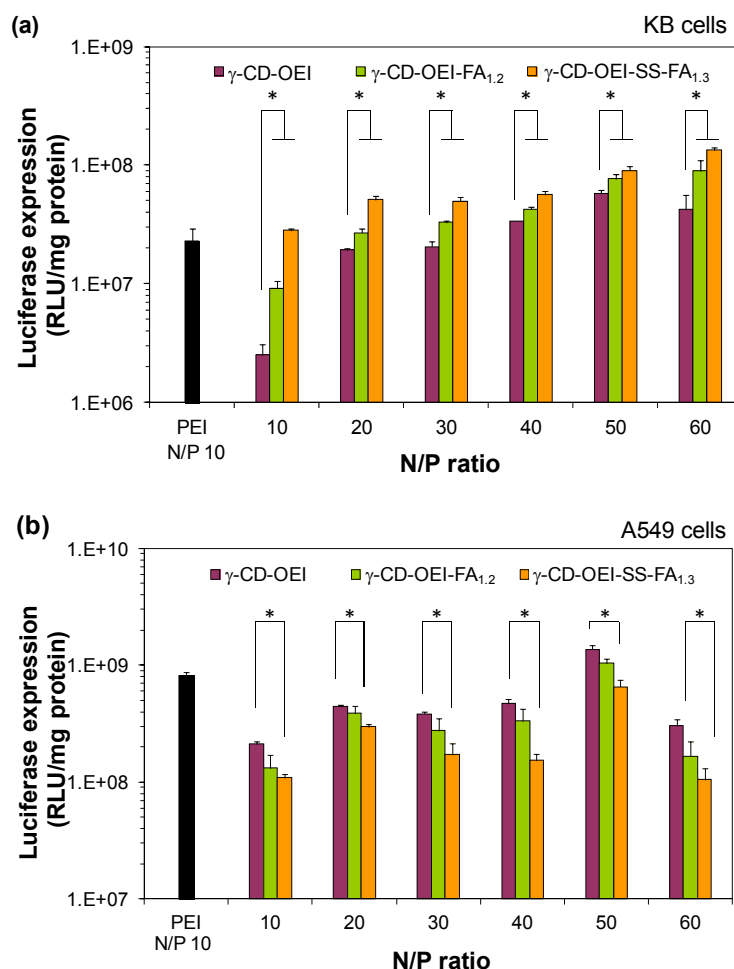


**Figure 4.9.** *In vitro* gene transfection efficiency of the pDNA polyplexes with PEI (25 kDa),  $\gamma$ -CD-OEI,  $\gamma$ -CD-OEI-FA<sub>1.2</sub>, and  $\gamma$ -CD-OEI-SS-FA<sub>1.3</sub> in KB cells (a) and A549 cells (b) in RPMI 1640 medium in the absence of FA. Data represent mean  $\pm$  standard deviation (\* $P$  < 0.05,  $n$  = 4).

Figure 4.9 shows the gene transfection efficiency of  $\gamma$ -CD-OEI-SS-FA<sub>1.3</sub> in KB and A549 cells in comparison with PEI (25 kDa),  $\gamma$ -CD-OEI, and  $\gamma$ -CD-OEI-FA<sub>1.2</sub> in RPMI 1640 medium (without FA in the medium). In FR-positive KB cells (Figure 4.9a), the gene transfection efficiency constantly followed the order  $\gamma$ -CD-OEI-SS-FA<sub>1.3</sub> >  $\gamma$ -CD-OEI-FA<sub>1.2</sub> >  $\gamma$ -CD-OEI. The gene transfection efficiency of  $\gamma$ -CD-OEI-SS-FA<sub>1.3</sub> was also constantly higher than that of PEI (25 kDa). The results indicate that FA-grafted polymers

significantly increased the gene transfection efficiency due to the FR-mediated cellular uptake. When comparing  $\gamma$ -CD-OEI-SS-FA<sub>1.3</sub> and  $\gamma$ -CD-OEI-FA<sub>1.2</sub>, the only difference is that the former had disulfide link between FA and  $\gamma$ -CD-OEI, and the disulfide link could be cleaved by GSH within the cells and then FA could be released (Figure 4.4). Therefore,  $\gamma$ -CD-OEI-SS-FA<sub>1.3</sub> could not only efficiently deliver pDNA into FR-positive cells through FR-mediated cellular uptake, but also cleave FA from the carrier to release FR within the cells, and then recover FR onto cellular membrane to promote continuous FR-mediated cellular uptake of pDNA carried by  $\gamma$ -CD-OEI-SS-FA<sub>1.3</sub>. This is the reason that the transfection efficiency of  $\gamma$ -CD-OEI-SS-FA<sub>1.3</sub> was constantly higher than that of  $\gamma$ -CD-OEI-FA<sub>1.2</sub>. At N/P ratio of 20 to 60, in general, the gene transfection efficiency of  $\gamma$ -CD-OEI-FA<sub>1.2</sub> was 1 to 2 folds higher than that of  $\gamma$ -CD-OEI, while  $\gamma$ -CD-OEI-SS-FA<sub>1.3</sub> was 2 to 4 folds higher than that of  $\gamma$ -CD-OEI, indicating that the significant improvement of the gene delivery efficiency was caused by the FA-conjugation as well as the incorporation of the disulfide bond. However, in FR-negative A549 cells (Figure 4.9b), FR-mediated cellular uptake was impossible, and the FA-conjugation showed no positive effect on the gene transfection efficiency. Inversely, the gene transfection efficiency constantly followed the order  $\gamma$ -CD-OEI >  $\gamma$ -CD-OEI-FA<sub>1.2</sub> >  $\gamma$ -CD-OEI-SS-FA<sub>1.3</sub>, probably due to that the grafted FA interfered the normal endocytosis of the DNA polyplexes.

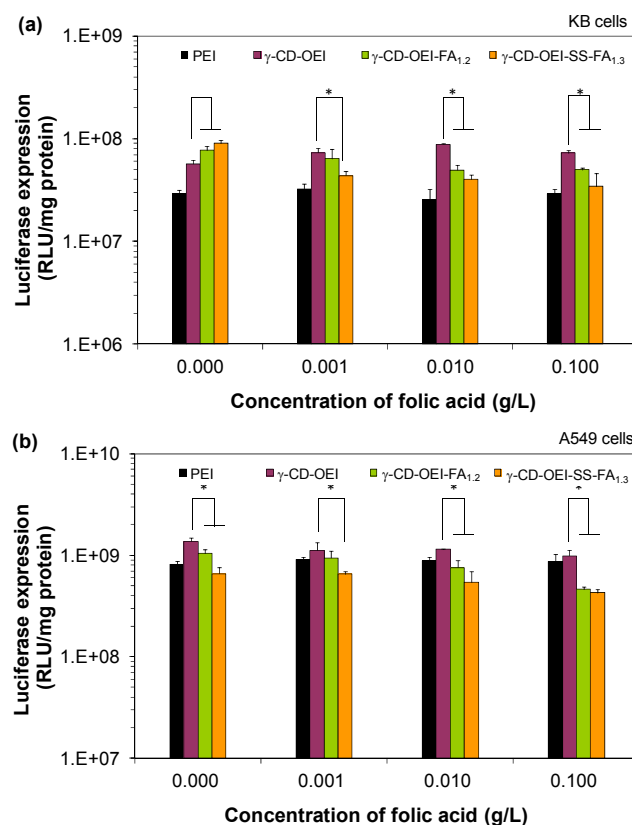


**Figure 4.10.** *In vitro* gene transfection efficiency of the pDNA polyplexes with  $\gamma$ -CD-OEI,  $\gamma$ -CD-OEI-FA<sub>1.2</sub>, and  $\gamma$ -CD-OEI-SS-FA<sub>1.3</sub> at N/P ratio of 50 in comparison with pDNA polyplexes with PEI (25 kDa) at N/P ratio of 10 in KB (a) and A549 (b) cells in RPMI 1640 medium treated with FA at different concentrations (0.000, 0.001, 0.010, and 0.100 g/L). Data represent mean  $\pm$  standard deviation (\* $P < 0.05$ ,  $n = 4$ ).

To further demonstrate the targeted effect of FA-grafted carriers, competition tests were carried out by addition of free FA at different concentrations (0.001, 0.010, and 0.100 g/L) to the cell culture medium during the gene transfection. As shown in Figure 4.10a, the gene transfection efficiency of both  $\gamma$ -CD-OEI-FA<sub>1.2</sub> and  $\gamma$ -CD-OEI-SS-FA<sub>1.3</sub> decreased with an increase in free FA concentration in FR-positive KB cells. In contrast, in Figure 4.10b, there were no significant changes in gene transfection efficiency for all carriers no matter whether there was FA-conjugation or not in FR-negative A549 cells.

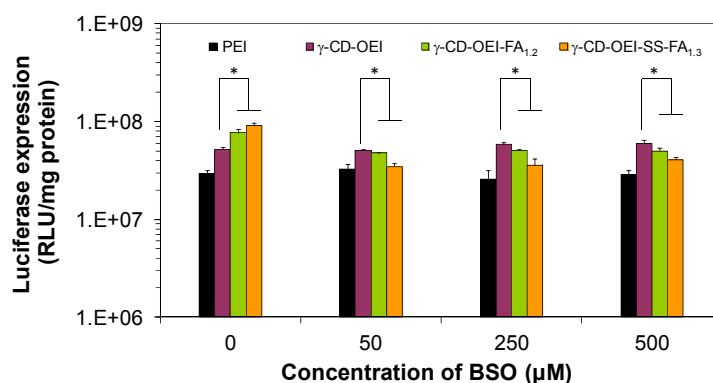


**Figure 4.11.** *In vitro* gene transfection efficiency of the pDNA polyplexes with PEI (25 kDa) at N/P ratio of 10 and pDNA polyplex with  $\gamma$ -CD-OEI,  $\gamma$ -CD-OEI-FA<sub>1,2</sub>, and  $\gamma$ -CD-OEI-SS-FA<sub>1,3</sub> at N/P ratio of 50 in KB cells in RPMI 1640 medium treated with BSO at different concentrations (0, 50, 250, and 500  $\mu$ M). Data represent mean  $\pm$  standard deviation (\* $P < 0.05$ ,  $n = 4$ ).

Sufficient FRs on the surface of cancer cells are a prerequisite for effect FR-mediated endocytosis.<sup>16</sup> Therefore, the continuous recovering and recycling of FRs after cellular endocytosis is necessary for FA-targeted delivery. The biodegradable disulfide bond was used in our gene carrier to recover and recycle the FRs. Figure 4.11 demonstrates the results of the inhibitory test of disulfide bond using BSO, which can reduce the intracellular glutathione concentration,<sup>35, 36</sup> resulting in inhibition of the cleavage of the disulfide bond. The transfection efficiency of  $\gamma$ -CD-OEI-SS-FA<sub>1,3</sub> was significantly affected by the addition of BSO. It was 2-fold higher than that of  $\gamma$ -CD-OEI in the absence of BSO, but lower than that of  $\gamma$ -CD-OEI when BSO was used to inhibit the recovering and recycling of FRs in the FR-positive KB cells. The results further support our hypothesis that the disulfide bond plays an important role in this targeted delivery system. The FA-targeted delivery system with incorporation of disulfide bond is much superior to previous systems.<sup>11</sup>

Finally, plasmid pEGFP-N1 encoding GFP was used to evaluate the GFP expression in KB cells. As shown in Figure 4.12, cells with strong green

fluorescence were observed for EGFP polyplexes with  $\gamma$ -CD-OEI-SS-FA<sub>1.3</sub>, which is significantly more than those of PEI (25 kDa),  $\gamma$ -CD-OEI, and  $\gamma$ -CD-OEI-FA<sub>1.2</sub>. This result further confirms that the gene delivery was enhanced by the FA-targeting moiety as well as the disulfide bond that links FA with the star-shaped cationic polymer.

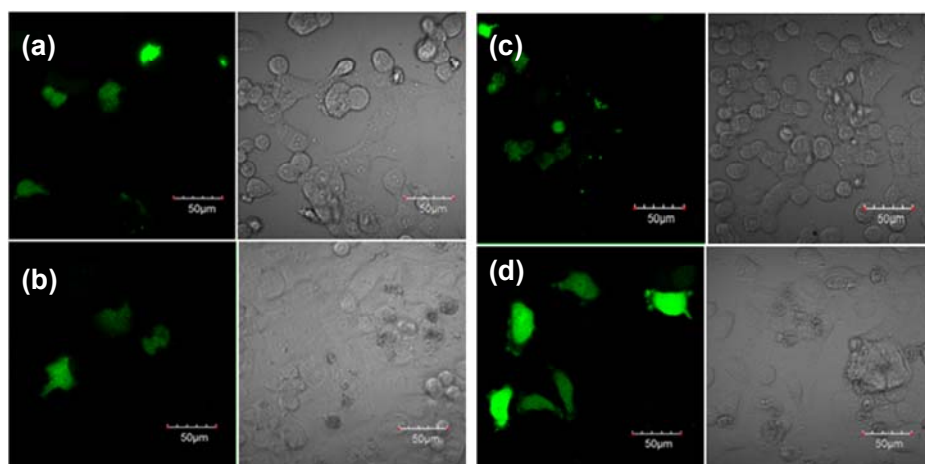


**Figure 4.12.** Confocal microscopy images of transfected KB cells by the EGFP polyplexes with PEI (25 kDa) (a),  $\gamma$ -CD-OEI (b),  $\gamma$ -CD-OEI-FA<sub>1.2</sub> (c), and  $\gamma$ -CD-OEI-SS-FA<sub>1.3</sub> (d) in RPMI 1640 medium in the absence of FA. N/P ratio was 10 for (a), and 50 for (b) – (d). For each experiment, the same field of cells was observed by fluorescent (left) and bright (right) fields to visualize GFP expression.

#### 4.4. Conclusions

This work has designed and synthesized a new star-shaped cationic polymer containing a  $\gamma$ -cyclodextrin ( $\gamma$ -CD) core and multiple oligoethylenimine (OEI) arms with folic acid (FA) linked by a biodegradable disulfide bond for efficient targeted gene delivery. Three samples of the star-shaped cationic  $\gamma$ -CD-OEI-SS-FA polymers were prepared with ratios of FA to  $\gamma$ -CD-OEI of 0.8, 1.3, and 1.7. The  $\gamma$ -CD-OEI-SS-FA polymers could be cleaved efficiently and FA was readily released under reductive condition similar to intracellular environment. The  $\gamma$ -CD-OEI-SS-FA polymers was

characterized and studied in terms of its gene delivery properties in FR-positive KB cells and FR-negative A549 cells under various conditions, in comparison with cationic polymers such as PEI (25 kDa),  $\gamma$ -CD-OEI star-shaped cationic polymer,  $\gamma$ -CD-OEI-FA polymer where FA was directed linked to the star polymer without disulfide linker. The  $\gamma$ -CD-OEI-SS-FA polymers showed similar cytotoxicity to  $\gamma$ -CD-OEI and  $\gamma$ -CD-OEI-FA polymers, and much lower cytotoxicity than PEI (25kDa). The  $\gamma$ -CD-OEI-SS-FA polymers showed good DNA condensation ability and could retard pDNA at N/P ratio of 2.5, which is similar to all comparison cationic polymers used in this study. The  $\gamma$ -CD-OEI-SS-FA polymers formed DNA nanoparticles of sizes ranging from 100 to 150 nm with positive zeta potential ranging from 20 – 40 mV at N/P ratios of 10 to 60.

It was found that  $\gamma$ -CD-OEI-SS-FA<sub>1.3</sub> with the FA to  $\gamma$ -CD-OEI ratio of 1.3 was the optimized composition for targeted gene delivery in FR-positive KB cells. The gene transfection efficiency of  $\gamma$ -CD-OEI-SS-FA<sub>1.3</sub> was up to 6 folds higher than that of PEI (25 kDa), 2 to 4 folds higher than that of  $\gamma$ -CD-OEI, and 2 folds higher than that of  $\gamma$ -CD-OEI-FA<sub>1.2</sub> in FR-positive KB cells. The disulfide linker of  $\gamma$ -CD-OEI-SS-FA<sub>1.3</sub> could be cleaved by GSH within the cells. Therefore,  $\gamma$ -CD-OEI-SS-FA<sub>1.3</sub> could not only efficiently deliver pDNA into FR-positive cells through FR-mediated cellular uptake, but also cleave FA from the carrier to release FR within the cells, and then recover FR onto cellular membrane to promote continuous FR-mediated cellular uptake of pDNA, to achieve very high levels of gene expression. FA competition and disulfide inhibitory tests demonstrated that the significantly enhanced gene expression was induced by the targeted effect of FA and the FR recovery and recycling facilitated by disulfide linker in FR-positive KB cells. Moreover, in FR-negative A549 cells, all the effects due to FA-conjugation and disulfide bond were not observed.

This study has expanded the strategy of FA-targeted delivery by combining the smart FR-recycling function to achieve the significant enhancement of gene expression. The new FA-targeted and biodegradable carrier may be a promising efficient gene delivery system for potential cancer gene therapy.

## 4.5 References

- (1) Mintzer, M. A.; Simanek, E. E., *Chemical Reviews* **2009**,*109*, 259-302.
- (2) Boussif, O.; Lezoualch, F.; Zanta, M. A.; Mergny, M. D.; Scherman, D.; Demeneix, B.; Behr, J. P., *P Natl Acad Sci USA* **1995**,*92*, 7297-7301.
- (3) Godbey, W. T.; Wu, K. K.; Mikos, A. G., *Journal of Biomedical Materials Research* **1999**,*45*, 268-275.
- (4) Fischer, D.; Li, Y. X.; Ahlemeyer, B.; Krieglstein, J.; Kissel, T., *Biomaterials* **2003**,*24*, 1121-1131.
- (5) Davis, M. E.; Brewster, M. E., *Nat Rev Drug Discov* **2004**,*3*, 1023-1035.
- (6) Uekama, K.; Hirayama, F.; Irie, T., *Chemical Reviews* **1998**,*98*, 2045-2076.
- (7) Gonzalez, H.; Hwang, S. J.; Davis, M. E., *Bioconjugate Chem* **1999**,*10*, 1068-1074.
- (8) Hwang, S. J.; Bellocq, N. C.; Davis, M. E., *Bioconjugate Chem* **2001**,*12*, 280-290.
- (9) Cheng, J. J.; Khin, K. T.; Jensen, G. S.; Liu, A. J.; Davis, M. E., *Bioconjugate Chem* **2003**,*14*, 1007-1017.
- (10) Pun, S. H.; Bellocq, N. C.; Liu, A. J.; Jensen, G.; Machemer, T.; Quijano, E.; Schluep, T.; Wen, S. F.; Engler, H.; Heidel, J.; Davis, M. E., *Bioconjugate Chem* **2004**,*15*, 831-840.
- (11) Yang, C. A.; Li, H. Z.; Goh, S. H.; Li, J., *Biomaterials* **2007**,*28*, 3245-3254.
- (12) Li, J.; Loh, X. J., *Adv Drug Deliver Rev* **2008**,*60*, 1000-1017.
- (13) Lu, Y. J.; Low, P. S., *Adv Drug Deliver Rev* **2002**,*54*, 675-693.
- (14) Leamon, C. P.; Low, P. S., *P Natl Acad Sci USA* **1991**,*88*, 5572-5576.
- (15) Turek, J. J.; Leamon, C. P.; Low, P. S., *Journal of Cell Science* **1993**,*106*, 423-430.
- (16) Paulos, C. M.; Reddy, J. A.; Leamon, C. P.; Turk, M. J.; Low, P. S., *Mol Pharmacol* **2004**,*66*, 1406-1414.
- (17) Haensler, J.; Szoka, F. C., *Bioconjugate Chem* **1993**,*4*, 372-379.
- (18) Gosselin, M. A.; Guo, W. J.; Lee, R. J., *Bioconjugate Chem* **2001**,*12*, 989-994.
- (19) Oupicky, D.; Parker, A. L.; Seymour, L. W., *Journal of the American Chemical Society* **2002**,*124*, 8-9.
- (20) Neu, M.; Sitterberg, J.; Bakowsky, U.; Kissel, T., *Biomacromolecules* **2006**,*7*, 3428-3438.
- (21) Kloeckner, J.; Wagner, E.; Ogris, M., *Eur J Pharm Sci* **2006**,*29*, 414-425.
- (22) Neu, M.; Germershaus, O.; Mao, S.; Voigt, K. H.; Behe, M.; Kissel, T., *Journal of Controlled Release* **2007**,*118*, 370-380.
- (23) Dauty, E.; Remy, J. S.; Zuber, G.; Behr, J. P., *Bioconjugate Chem* **2002**,*13*, 831-839.



- (24) Saeed, A. O.; Magnusson, J. P.; Moradi, E.; Soliman, M.; Wang, W. X.; Stolnik, S.; Thurecht, K. J.; Howdle, S. M.; Alexander, C., *Bioconjugate Chem* **2011**, *22*, 156-168.
- (25) Chittimalla, C.; Dalkara, D.; Zuber, G., *Lett Drug Des Discov* **2007**, *4*, 92-98.
- (26) Yang, J. J.; Kularatne, S. A.; Chen, X. M.; Low, P. S.; Wang, E., *Molecular pharmaceutics* **2012**, *9*, 310-317.
- (27) Leamon, C. P.; Reddy, J. A.; Vlahov, L. R.; Westrick, E.; Parker, N.; Nicoson, J. S.; Vetzal, M., *International journal of cancer. Journal international du cancer* **2007**, *121*, 1585-1592.
- (28) Leamon, C. P.; Reddy, J. A.; Vlahov, I. R.; Westrick, E.; Dawson, A.; Dorton, R.; Vetzal, M.; Santhapuram, H. K.; Wang, V., *Molecular pharmaceutics* **2007**, *4*, 659-667.
- (29) Henne, W. A.; Doorneweerd, D. D.; Hilgenbrink, A. R.; Kularatne, S. A.; Low, P. S., *Bioorganic & medicinal chemistry letters* **2006**, *16*, 5350-5355.
- (30) Guo, R.; Li, L. L.; Zhao, W. H.; Chen, Y. X.; Wang, X. Z.; Fang, C. J.; Feng, W.; Zhang, T. L.; Ma, X.; Lu, M.; Peng, S. Q.; Yan, C. H., *Nanoscale* **2012**, *4*, 3577-3583.
- (31) Ishida, O.; Maruyama, K.; Sasaki, K.; Iwatsuru, M., *International journal of pharmaceutics* **1999**, *190*, 49-56.
- (32) Kong, G.; Braun, R. D.; Dewhirst, M. W., *Cancer Res* **2000**, *60*, 4440-4445.
- (33) Fischer, D.; Bieber, T.; Li, Y. X.; Elsasser, H. P.; Kissel, T., *Pharmaceut Res* **1999**, *16*, 1273-1279.
- (34) Troen, A. M.; Mitchell, B.; Sorensen, B.; Wener, M. H.; Johnston, A.; Wood, B.; Selhub, J.; McTiernan, A.; Yasui, Y.; Oral, E.; Potter, J. D.; Ulrich, C. M., *Journal of Nutrition* **2006**, *136*, 189-194.
- (35) Xu, K.; Thornalley, P. J., *Biochem Pharmacol* **2001**, *61*, 165-177.
- (36) Song, J. J.; Lee, Y. J., *The Biochemical journal* **2003**, *373*, 845-853.

## **CHAPTER 5 A MULTIFUNCTIONAL SUPRAMOLECULAR SELF-ASSEMBLY FORMING A SYNERGISTIC TARGETED AND CO-DELIVERY SYSTEM OF GENE AND DRUG FOR POTENTIAL CANCER THERAPY**

### **5.1. Introduction**

Combination of two or more different therapeutic and delivery strategies with synergistic and enhancement effects is becoming a promising approach for cancer therapy.<sup>1-5</sup> Paclitaxel (PTX) is one of the most commonly used chemotherapeutic drugs against ovarian, breast, head and neck, and non-small-cell lung cancers.<sup>6, 7</sup> PTX binds to tubulin and promotes tubulin polymerization and stabilization of microtubules against depolymerization.<sup>8, 9</sup> As a result, PTX-induced microtubule stabilization leads to G2/M cell cycle arrest and cell death.<sup>10</sup> One of the major problems for PTX application is its low aqueous solubility (0.3 µg/mL).<sup>11</sup> On the other hand, chemotherapy is generally limited by the side effects and multidrug resistance.

Gene therapy has obtained great attention over the past two decades as an alternative method to conventional chemotherapy.<sup>12, 13</sup> Tumor suppressor

protein gene, such as p53, is one of the most frequently delivered genes for effective cancer therapy. The p53 protein plays a role as a prevailing guardian in damaged or transformed cells, which induces cell growth arrest or apoptosis.<sup>14</sup> Cells cannot control their growth if normal protective function of p53 is lost, resulting in rapid growth and progression toward malignancy.<sup>15, 16</sup> Moreover, mutant or loss of p53 gene has been found in around 50% of human cancers,<sup>17</sup> and the loss of p53 may also result in resistance to radiotherapy or chemotherapy.<sup>18</sup> Therefore, the reinstatement of wild-type p53 expression is a reasonable approach for cancer therapy.

Co-delivery of DNA and anticancer drug, such as doxorubicin and PTX has shown great promise to achieve the synergistic or combined effects in cancer therapy.<sup>19-25</sup> The co-delivery of paclitaxel and plasmid DNA by cationic core-shell nanoparticles improved gene transfection both *in vitro* and *in vivo*.<sup>21</sup> The co-delivery of doxorubicin and p53 gene by micelles increased p53 mRNA expression level as well as cytotoxicity towards HepG2 cells.<sup>19</sup> The presence of PTX would enhance gene expression possibly due to its anti-mitotic function.<sup>26, 27</sup> Although PTX-induced apoptosis is p53-independent,<sup>10, 28</sup> the status of p53 may influence the cell-cycle progression following mitotic arrest.<sup>29, 30</sup> Adenovirus-mediated p53 gene therapy with PTX had synergistic effect in many cancer cell lines.<sup>31</sup>

Cyclodextrins ( $\alpha$ -,  $\beta$ -, and  $\gamma$ -CD) are a series of natural cyclic oligosaccharides consisting of 6, 7, or 8 D(+)-glucose units, taking a torus-like structure with a hydrophobic cavity.<sup>32</sup> These water-soluble molecules have low toxicity in animals and humans.<sup>33</sup> CDs are potential candidates for drug delivery thanks to their ability to form inclusion complexes with guest molecules and consequently change their physical, chemical, and biological properties.<sup>34</sup> Inclusion complexes between CD derivatives and PTX to improve the physical properties of PTX have been widely investigated in the last two decades.<sup>35-41</sup> Davis' group synthesized CD-based cationic polymers

for gene delivery.<sup>42-45</sup> Our group also reported a series of CD-based cationic star-shape or supramolecular polymers by grafting oligoethylenimine (OEI) chains to CD rings as non-viral gene delivery vectors,<sup>46-49</sup> which showed much lower cytotoxicity and improved gene transfection efficiency that were comparable to or even higher than that of high molecular weight branched PEI (25 kDa). We recently developed folic acid (FA) modified  $\gamma$ -CD-OEI with bio-reducible disulfide linker ( $\gamma$ -CD-OEI-SS-FA) as an efficient gene delivery carrier.<sup>50</sup> The new  $\gamma$ -CD-OEI-SS-FA carrier can specifically target and deliver DNA to cancer cells that overexpress folate receptors (FRs) due to the ligand-receptor interaction and the recycling of FRs onto cellular membranes to assist FR-mediated endocytosis induced by the reduction of disulfide linker within the cells.

In this work, the  $\gamma$ -CD-OEI-SS-FA gene carrier has been developed into a multifunctional drug and gene co-delivery system through supramolecular self-assembly to form inclusion complexation between the  $\gamma$ -CD core and PTX followed by polyplexing plasmid DNA (pDNA) encoding luciferase or *p53* gene (Scheme 5.1). Our data have demonstrated that the multifunctional  $\gamma$ -CD-OEI-SS-FA/PTX self-assembly co-delivery system showed the combined and synergistic effects of the PTX-enhanced gene transfection, the FA-targeted delivery, and the disulfide linker mediated FR-recycling. The multifunctional synergistic effects resulted in very effective delivery of wild-type *p53* gene into FR-overexpressed KB cancer cells at very low N/P ratios to induce an efficient cell apoptosis for potential cancer therapy.

## **5.2. Experimental Section**

### **5.2.1. Materials**

Paclitaxel (PTX) was purchased from LC Laboratories (MA, USA). *N,N'*-dicyclohexylcarbodiimide (DCC), 4-dimethylaminopyridine (DMAP), rhodamine B (Rhd), fluorescein isothiocyanate (FITC), buthionine

sulphoximine (BSO), and anhydrous dimethyl sulfoxide (DMSO) were purchased from Sigma-Aldrich. 3-(4,5-Dimethyl-thiazol-2-yl)-2,5-diphenyl tetrazodium bromide (MTT) was obtained from Alfa Aesar (MA, USA). D<sub>2</sub>O and CDCl<sub>3</sub> used as solvents in the NMR measurement were purchased from Cambridge Isotope Laboratories, Inc. (Andover, USA).  $\gamma$ -CD-OEI-SS-FA and its control compounds  $\gamma$ -CD-OEI and  $\gamma$ -CD-OEI-FA were synthesized according to our previous report.<sup>50</sup>

### 5.2.2. Preparation of Inclusion Complexes

The general synthesis procedure of inclusion complexes of  $\gamma$ -CD-OEI-SS-FA (or the control compounds) with PTX is as follows. To a solution of  $\gamma$ -CD-OEI-SS-FA (10  $\mu$ mol) in water (1 mL) was added a solution of PTX (8.5 mg, 10  $\mu$ mol) in ethanol (1 mL). The suspension was then stirred for five days in the dark until a clear solution formed. The mixture was concentrated under vacuum to a volume of c.a. 1 mL, centrifuged to remove unreacted PTX, and then freeze dried to yield the product.

$\gamma$ -CD-OEI/PTX inclusion complex was colorless solid (65 mg, yield 99%). <sup>1</sup>H NMR: (400 MHz, D<sub>2</sub>O):  $\delta$  7.22 – 8.13 (m, 15 H, ArH of PTX), 4.80 – 5.65 (m, 12 H, H-1 of  $\gamma$ -CD, H of PTX), 2.87 – 4.55 (m, 69 H, H-2-6 of  $\gamma$ -CD, -CONHCH<sub>2</sub>- of OEI, H of PTX), 2.00 – 2.87 (m, 407 H, -CH<sub>2</sub>CH<sub>2</sub>NH- of OEI, H of PTX), 0.80 – 2.00 (m, 18 H, H of PTX).

$\gamma$ -CD-OEI-FA/PTX inclusion complex was yellow solid (68 mg, yield 97%). <sup>1</sup>H NMR: (400 MHz, D<sub>2</sub>O):  $\delta$  8.52 (s, 1.2 H, -CH- of pyrazine on FA), 7.20 – 8.12 (m, 17.4 H, ArH of PTX, 2.4 H, -CH- of phenyl ring on FA), 6.69 (d, 2.4 H, -CH- of phenyl ring on FA), 4.70 – 5.62 (m, 12 H, H-1 of  $\gamma$ -CD, H of PTX), 2.93 – 4.52 (m, 77 H, H-2-6 of  $\gamma$ -CD, -CONHCH<sub>2</sub>- of OEI, H of PTX), 2.00 – 2.93 (m, 407 H, -CH<sub>2</sub>CH<sub>2</sub>NH- of OEI, H of PTX), 0.80 – 2.00 (m, 18 H, H of PTX).

$\gamma$ -CD-OEI-SS-FA/PTX inclusion complex was yellow solid (72 mg, yield 97%).  $^1\text{H}$  NMR: (400 MHz,  $\text{D}_2\text{O}$ ):  $\delta$  8.40 – 8.60 (m, 1.3 H, -CH- of pyrazine on FA), 7.20 – 8.12 (m, 17.6 H, ArH of PTX, 2.6 H, -CH- of phenyl ring on FA), 6.60 – 6.80 (m, 2.6 H, -CH- of phenyl ring on FA), 6.69 (d, 2.4 H, -CH- of phenyl ring on FA), 4.72 – 5.65 (m, 12 H, H-1 of  $\gamma$ -CD, H of PTX), 2.97 – 4.52 (m, 77 H, H-2-6 of  $\gamma$ -CD, -CONHCH<sub>2</sub>- of OEI, H of PTX), 2.00 – 2.97 (m, 407 H, -CH<sub>2</sub>CH<sub>2</sub>NH- of OEI, H of PTX), 0.80 – 2.00 (m, 18 H, H of PTX).

*Fluorescence Labeling:* The general synthesis procedure of rhodamine-grafted  $\gamma$ -CD-OEI-SS-FA (or the control compounds) is as follows. To a solution of  $\gamma$ -CD-OEI derivatives (2  $\mu\text{mol}$ ) in anhydrous DMSO (1 mL) was added rhodamine B (1.4 mg, 3  $\mu\text{mol}$ ), DCC (0.8 mg, 4  $\mu\text{mol}$ ), and DMAP (0.05 mg, 0.4  $\mu\text{mol}$ ). The mixture was then stirred at room temperature for one day in the dark. Purification by dialysis (MWCO 2000) against water was conducted in the dark for five days. The mixture was freeze dried to yield red oil product. Three rhodamine-grafted carriers were synthesized, including  $\gamma$ -CD-OEI-Rhd,  $\gamma$ -CD-OEI-FA-Rhd, and  $\gamma$ -CD-OEI-SS-FA-Rhd.

*PTX Labeling:* The synthesis method for PTX-FITC was adopted from previous report.<sup>51</sup> According to the reference, the 7-substituted fluorescent PTX maintains its bioactivity. Moreover, the modification of 7-position will not influence the formation of inclusion complex with CD, since the A and B phenyl rings of PTX are the binding groups within the cavity of CD.<sup>37, 38</sup>

### **5.2.3. Characterization Methods**

*Gel Permeation Chromatography:* Gel permeation chromatography (GPC) analysis was conducted on a Shimadzu SCL-10A and LC-10AT system equipped with a Sephadex G-75 column (size: 2.5  $\times$  32 cm) and a Shimadzu RID-10A refractive index detector. PBS buffer solution (0.5  $\times$ ) was used as the eluent, and the fractions were collected per 2 mL and were further detected

with a HORIBA SEPA-300 high speed accurate polarimeter at wavelength 589 nm with cell length 10 cm and response 2 s.

*<sup>1</sup>H NMR Spectroscopy:* <sup>1</sup>H NMR spectra were measured on a Bruker AV-400 NMR spectrometer at 400 MHz. The <sup>1</sup>H NMR measurements were carried out with an acquisition time of 3.2 s, a pulse repetition time of 2.0 s, a 30° pulse width, 5208 Hz spectral width, and 32 K data points. Chemical shifts were referenced to the solvent peak ( $\delta = 4.70$  ppm for D<sub>2</sub>O).

*UV-vis Spectroscopy:* All absorption spectra were recorded on a Shimadzu UV 2501 spectrophotometer against water blank. Absorption was measured in quartz cuvettes (frosted wall, 0.7 mL). All the samples were diluted to 0.1 mg/mL of aqueous solutions.

### 5.2.4. Biological Characterization Methods

*Plasmids:* The plasmid pRL-CMV encoding a *Renilla* luciferase reporter gene was purchased from Promega (Madison, USA). The plasmid pCMV-p53 (wild type) and pCMV-p53mt135 (dominant-negative) were purchased from Clontech Laboratories Inc. (Mountain View, USA). All these plasmids were amplified in *Escherichia coli* and purified according to the protocol of suppliers (Qiagen, Hilden, Germany). The concentrations of the purified plasmid DNA were measured by UV spectroscopy under optical density at 260 and 280 nm. The quality was analyzed by gel electrophoresis. The plasmids were resuspended in TE buffer (10 mM Tris-Cl, pH 7.5, 1 mM EDTA) and kept at a concentration of 0.5 mg/mL for storage.

*Cells and Media:* KB and A549 cell lines were purchased from ATCC (Rockville, MD). KB cells are FR-positive human nasopharyngeal cells, cultured in Minimum Essential Medium (MEM) supplemented with 10% heat-inactivated fetal bovine serum (FBS), 0.3 g/L of L-glutamine, 0.1 g/L of sodium pyruvate, 100 units/mg of penicillin, and 100  $\mu$ g/mL of streptomycin. The A549 human lung epithelial carcinoma cell line was cultured in Ham's

F-12 Nutrient Mixture (F-12) supplemented with 10% FBS, 100 units/mg of penicillin, and 100 µg/mL of streptomycin. Roswell Park Memorial Institute (RPMI) 1640 medium (FA free) supplemented with 10% FBS, 100 units/mg of penicillin, and 100 µg/mL of streptomycin was used during cell viability and gene delivery test. All the cells were cultured in an incubator at 37 °C with 5% CO<sub>2</sub>, and 95% relative humidity. MEM, F-12, and FA-free RPMI 1640 medium were purchased from Gibco BRL (Invitrogen, Singapore).

*Gel Retardation Assay:* Gel electrophoresis was used to assay the binding ability of all the synthesized polymers with plasmid pRL-CMV. Briefly, 5 µL of polymer solutions were added into 5 µL of plasmid solutions (0.1 mg/mL) to prepare various nitrogen/phosphate (N/P) ratio solutions from 0 to 4. The polyplexes were incubated for 30 min at room temperature, and then mixed with 1 µL of loading buffer (10×) before loading to 1% agarose gel containing 0.5 µg/mL of ethidium bromide (EtBr). Gel electrophoresis was carried out in TAE buffer (40 mM Tris-acetate, 1 mM EDTA) at 100 V for 30 min in a Sub-Cell system (Bio-Rad Laboratories, CA). DNA bands were visualized by a UV lamp with MULTI GENIUS BioImaging System (Syngene, UK).

*Dynamic Light Scattering and Zeta-potential Measurements:* Particle size and zeta potential of the polymer/pRL-CMV polyplexes were tested by a Zetasizer Nano ZS (Malvern Instruments, Southborough, USA) with a laser light wavelength of 633 nm at a 173° scattering angle. In general, 50 µL of polymer solutions were added into 50 µL of plasmid solutions (0.1 mg/mL) to prepare various solutions with N/P ratios ranging from 10 to 50. The mixtures were vortexed for 20 s and incubated at room temperature for 30 min. The polyplexes were diluted with 0.9 mL of distilled water and vortexed for 20 s before test. The particle size measurement was done at 25 °C. The deconvolution of the measured correlation curve to an intensity size distribution was accomplished using a nonnegative least squares algorithm. The Z-average hydrodynamic diameters of the particles were provided by the



instrument. The Z-average size is the intensity weighted mean diameter derived from a Cumulants or single-exponential fit of the intensity autocorrelation function. The zeta potential measurement was tested using a capillary zeta potential cell in automatic mode.

*Cell Viability Assay:* 100  $\mu\text{L}$  of FA-free RPMI 1640 medium with  $1.5 \times 10^4$  KB cells was seeded into 96-well plates (NUNC, Wiesbaden, Germany). After 24 h, the culture media were replaced with fresh media containing serial dilutions of polymers, and then the cells were cultured for an additional 20 h. Then, 10  $\mu\text{L}$  of sterile filtered MTT (5 mg/mL) stock solution in PBS was added to each well. After incubation for 4 h, the medium were removed by aspiration. The formazan crystals were dissolved in 100  $\mu\text{L}$ /well of DMSO. Then the absorbance was measured by a microplate reader (Spectra Plus, TECAN) at a wavelength of 570 nm. The relative cell growth (%) related to control cells without polymer was calculated by  $[A]_{\text{test}}/[A]_{\text{control}} \times 100\%$ .

*In vitro Transfection and Luciferase Assay:* Gene transfection efficiency was tested using pRL-CMV as reporter gene in KB and A549 cells. Cells with a density of  $8 \times 10^4$ /well (KB cells) or  $6 \times 10^4$ /well (A549 cells) were seeded into 24-well plates for 24 hours. 10  $\mu\text{L}$  of polymer solutions were added into 10  $\mu\text{L}$  of plasmid solutions (0.1 mg/mL) to prepare various solutions with N/P ratios ranging from 10 to 50. The polyplexes were vortexed for 20 s and incubated for 30 min at room temperature before the transfection. Each well was first replaced with 400  $\mu\text{L}$  of fresh FA-free RPMI 1640 medium, and then added 20  $\mu\text{L}$  of polymer/DNA polyplexes. After incubation for 4 hours, the medium was replaced with 500  $\mu\text{L}$  of fresh FA-free RPMI 1640 medium, and the cells were further incubated for 20 hours under the same conditions. At the end of transfection, cells were washed with PBS twice and added 100  $\mu\text{L}$  of lysis reagent (Promega, Cergy Pontoise, France). The plates were shook at 1000 rpm for 1 hour at room temperature before test. Luciferase gene expression was tested using a commercial kit (Promega, Cergy Pontoise,

France) by a luminometer (Berthold Centro LB 960, Germany). The Protein concentrations were measured by Commassie Plus<sup>TM</sup> Protein Assay Reagent (Pierce). Absorption was measured using a microplate reader (Spectra Plus, TECAN) at 595 nm and compared to a standard curve calibrated by BSA solutions. The results are expressed as relative light units per milligram of cell protein lysate (RLU/mg protein).

*FA Competition and BSO Inhibitory Test:* FA competition and BSO inhibitory test were carried out to inhibit the FR-mediated endocytosis and disulfide linker-mediated FR recycling function. The transfection procedure is the same as previous described luciferase assay. RPMI 1640 medium with 0.001 g/L of FA or 250  $\mu$ M of BSO was used in these two experiments, respectively. The optimal N/P ratio of 15 was adopted at which the PTX inclusion complexes have the highest transfection efficiency.

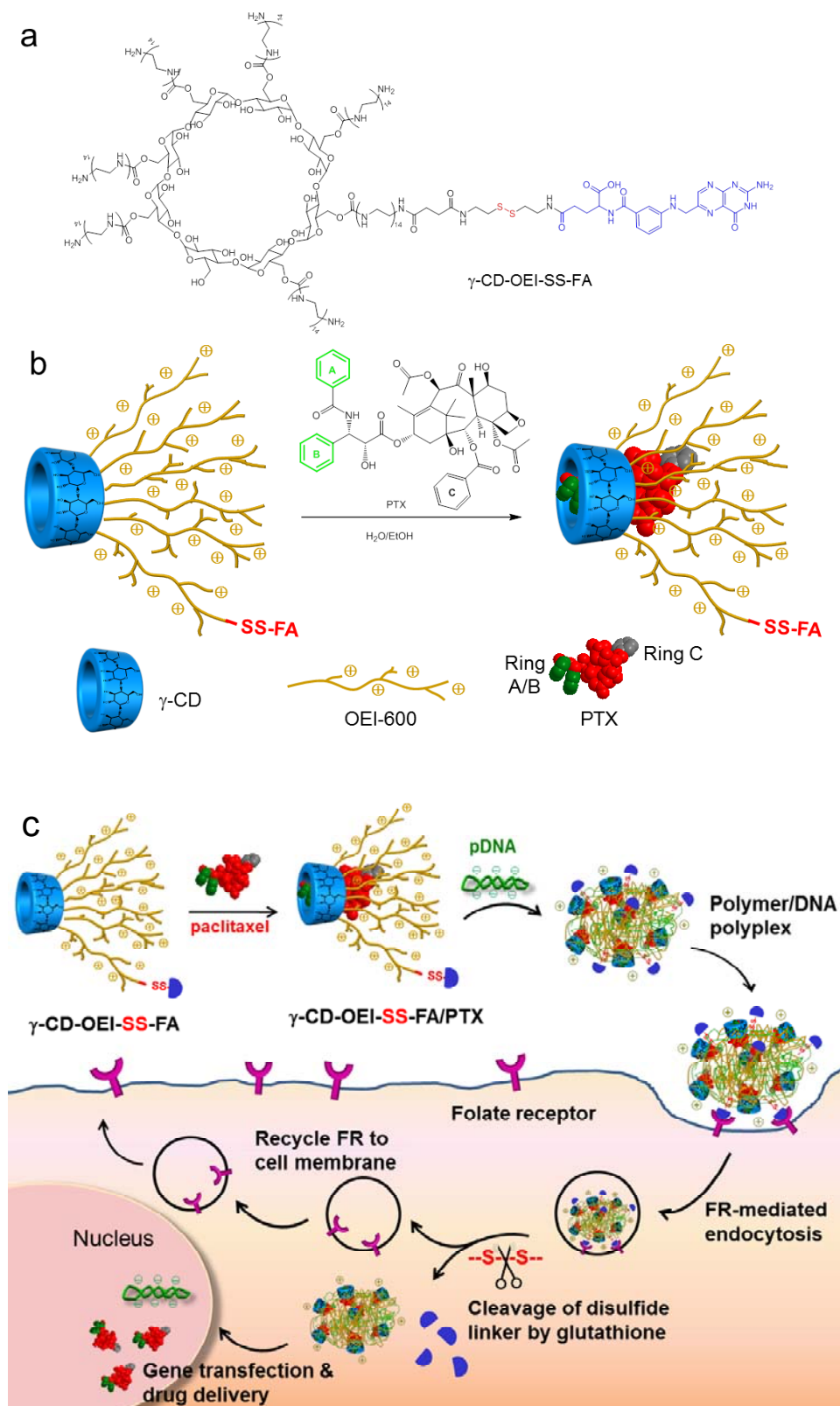
*Cell Cycle Analysis:* Two plasmids pCMV-p53 and mutant pCMV-p53mt135 were delivered into FR-positive KB cells and FR-negative A549 cells by the cationic polymers to assay the cell growth inhibition. The pCMV-p53 expresses the wild-type p53 tumor suppression protein while the pCMV-p53mt135 expresses a dominant-negative mutant. The procedure of transfection is the same as previously described. At the end of transfection, the cells were washed with PBS twice and added 300  $\mu$ L of 1 $\times$  trypsin. After incubation for 8 min, 500  $\mu$ L of medium was added. The cells were collected by centrifuge at 2000 rpm for 5 min, washed with PBS, and fixed with 70% ethanol for 2 h at 4  $^{\circ}$ C. After washing with PBS, the cells were suspended into PBS solutions with 0.2% Triton X-100, 20  $\mu$ g/mL of propidium iodide, and 0.2 mg/mL of RNase (BD Biosciences, San Diego, CA). The mixtures were incubated at 37  $^{\circ}$ C for 20 min and stored at 4  $^{\circ}$ C before test. The distribution of cells in the various phases of cell cycle (sub G1, G0/G1, S, and G2/M) was measured using flow cytometry (FACSCalibur, Becton Dickinson, NJ).

*Confocal Microscopy:* Confocal microscopy was conducted to assay the cellular uptake of pRL-CMV polyplexes with the rhodamine stained cationic polymers and their inclusion complexes with FITC stained PTX. In brief, a density of  $1.5 \times 10^4$ /well KB cells in 0.3 ml of FA-free RPMI 1640 medium were seeded onto a Lab-Tekfour-chambered coverglass system (Nalge-Nane International, Naperville, IL). After 24 h, the pRL-CMV polyplexes with  $\gamma$ -CD-OEI-Rhd,  $\gamma$ -CD-OEI-FA-Rhd,  $\gamma$ -CD-OEI-SS-FA-Rhd, and the inclusion complexes of  $\gamma$ -CD-OEI-Rhd/PTX-FITC,  $\gamma$ -CD-OEI-FA-Rhd/PTX-FITC,  $\gamma$ -CD-OEI-SS-FA-Rhd/PTX-FITC, and  $\gamma$ -CD-OEI-SS-FA/PTX-FITC at N/P ratio of 15 were added into the transfection medium. After incubation for 1 h, the medium was replaced with 0.3 mL of fresh medium and imaged using an Olympus Fluoview FV500 confocal laser scanning microscope (Olympus, Japan). The excitation wavelength was set at 488 nm for FITC and 559 nm for rhodamine. The optical filter for emission signal of FITC and rhodamine is 515 nm and 575 to 675 nm, respectively.

*Statistical Analysis:* Statistical analysis was performed by a standard Student's *t*-test with a minimum confidence level of 0.05 as significant statistical difference. All the data are reported as mean  $\pm$  standard deviation.

## 5.3. Results and Discussion

### 5.3.1. Synthesis of Self-assembled Inclusion Complexes



**Scheme 5.1.** (a) Structures of  $\gamma$ -CD-OEI-SS-FA. (b) Schematic presentation of the supramolecular self-assembly process for formation of the  $\gamma$ -CD-OEI-SS-FA/PTX inclusion complex. (c) Illustration of the concept of the drug and gene co-delivery mediated by the multifunctional supramolecular self-assembly.

The  $\gamma$ -CD-based gene carriers, including  $\gamma$ -CD-OEI,  $\gamma$ -CD-OEI-FA, and  $\gamma$ -CD-OEI-SS-FA were synthesized according to our previous reported procedures,<sup>50</sup> and their structures are shown in Scheme 5.1. The  $\gamma$ -CD core of these gene carriers should be capable of forming inclusion complexes with hydrophobic drugs such as PTX. To synthesize the inclusion complexes of PTX with these  $\gamma$ -CD-based gene carriers, 1:1 ratio of  $\gamma$ -CD-based cationic polymers and PTX were dissolved in a mixture of water and ethanol (v:v = 1:1) and stirred at room temperature for five days in the dark. As the PTX was gradually included into the hydrophobic cavity of the  $\gamma$ -CD ring, the reaction mixture turned from a suspension to a clear solution after rigorous stirring. The formation of clear solution was considered completion of the inclusion complexation, and the time required for the completion of complexation followed the order  $\gamma$ -CD-OEI <  $\gamma$ -CD-OEI-FA  $\leq$   $\gamma$ -CD-OEI-SS-FA due to the steric effects.

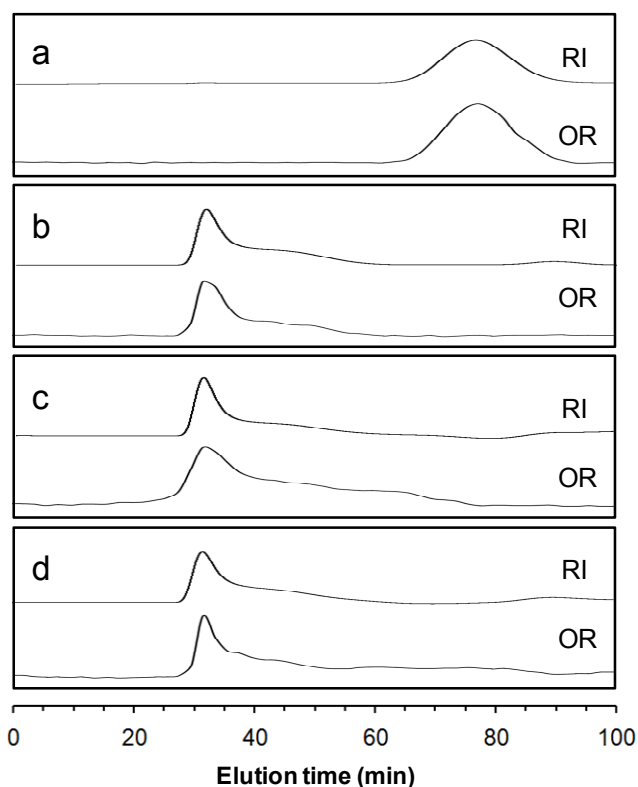


**Figure 5.1.** Size exclusion chromatography diagrams of  $\gamma$ -CD (a),  $\gamma$ -CD-OEI (b),  $\gamma$ -CD-OEI-SS-FA (c), and  $\gamma$ -CD-OEI-SS-FA/PTX (d) recorded with refractive index (RI) and optical rotation (OR).

Figure 5.1 shows the size exclusion chromatography diagrams of  $\gamma$ -CD-OEI-SS-FA/PTX inclusion complex in comparison with  $\gamma$ -CD-OEI-SS-FA,  $\gamma$ -CD-OEI, and  $\gamma$ -CD. Free  $\gamma$ -CD (MW 1297) has small molecular size, whose peak was observed at the low molecular weight range of the diagram. The peaks of  $\gamma$ -CD-OEI,  $\gamma$ -CD-OEI-SS-FA, and  $\gamma$ -CD-OEI-SS-FA/PTX complex were observed at high molecular weight range, showing similar elution times due to the similar molecular weights (5686, 6542, and 7396 Da, respectively).

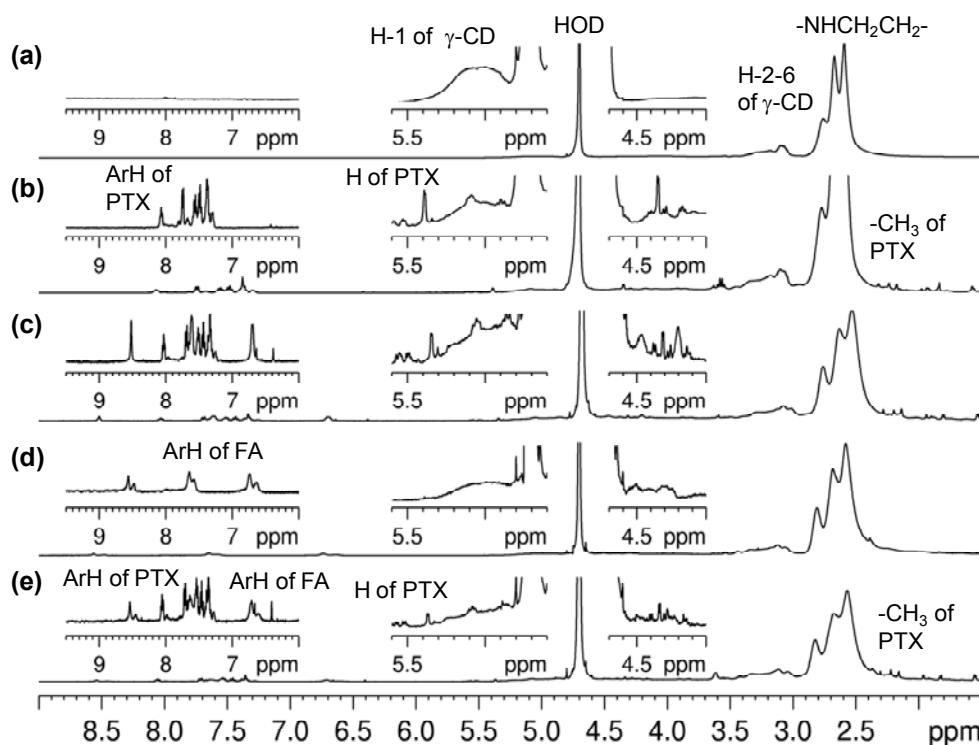


**Figure 5.2.**  $^1\text{H}$  NMR spectra of  $\gamma\text{-CD-OEI}$  (a),  $\gamma\text{-CD-OEI/PTX}$  (b),  $\gamma\text{-CD-OEI-FA/PTX}$  (c),  $\gamma\text{-CD-OEI-SS-FA}$  (d), and  $\gamma\text{-CD-OEI-SS-FA/PTX}$  (e) in  $\text{D}_2\text{O}$ .

PTX has very poor water solubility,<sup>11</sup> which gives no signals in  $^1\text{H}$  NMR and UV-vis spectroscopy when  $\text{D}_2\text{O}$  and water were used as solvent, respectively. Therefore, the successful complexation of PTX in  $\gamma\text{-CD}$  can be proved by the appearance of the  $^1\text{H}$  NMR peaks and UV-vis absorption when the complexes are dissolved in  $\text{D}_2\text{O}$  or water. Figure 5.2 shows the  $^1\text{H}$  NMR spectra of the inclusion complexes  $\gamma\text{-CD-OEI/PTX}$ ,  $\gamma\text{-CD-OEI-FA/PTX}$ , and  $\gamma\text{-CD-OEI-SS-FA/PTX}$  in comparison with  $\gamma\text{-CD-OEI}$  and  $\gamma\text{-CD-OEI-SS-FA}$ . The typical signals of PTX phenyl rings can be observed at  $\delta$  7.2 – 8.2, and the stoichiometry can be calculated by comparing the integral strengths of PTX phenyl rings and OEI arms. As a result, one PTX molecule is included in one  $\gamma\text{-CD}$  cavity, corresponding to 13.0, 11.5, and 10.4% loading level of PTX in the inclusion complexes. To further confirm the formation of the inclusion complexes, UV-vis spectra were measured. As shown in Figure 5.3, all the

inclusion complexes, including  $\gamma$ -CD-OEI/PTX,  $\gamma$ -CD-OEI-FA/PTX, and  $\gamma$ -CD-OEI-SS-FA/PTX, have obvious absorption peaks at 230 nm, indicating the successful complexation of PTX in the  $\gamma$ -CD cavity.

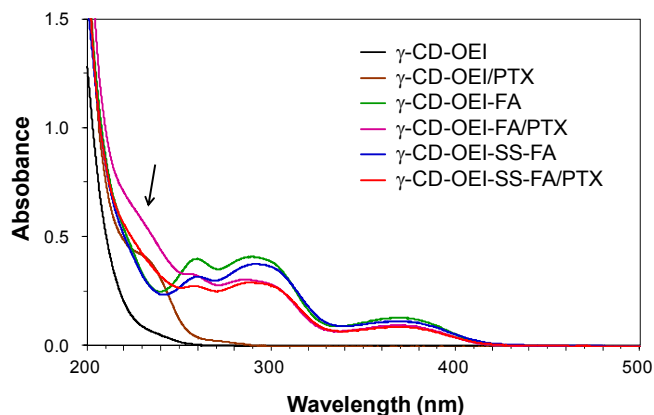


**Figure 5.3.** UV-vis spectra of  $\gamma$ -CD-OEI,  $\gamma$ -CD-OEI/PTX,  $\gamma$ -CD-OEI-FA,  $\gamma$ -CD-OEI-FA/PTX,  $\gamma$ -CD-OEI-SS-FA, and  $\gamma$ -CD-OEI-SS-FA/PTX at 0.1 mg/mL in H<sub>2</sub>O. The arrow indicates UV absorption of PTX at 230 nm.

### 5.3.2. Formation of Polyplexes with pDNA

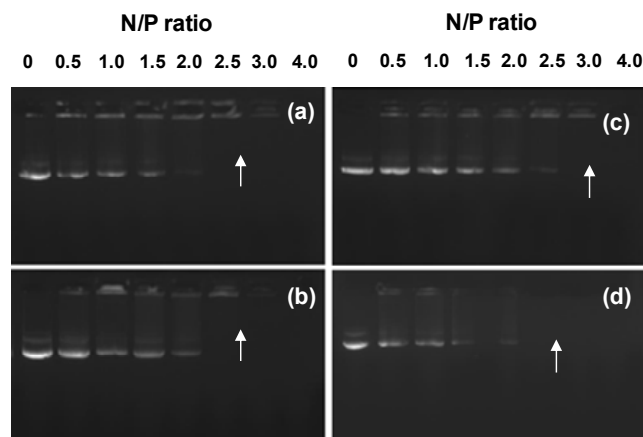


**Figure 5.4.** Electrophoretic mobility of pDNA in the polyplexes formed with PEI (a),  $\gamma$ -CD-OEI/PTX (b),  $\gamma$ -CD-OEI-FA/PTX (c), and  $\gamma$ -CD-OEI-SS-FA/PTX (d). The arrows indicate the N/P ratios where the DNA mobility is completely retarded.

The binding ability of the  $\gamma$ -CD-OEI/PTX,  $\gamma$ -CD-OEI-FA/PTX, and  $\gamma$ -CD-OEI-SS-FA/PTX inclusion complexes to pDNA *pRL-CMV* was



analyzed by agarose gel electrophoresis in comparison with PEI (25 kDa). Figure 5.4 shows that PEI,  $\gamma$ -CD-OEI/PTX,  $\gamma$ -CD-OEI-FA/PTX, and  $\gamma$ -CD-OEI-SS-FA/PTX entirely compacted pDNA at N/P ratios of 2.5, 2.5, 3.0, and 2.5, respectively. The results indicate that the binding ability of the inclusion complexes is strong, which is similar to that of PEI, as well as to that of the PTX-free  $\gamma$ -CD-OEI,  $\gamma$ -CD-OEI-FA, and  $\gamma$ -CD-OEI-SS-FA<sup>50</sup>.

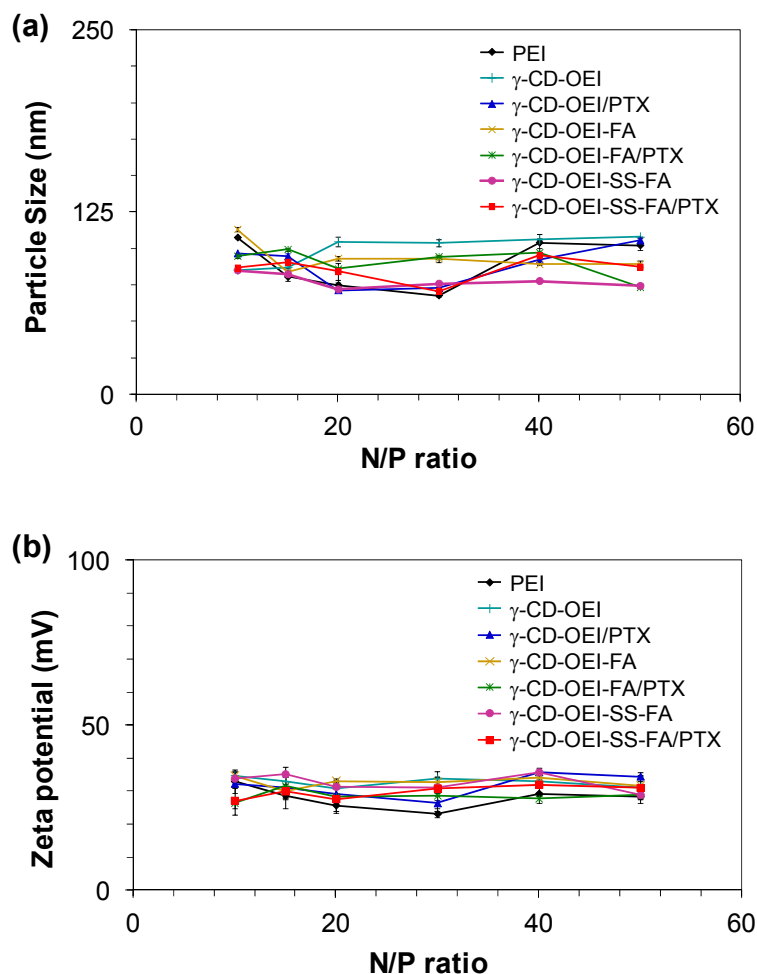


**Figure 5.5.** Particle size (a) and zeta potential (b) of the pDNA polyplexes with PEI (25 kDa),  $\gamma$ -CD-OEI,  $\gamma$ -CD-OEI/PTX,  $\gamma$ -CD-OEI-FA,  $\gamma$ -CD-OEI-FA/PTX,  $\gamma$ -CD-OEI-SS-FA, and  $\gamma$ -CD-OEI-SS-FA/PTX at various N/P ratios.

Figure 5.5 displays the particle size and zeta potential of the pDNA polyplexes with PEI, the three precursors ( $\gamma$ -CD-OEI,  $\gamma$ -CD-OEI-FA, and  $\gamma$ -CD-OEI-SS-FA), and the inclusion complexes ( $\gamma$ -CD-OEI/PTX,  $\gamma$ -CD-OEI-FA/PTX, and  $\gamma$ -CD-OEI-SS-FA/PTX) at various N/P ratios. As

shown in Figure 5.5a, all the cationic polymers efficiently compact pDNA into small nanoparticles with particle sizes around 70 to 110 nm. Their surface charge density in terms of zeta potential ranges from 25 to 36 mV as shown in Figure 5.5b. The formation of inclusion complexes with PTX did not significantly change the particle size and surface charge density of the polyplexes.

### 5.3.3. Cytotoxicity

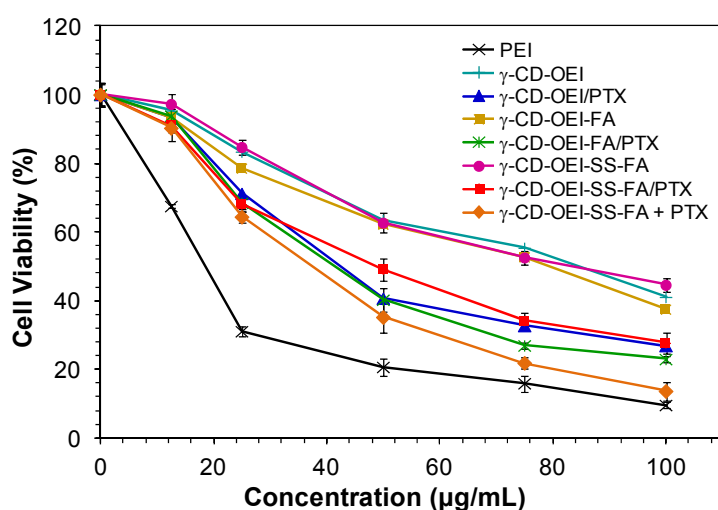


**Figure 5.6.** Cell viability assay in KB cells. The KB cells were treated with PEI (25 kDa),  $\gamma$ -CD-OEI,  $\gamma$ -CD-OEI/PTX,  $\gamma$ -CD-OEI-FA,  $\gamma$ -CD-OEI-FA/PTX,  $\gamma$ -CD-OEI-SS-FA,  $\gamma$ -CD-OEI-SS-FA/PTX, and physical mixture of  $\gamma$ -CD-OEI-SS-FA and PTX (denoted by  $\gamma$ -CD-OEI-SS-FA + PTX) at various concentrations for 24 hours in FA-free RPMI 1640 medium. Data represent mean  $\pm$  standard deviation ( $n = 4$ ).

Figure 5.6 shows the cell cytotoxicity results in KB cells. As a result, all the PTX-free  $\gamma$ -CD-OEI,  $\gamma$ -CD-OEI-FA, and  $\gamma$ -CD-OEI-SS-FA showed lower cytotoxicity than PEI because the introduction of CD ring could decrease the cytotoxicity. The formation of inclusion complexes with PTX considerably increased the cytotoxicity of these compounds, obviously due to the introduction the toxic PTX. The physical mixture of  $\gamma$ -CD-OEI-SS-FA and

PTX with DMSO as solubilizer showed much higher cytotoxicity due to the free PTX that is available immediately.

### 5.3.4. In vitro Luciferase Gene Transfection

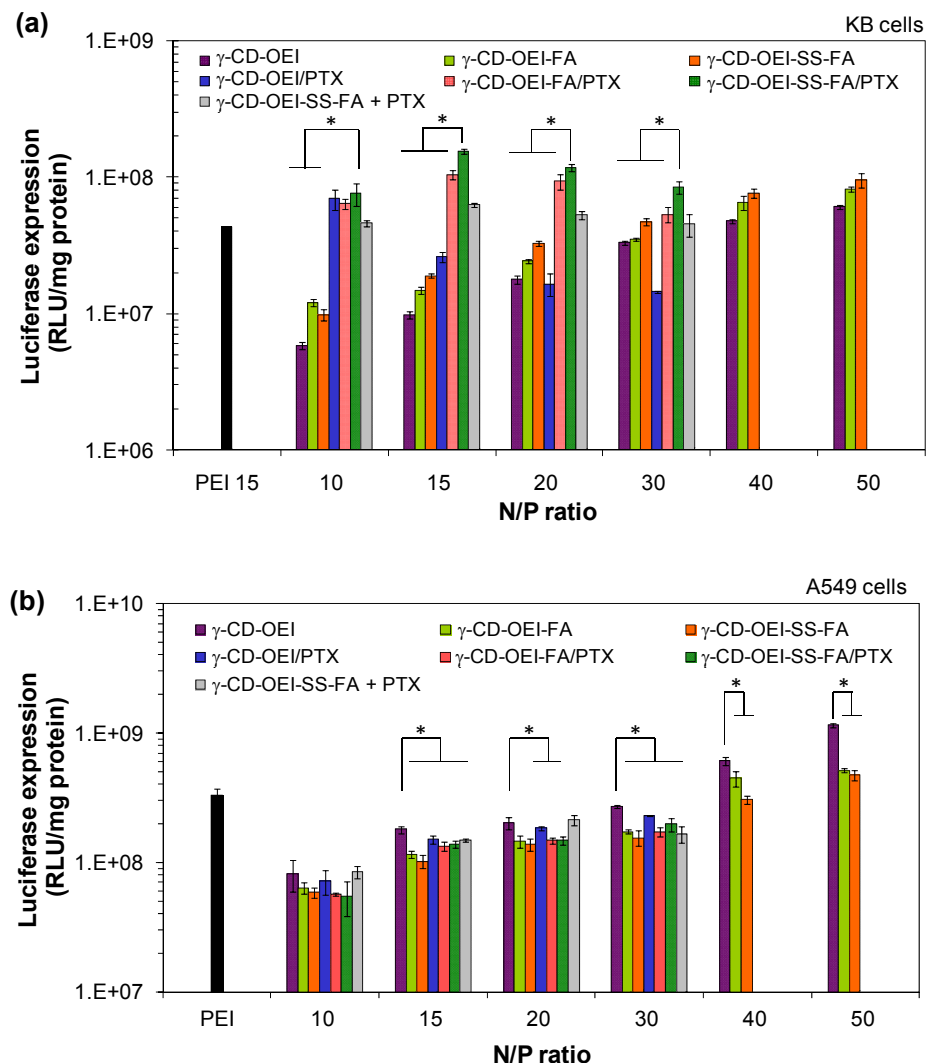


**Figure 5.7.** *In vitro* gene transfection efficiency of the pDNA polyplexes with PEI (25 kDa),  $\gamma$ -CD-OEI,  $\gamma$ -CD-OEI-FA,  $\gamma$ -CD-OEI-SS-FA,  $\gamma$ -CD-OEI/PTX,  $\gamma$ -CD-OEI-FA/PTX,  $\gamma$ -CD-OEI-SS-FA/PTX, and physical mixture of  $\gamma$ -CD-OEI-SS-FA and PTX (denoted by  $\gamma$ -CD-OEI-SS-FA + PTX) at different N/P ratios in KB cells (a) and A549 cells (b) in FA-free RPMI 1640 medium. Data represent mean  $\pm$  standard deviation (\* $P < 0.005$ ,  $n = 4$ ).

The FR-mediated targeted gene delivery and enhanced gene expression by co-delivery of anti-cancer drug PTX and gene were studied using luciferase

assay in FR-positive KB cells and FR-negative A549 cells. The gene transfection efficiency of  $\gamma$ -CD-OEI-SS-FA/PTX in KB cells (Figure 5.7a) and A549 cells (Figure 5.7b) was evaluated in comparison with PEI,  $\gamma$ -CD-OEI,  $\gamma$ -CD-OEI-FA,  $\gamma$ -CD-OEI-SS-FA,  $\gamma$ -CD-OEI/PTX,  $\gamma$ -CD-OEI-FA/PTX, and physical mixture of  $\gamma$ -CD-OEI-SS-FA and PTX in FA-free RPMI 1640 medium. The structural difference of  $\gamma$ -CD-OEI-SS-FA and  $\gamma$ -CD-OEI-FA is that the former possesses a disulfide linker between FA and  $\gamma$ -CD-OEI. This disulfide linker can be reduced by glutathione (GSH) after FR-mediated endocytosis and then the FR could be readily released and recycled to cell membrane. As discussed in our previous work, the FA-targeted delivery combined with the smart FR-recycling function can achieve a significant enhancement of gene expression.<sup>50</sup> The cytotoxicity of the PTX inclusion complexes was obvious at N/P ratio of 40 and 50, so the gene expression data were not shown in Figure 5.7.

In FR-positive KB cells (Figure 5.7a), co-delivery of PTX could further enhance the gene transfection efficiency following the order  $\gamma$ -CD-OEI-SS-FA/PTX >  $\gamma$ -CD-OEI-FA/PTX >  $\gamma$ -CD-OEI/PTX. For PTX-free carriers, the gene transfection efficiency followed a similar order  $\gamma$ -CD-OEI-SS-FA >  $\gamma$ -CD-OEI-FA >  $\gamma$ -CD-OEI. The gene transfection efficiency of  $\gamma$ -CD-OEI-SS-FA/PTX was constantly higher than that of PEI (25 kDa) and all the other carriers. Generally, all the three PTX-complexed gene carriers showed significantly higher gene transfection efficiency at low N/P ratios ranging from 10 to 20 than that of their PTX-free counterparts. According to the cell viability results, these PTX-complexed carriers had comparatively high cytotoxicity due to the complexed PTX. In this work, the increase of N/P ratios to high level resulted in a decrease of gene transfection efficiency because of the high cytotoxicity of PTX. So, we focus our discussion on the gene transfection experiments involving these PTX-complexed gene carriers at low N/P ratio range from 10 to 30. At N/P

ratio of 15,  $\gamma$ -CD-OEI-SS-FA/PTX showed optimal gene transfection efficiency, which was also significantly higher than that of  $\gamma$ -CD-OEI-SS-FA,  $\gamma$ -CD-OEI-FA/PTX,  $\gamma$ -CD-OEI-FA,  $\gamma$ -CD-OEI/PTX, and  $\gamma$ -CD-OEI, by 8-fold, 1-fold, 10-fold, 6-fold, and 21-fold, respectively. Further, even  $\gamma$ -CD-OEI/PTX without target group showed considerably enhanced gene transfection efficiency, which is 4-fold higher than that of  $\gamma$ -CD-OEI. These results proved the synergistic or combined effect of co-delivery of PTX with DNA to enhance the gene transfection, as well as the enhancement effects induced by the FA-targeted group and the reducible disulfide linker. In contrast, in FR-negative A549 cells (Figure 5.7b), the FA and disulfide linker showed no enhancement effect on gene expression due to the lack of FR-mediated endocytosis, and the complexation of PTX also had no enhancement on gene transfection.

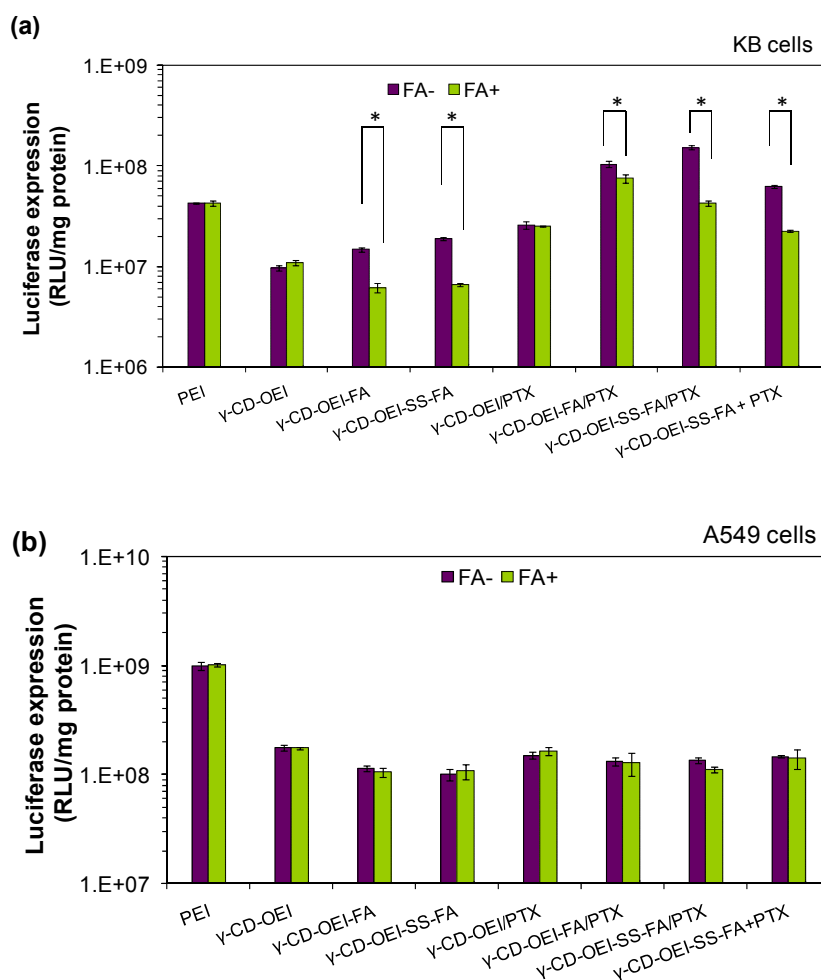


**Figure 5.8.** *In vitro* gene transfection efficiency of the pDNA polyplexes with by PEI (25 kDa),  $\gamma$ -CD-OEI,  $\gamma$ -CD-OEI-FA,  $\gamma$ -CD-OEI-SS-FA,  $\gamma$ -CD-OEI/PTX,  $\gamma$ -CD-OEI-FA/PTX,  $\gamma$ -CD-OEI-SS-FA/PTX, and physical mixture of  $\gamma$ -CD-OEI-SS-FA and PTX (denoted by  $\gamma$ -CD-OEI-SS-FA + PTX) at N/P ratio of 15 in KB cells (a) and A549 cells (b) in the absence and presence of 0.001 g/L of FA in the culture medium. Data represent mean  $\pm$  standard deviation (\* $P < 0.005$ ,  $n = 4$ ).

To further demonstrate the effects of the supramolecular self-assembly and the FA group attached to the carrier, FA competition tests were carried out by comparison of gene transfection efficiency in the absence and presence of FA in the cell culture medium. As shown in Figure 5.8a, the gene transfection efficiency of both FA-modified carriers ( $\gamma$ -CD-OEI-FA, and  $\gamma$ -CD-OEI-SS-FA) and their PTX-complexed self-assemblies ( $\gamma$ -CD-OEI-FA/PTX, and  $\gamma$ -CD-OEI-SS-FA/PTX) was reduced when the FR-positive KB cells were treated with FA-containing culture medium. In contrast, other carriers without FA group, such as PEI,  $\gamma$ -CD-OEI, and  $\gamma$ -CD-OEI/PTX had almost no difference in the absence and presence of FA in the culture medium. In addition, although the effect was considerably weakened because of the competition of FRs by free FA in the FA-containing medium, the PTX-complexed self-assembly carriers ( $\gamma$ -CD-OEI-SS-FA/PTX and  $\gamma$ -CD-OEI-FA/PTX) still had higher gene transfection efficiency than all other carriers. The physical mixture of  $\gamma$ -CD-OEI-SS-FA and PTX showed higher gene transfection than  $\gamma$ -CD-OEI-SS-FA, but lower than  $\gamma$ -CD-OEI-SS-FA/PTX and  $\gamma$ -CD-OEI-FA/PTX. Moreover, the gene transfection efficiency for this physical mixture system was also reduced when the FA-containing medium was applied. These results indicate that the FA group in  $\gamma$ -CD-OEI-SS-FA was an important factor to improve the gene transfection, and the PTX-complexed self-assembly system showed double effects in enhancing the gene transfection efficiency. In contrast, when the

experiments were done in FR-negative A549 cells, the transfection efficiency for each carrier showed no difference in the absence and presence of FA in the culture medium (Figure 5.8b). Also, generally all  $\gamma$ -CD-based carriers with or without FA modification showed low gene transfection efficiency at this low N/P ratio of 15, which is much lower than that of PEI. FA-modified carriers in FR-negative A549 cells showed low transfection efficiency due to the lack of FR-mediated endocytosis effect. There was also no PTX co-delivery effect at the low N/P ratio of 15 in FR-negative A549 cells, probably due to the generally low gene transfection efficiency.

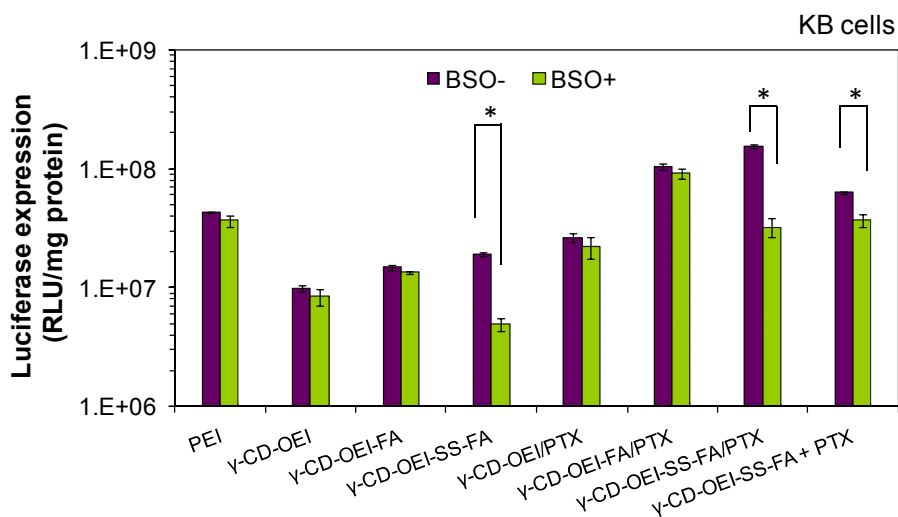


**Figure 5.9.** *In vitro* gene transfection efficiency of the pDNA polyplexes with PEI (25 kDa),  $\gamma$ -CD-OEI,  $\gamma$ -CD-OEI-FA,  $\gamma$ -CD-OEI-SS-FA,  $\gamma$ -CD-OEI/PTX,  $\gamma$ -CD-OEI-FA/PTX,  $\gamma$ -CD-OEI-SS-FA/PTX, and physical mixture of  $\gamma$ -CD-OEI-SS-FA and PTX (denoted by  $\gamma$ -CD-OEI-SS-FA + PTX) at N/P ratio of 15 in KB cells in the absence and presence of 250  $\mu$ M of BSO in the culture medium. Data represent mean  $\pm$  standard deviation (\* $P$  < 0.005,  $n$  = 4)

BSO can reduce the intracellular glutathione concentration and inhibit the reduction of disulfide linker<sup>52, 53, 50, 51</sup>. At the presence of BSO, the effect of the disulfide linker in the disulfide-containing carrier systems will be weakened. As shown in Figure 5.9, the gene transfection efficiency of disulfide-modified

systems including  $\gamma$ -CD-OEI-SS-FA, its PTX-complexed  $\gamma$ -CD-OEI-SS-FA/PTX, and the physical mixture of  $\gamma$ -CD-OEI-SS-FA and PTX was significantly decreased when the KB cells were treated with BSO-containing medium. In contrast, the systems without disulfide bond showed almost no changes. We previously reported that the reducible disulfide linker in the  $\gamma$ -CD-OEI-SS-FA system can lead to the detachment of the FA groups from the polymeric carrier after the FR-mediated endocytosis, which results in the release of the bound FRs followed by the recycling of the FRs from the cytosol onto the cell membrane surface, facilitating continuous FR-mediated endocytosis to achieve enhanced gene transfection.<sup>50</sup>

Figure 5.10 gives the confocal microscopy images showing the cellular uptake of the pDNA polyplexes with all  $\gamma$ -CD-based carriers and their PTX-complexed self-assemblies. PTX was labeled with FITC giving green fluorescence and the cationic  $\gamma$ -CD-based carriers with rhodamine that is red. After treating the FR-positive KB cells with the pRL-CMV polyplexes for 2 hours in FA-free medium, the cellular uptake rate follows an order  $\gamma$ -CD-OEI-SS-FA/PTX =  $\gamma$ -CD-OEI-SS-FA >  $\gamma$ -CD-OEI-FA/PTX =  $\gamma$ -CD-OEI-FA >  $\gamma$ -CD-OEI/PTX =  $\gamma$ -CD-OEI, which is consistent with the results of gene transfection experiments. Most of the green and red fluorescence polyplexes appeared overlapped. Some free green fluorescence dots could also be observed due to the release of the complexed PTX, which explains the cell viability results that all the three PTX-complexed self-assembly systems had higher cytotoxicity.



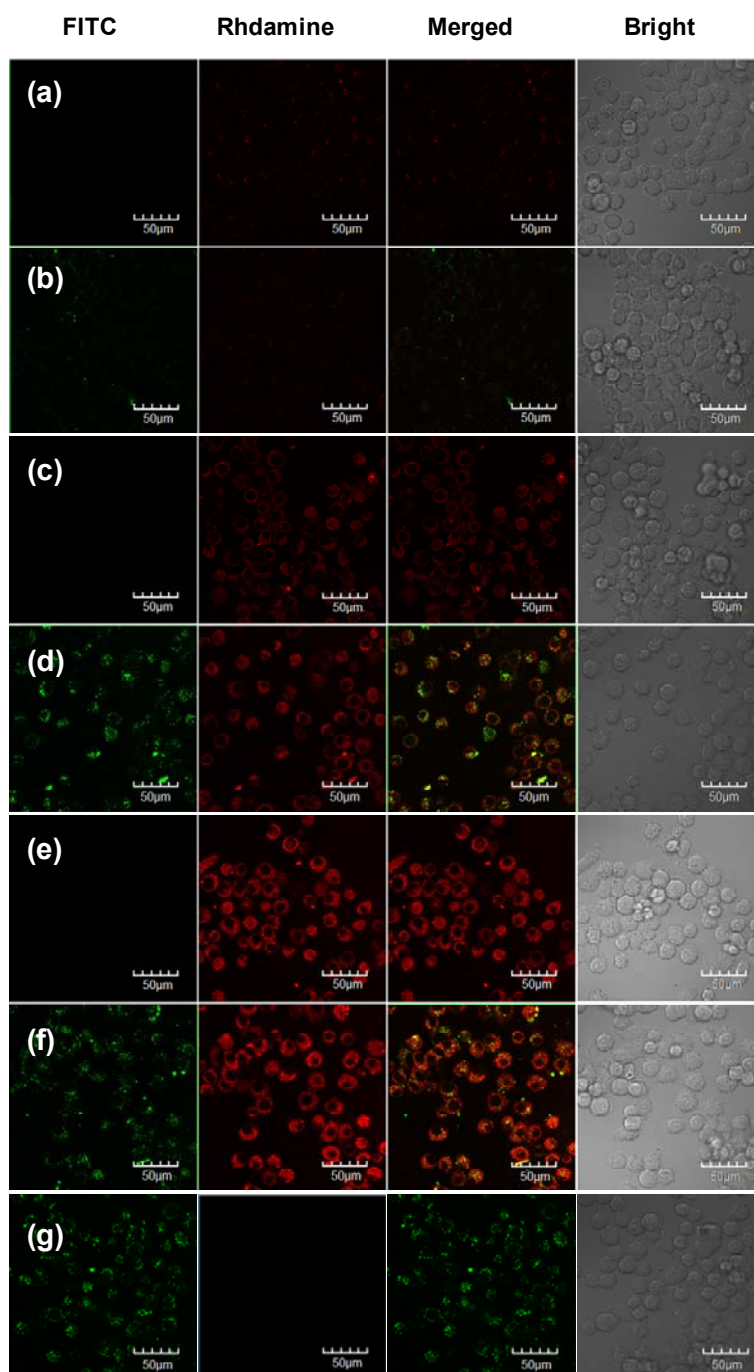


**Figure 5.10.** Confocal microscopy images of the KB cells transfected by the pDNA polyplexes with  $\gamma$ -CD-OEI-Rhd (a),  $\gamma$ -CD-OEI-Rhd/PTX-FITC (b),  $\gamma$ -CD-OEI-FA-Rhd (c),  $\gamma$ -CD-OEI-FA-Rhd/PTX-FITC (d),  $\gamma$ -CD-OEI-SS-FA-Rhd (e),  $\gamma$ -CD-OEI-SS-FA-Rhd/PTX-FITC (f), and  $\gamma$ -CD-OEI-SS-FA/PTX-FITC (g) at N/P ratio of 15 in FA-free RPMI 1640 medium. PTX and  $\gamma$ -CD-OEI derivatives were labeled with FITC (green) and rhodamine (red), respectively.

## 5.3.5. Delivery of Wild Type p53 Gene for Cancer Cell Apoptosis

The protein encoded by *p53* gene is a common tumor suppressor which plays a critical role in diverse cellular pathways, such as DNA repair, regulation of cell cycle, and cell apoptosis.<sup>54</sup> It has been reported that *p53* gene is mutated nearly in 50% of human cancers. Mutant *p53* gene loses its ability to control cell cycle and cell apoptosis, resulting in tumor growth. Hence, functional restoration of wild type *p53* gene in cancer cells can suppress cell proliferation and stimulate apoptosis. This was evidenced by the fact that adenovirus-mediated *p53* gene delivery showed tumor regression in clinical trials, although this method has been limited in intra-tumor injection.<sup>55</sup>

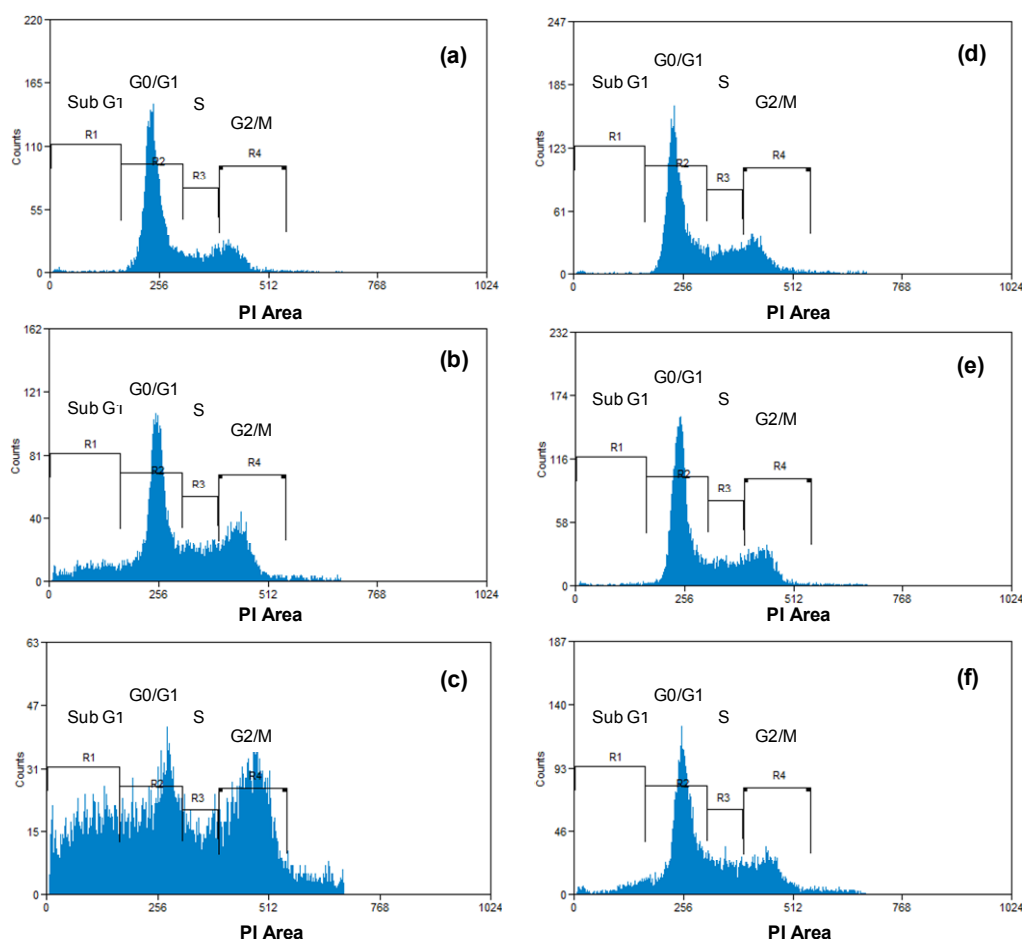


**Figure 5.11.** Representative cell cycle diagrams of KB cells transfected with pCMV-p53 mediated by  $\gamma$ -CD-OEI/PTX (a),  $\gamma$ -CD-OEI-FA/PTX (b),  $\gamma$ -CD-OEI-SS-FA/PTX (c), and transfected with pCMV-p53mt135 mediated by

$\gamma$ -CD-OEI/PTX (d),  $\gamma$ -CD-OEI-FA/PTX (e), and  $\gamma$ -CD-OEI-SS-FA/PTX (f) at N/P ratio of 15 in FA-free RPMI 1640 medium.

Herein we have applied the multifunctional supramolecular self-assembly drug and gene co-carrier for delivery of wild type *p53* gene into KB cells to efficiently control the cancer cell apoptosis. For this purpose, two plasmids pCMV-*p53* and pCMV-*p53*mt135 were used. pCMV-*p53* expresses the wild-type *p53* tumor suppression protein and pCMV-*p53*mt135 expresses a mutant *p53* protein that does not have tumor suppression effect, which is used as negative control.

Figure 5.11 shows the cell cycle diagrams of FR-positive KB cells transfected with pCMV-*p53* and pCMV-*p53*mt135 genes with different carrier systems. Table 5.1 and Table 5.2 summarize the cell cycle analysis results for FR-positive KB cells and FR-negative cells transfected with pCMV-*p53* and pCMV-*p53*mt135 genes mediated by different carrier systems. In FR-positive KB cells, the PTX-complexed  $\gamma$ -CD-OEI-SS-FA/PTX self-assembly system resulted in remarkably larger cell population at sub G1 phase (23.48%) than any other carrier systems (Figure 5.11c, Table 5.1). Moreover, the G2/M phase for these KB cells was 31.54%, indicating that the PTX-induced microtubule stabilization led to G2/M cell cycle arrest. As also supported by our luciferase gene transfection results, we can reasonably conclude that the very efficient *p53* gene delivery mediated by the  $\gamma$ -CD-OEI-SS-FA/PTX self-assembly system was a result from the combined and synergistic effects of the PTX-enhanced gene transfection, the FA-targeted delivery, and the disulfide linker mediated FR-recycling.

**Table 5.1.** Cell cycle analysis results of FR-positive KB cells transfected with pCMV-*p53* and pCMV-*p53*mt135 mediated by PEI (25 KDa),  $\gamma$ -CD-OEI,  $\gamma$ -CD-OEI-FA,  $\gamma$ -CD-OEI-SS-FA,  $\gamma$ -CD-OEI/PTX,  $\gamma$ -CD-OEI-FA/PTX,  $\gamma$ -CD-OEI-SS-FA/PTX, and physical mixture of  $\gamma$ -CD-OEI-SS-FA and PTX at N/P ratio of 15 in FA-free RPMI 1640 medium.

Polymers	pCMV-p53				pCMV-p53mt135			
	sub G1	G0/G1	S	G2/M	sub G1	G0/G1	S	G2/M
PEI	1.39	71.33	11.06	16.18	1.65	65.23	14.98	17.84
$\gamma$ -CD-OEI	1.62	67.69	12.10	18.17	0.77	59.50	15.84	22.78
$\gamma$ -CD-OEI/PTX	1.15	71.46	12.80	14.25	0.54	64.19	15.97	18.52
$\gamma$ -CD-OEI-FA	1.17	70.02	13.59	14.99	0.73	62.94	17.38	18.13
$\gamma$ -CD-OEI-FA/PTX	9.73	50.40	15.60	23.14	1.08	63.33	14.69	20.33
$\gamma$ -CD-OEI-SS-FA	1.90	71.14	13.50	13.33	0.81	61.30	16.11	20.67
$\gamma$ -CD-OEI-SS-FA/PTX	23.48	29.41	11.91	31.54	5.10	54.80	16.96	21.28
$\gamma$ -CD-OEI-SS-FA+PTX	0.92	71.54	12.42	15.05	0.71	64.07	16.28	18.21

**Table 5.2.** Cell cycle analysis results of FR-negative A549 cells transfected with pCMV-p53 and pCMV-p53mt135 mediated by PEI (25 KDa),  $\gamma$ -CD-OEI,  $\gamma$ -CD-OEI-FA,  $\gamma$ -CD-OEI-SS-FA,  $\gamma$ -CD-OEI/PTX,  $\gamma$ -CD-OEI-FA/PTX,  $\gamma$ -CD-OEI-SS-FA/PTX, and physical mixture of  $\gamma$ -CD-OEI-SS-FA and PTX at N/P ratio of 15 in FA-free RPMI 1640 medium.

Polymers	pCMV-p53				pCMV-p53mt135			
	sub G1	G0/G1	S	G2/M	sub G1	G0/G1	S	G2/M
PEI	0.53	57.97	12.59	27.45	0.51	58.66	13.15	26.59
$\gamma$ -CD-OEI	0.42	53.81	13.65	30.23	0.87	54.66	13.99	28.55
$\gamma$ -CD-OEI/PTX	0.29	52.08	13.58	32.06	0.38	53.96	12.78	31.18
$\gamma$ -CD-OEI-FA	0.44	54.95	12.77	30.24	0.37	57.34	13.10	27.63
$\gamma$ -CD-OEI-FA/PTX	0.39	55.48	13.48	28.73	0.32	55.36	12.77	29.78
$\gamma$ -CD-OEI-SS-FA	0.35	52.45	14.55	29.92	0.44	56.39	13.34	28.12
$\gamma$ -CD-OEI-SS-FA/PTX	0.32	51.62	13.58	31.82	0.55	54.48	13.30	29.75
$\gamma$ -CD-OEI-SS-FA+PTX	9.16	15.39	14.34	60.62	10.96	13.95	10.85	64.07

In comparison, when the mutant pCMV-p53mt135 was used in KB cells, all carrier systems showed no effects on the cell apoptosis and G2/M cell cycle arrest induced by PTX (Figure 5.11, Table 5.1), since pCMV-p53mt135 only expresses a mutant *p53* protein that does not have tumor suppression effect. When both pCMV-p53 and pCMV-p53mt135 were used in FR-negative A549 cells, also all carrier systems showed no effects on the cell apoptosis and G2/M cell cycle arrest induced by PTX (Table 5.2), since there had no effects of the FA-targeted delivery, and the disulfide linker mediated FR-recycling.

## **5.4. Conclusions**

Self-assembled inclusion complex between the star-shaped cationic polymer  $\gamma$ -CD-OEI-SS-FA and anticancer drug PTX was prepared, as the precursor of the multifunctional supramolecular self-assembly co-delivery system for PTX and pDNA. PTX was included in the  $\gamma$ -CD ring of  $\gamma$ -CD-OEI-SS-FA to form a 1:1 complex, corresponding to a 10.4% loading level of PTX. The  $\gamma$ -CD-OEI-SS-FA/PTX complex had good solubility in water, although PTX is water-insoluble. The  $\gamma$ -CD-OEI-SS-FA/PTX complex could form polyplexes with pDNA to give positively charged nanoparticles with size ranging from 70 to 110 nm, forming the multifunctional supramolecular self-assembly co-delivery system for PTX and pDNA.

The gene transfection experiments using luciferase marker gene were carried out in FR-positive KB cells and FR-negative A549 cells under various conditions. The results showed that the FA-targeted delivery induced higher gene transfection efficiency in the FR-positive KB cells. In addition, the reducible disulfide linker in the  $\gamma$ -CD-OEI-SS-FA/PTX self-assembly system led to the detachment of the FA groups from the carrier after the FR-mediated endocytosis, which resulted in the release of the bound FRs followed by the recycling of the FRs from the cytosol onto the cell membrane surface, facilitating continuous FR-mediated endocytosis to achieve the enhanced gene transfection. Moreover, the complexed PTX was co-delivered to the cells with pDNA, and the co-delivered PTX further enhanced the gene transfection even at a low N/P ratio of 15 in the FR-positive KB cells.

Finally, the  $\gamma$ -CD-OEI-SS-FA/PTX self-assembly co-delivery system was used to deliver wild-type p53 gene in KB cells. From the cell cycle analysis, the transfected KB cells showed large cell population at sub G1 and G2/M phases, indicating the efficient delivery of p53 gene that induced significant cell apoptosis. The data in this study have demonstrated that the

multifunctional  $\gamma$ -CD-OEI-SS-FA/PTX self-assembly co-delivery system showed the combined and synergistic effects of the PTX-enhanced gene transfection, the FA-targeted delivery, and the redox-sensitive FR-recycling. The multifunctional synergistic effects resulted in the very effective deliver of wild-type *p53* gene into FR-overexpressed KB cancer cells at low N/P ratios to induce an efficient cell apoptosis. Therefore, the novel multifunctional supramolecular self-assembly delivery system may be a promising candidate for potential cancer therapeutic application.

## 5.5. References

- (1) Greco, F.; Vicent, M. J., *Adv Drug Deliver Rev* **2009**,*61*, 1203-1213.
- (2) Lane, D., *Nat Biotechnol* **2006**,*24*, 163-164.
- (3) Rubinfeld, B.; Upadhyay, A.; Clark, S. L.; Fong, S. E.; Smith, V.; Koeppen, H.; Ross, S.; Polakis, P., *Nat Biotechnol* **2006**,*24*, 205-209.
- (4) Lebedeva, I. V.; Washington, I.; Sarkar, D.; Clark, J. A.; Fine, R. L.; Dent, P.; Curiel, D. T.; Turro, N. J.; Fisher, P. B., *P Natl Acad Sci USA* **2007**,*104*, 3484-3489.
- (5) Sun, T. M.; Du, J. Z.; Yao, Y. D.; Mao, C. Q.; Dou, S.; Huang, S. Y.; Zhang, P. Z.; Leong, K. W.; Song, E. W.; Wang, J., *ACS nano* **2011**,*5*, 1483-1494.
- (6) Tamura, M.; De, G.; Ueno, A., *Chemistry* **2001**,*7*, 1390-1397.
- (7) Michels, J. J.; O'Connell, M. J.; Taylor, P. N.; Wilson, J. S.; Cacialli, F.; Anderson, H. L., *Chemistry* **2003**,*9*, 6167-6176.
- (8) Cragg, G. M., *Medicinal Research Reviews* **1998**,*18*, 315-331.
- (9) Manfredi, J. J.; Horwitz, S. B., *Pharmacology & Therapeutics* **1984**,*25*, 83-125.
- (10) Woods, C. M.; Zhu, J.; Mcquaney, P. A.; Bollag, D.; Lazarides, E., *Mol Med* **1995**,*1*, 506-526.
- (11) Suffness, M., *Annu Rep Med Chem* **1993**,*28*, 305-314.
- (12) Culver, K. W.; Blaese, R. M., *Trends Genet* **1994**,*10*, 174-178.
- (13) Yang, Z. R.; Wang, H. F.; Zhao, J.; Peng, Y. Y.; Wang, J.; Guinn, B. A.; Huang, L. Q., *Cancer Gene Ther* **2007**,*14*, 599-615.
- (14) Junttila, M. R.; Evan, G. I., *Nat Rev Cancer* **2009**,*9*, 821-829.
- (15) Karmakar, A.; Bratton, S. M.; Dervishi, E.; Ghosh, A.; Mahmood, M.; Xu, Y.; Saeed, L. M.; Mustafa, T.; Casciano, D.; Radominska-Pandya, A.; Biris, A. S., *Int J Nanomed* **2011**,*6*, 1045-1055.
- (16) Levine, A. J.; Momand, J.; Finlay, C. A., *Nature* **1991**,*351*, 453-456.
- (17) Evan, G. I.; Vousden, K. H., *Nature* **2001**,*411*, 342-348.
- (18) Li, Y. X.; Lin, Z. B.; Tan, H. R., *Acta Pharmacol Sin* **2004**,*25*, 76-82.
- (19) Wiradharma, N.; Tong, Y. W.; Yang, Y. Y., *Biomaterials* **2009**,*30*, 3100-3109.
- (20) Xu, Z. H.; Zhang, Z. W.; Chen, Y.; Chen, L. L.; Lin, L. P.; Li, Y. P., *Biomaterials* **2010**,*31*, 916-922.
- (21) Wang, Y.; Gao, S. J.; Ye, W. H.; Yoon, H. S.; Yang, Y. Y., *Nature Materials* **2006**,*5*, 791-796.
- (22) Yue, X. Y.; Qiao, Y.; Qiao, N.; Guo, S. T.; Xing, J. F.; Deng, L. D.; Xu, J. Q.; Dong, A. J., *Biomacromolecules* **2010**,*11*, 2306-2312.
- (23) Wang, H. J.; Zhao, P. Q.; Su, W. Y.; Wang, S.; Liao, Z. Y.; Niu, R. F.; Chang, J., *Biomaterials* **2010**,*31*, 8741-8748.
- (24) Hu, Q. D.; Fan, H.; Ping, Y.; Liang, W. Q.; Tang, G. P.; Li, J., *Chemical Communications* **2011**,*47*, 5572-5574.

- (25) Wu, Y. L.; Yin, H.; Zhao, F.; Li, J., *Adv. Healthc. Mater.* **2013**,*2*, 297-301.
- (26) Son, K.; Huang, L., *Gene Ther* **1996**,*3*, 630-634.
- (27) Nair, R. R.; Rodgers, J. R.; Schwarz, L. A., *Molecular therapy : the journal of the American Society of Gene Therapy* **2002**,*5*, 455-462.
- (28) Bhalla, K.; Ibrado, A. M.; Tourkina, E.; Tang, C.; Mahoney, M. E.; Huang, Y., *Leukemia : official journal of the Leukemia Society of America, Leukemia Research Fund, U.K* **1993**,*7*, 563-568.
- (29) Sorger, P. K.; Dobles, M.; Tournebise, R.; Hyman, A. A., *Current opinion in cell biology* **1997**,*9*, 807-814.
- (30) Blagosklonny, M. V.; Fojo, T., *Int J Cancer* **1999**,*83*, 151-156.
- (31) Nielsen, L. L.; Lipari, P.; Dell, J.; Gurnani, M.; Hajian, G., *Clin Cancer Res* **1998**,*4*, 835-846.
- (32) Szejtli, J., *Chemical Reviews* **1998**,*98*, 1743-1753.
- (33) Davis, M. E.; Brewster, M. E., *Nat Rev Drug Discov* **2004**,*3*, 1023-1035.
- (34) Uekama, K.; Hirayama, F.; Irie, T., *Chemical Reviews* **1998**,*98*, 2045-2076.
- (35) Sharma, U. S.; Balasubramanian, S. V.; Straubinger, R. M., *J Pharm Sci* **1995**,*84*, 1223-1230.
- (36) Cserhati, T.; Forgacs, E.; Hollo, J., *J. Pharm. Biomed. Anal.* **1995**,*13*, 533-541.
- (37) Liu, Y.; Chen, G. S.; Li, L.; Zhang, H. Y.; Cao, D. X.; Yuan, Y. J., *Journal of medicinal chemistry* **2003**,*46*, 4634-4637.
- (38) Liu, Y.; Chen, G. S.; Chen, Y.; Cao, D. X.; Ge, Z. Q.; Yuan, Y. J., *Bioorg. Med. Chem.* **2004**,*12*, 5767-5775.
- (39) Hamada, H.; Ishihara, K.; Masuoka, N.; Mikuni, K.; Nakajima, N., *J. Biosci. Bioeng.* **2006**,*102*, 369-371.
- (40) Bouquet, W.; Ceelen, W.; Fritzing, B.; Pattyn, P.; Peeters, M.; Remon, J. P.; Vervaet, C., *Eur J Pharm Biopharm* **2007**,*66*, 391-397.
- (41) Fenyvesi, F.; Kiss, T.; Fenyvesi, E.; Szente, L.; Veszeka, S.; Deli, M. A.; Varadi, J.; Feher, P.; Ujhelyi, Z.; Tosaki, A.; Vecsernyes, M.; Bacska, I., *J Pharm Sci* **2011**,*100*, 4734-4744.
- (42) Gonzalez, H.; Hwang, S. J.; Davis, M. E., *Bioconjugate Chem* **1999**,*10*, 1068-1074.
- (43) Hwang, S. J.; Bellocq, N. C.; Davis, M. E., *Bioconjugate Chem* **2001**,*12*, 280-290.
- (44) Cheng, J. J.; Khin, K. T.; Jensen, G. S.; Liu, A. J.; Davis, M. E., *Bioconjugate Chem* **2003**,*14*, 1007-1017.
- (45) Pun, S. H.; Bellocq, N. C.; Liu, A. J.; Jensen, G.; Machemer, T.; Quijano, E.; Schluep, T.; Wen, S. F.; Engler, H.; Heidel, J.; Davis, M. E., *Bioconjugate Chem* **2004**,*15*, 831-840.
- (46) Yang, C. A.; Li, H. Z.; Goh, S. H.; Li, J., *Biomaterials* **2007**,*28*, 3245-3254.
- (47) Li, J.; Loh, X. J., *Adv Drug Deliver Rev* **2008**,*60*, 1000-1017.



- (48) Li, J.; Yang, C.; Li, H. Z.; Wang, X.; Goh, S. H.; Ding, J. L.; Wang, D. Y.; Leong, K. W., *Advanced Materials* **2006**, *18*, 2969-2974.
- (49) Tokuoka, R.; Abe, M.; Fujiwara, T.; Tomita, K.; Saenger, W., *Chem. Lett.* **1980**, 491-494.
- (50) Zhao, F.; Yin, H.; Zhang, Z.; Li, J., *Biomacromolecules* **2013**, *14*, 476-84.
- (51) Rao, C. S.; Chu, J. J.; Liu, R. S.; Lai, Y. K., *Bioorganic & medicinal chemistry* **1998**, *6*, 2193-2204.
- (52) Xu, K.; Thornalley, P. J., *Biochem Pharmacol* **2001**, *61*, 165-177.
- (53) Song, J. J.; Lee, Y. J., *The Biochemical journal* **2003**, *373*, 845-853.
- (54) Yoshida, K.; Miki, Y., *Cancer Sci* **2010**, *101*, 831-835.
- (55) Wiman, K. G., *Adv Cancer Res* **2007**, *97*, 321-338.

## CHAPTER 6 CONCLUSIONS AND FUTURE WORK

### 6.1. Conclusions

This research studied on synthesis of novel multi-functional cyclodextrin-based cationic star polymers for drug and gene delivery. Generally, the host-guest structure between cyclodextrin (CD) ring with hydrophobic cavity and hydrophobic anticancer drug was synthesized to alter the solubility and cytotoxicity of drug. Cyclodextrin-oligoethylenimines (CD-OEIs) modified with targeted groups and biodegradable linkers were prepared for site-specific and enhanced gene delivery. Moreover, the CD ring was included anticancer drug for potential drug and gene co-delivery. These CD-based cationic polymers have potential applications in cancer therapy.

In detail, this study reported a synthesis of OEI-conjugated  $\alpha$ -,  $\beta$ -, and  $\gamma$ -CD as a carrier for anticancer drug paclitaxel (PTX). As a result, structure modification by OEI significantly increase the water solubility of  $\beta$ -CD, which are widely used in oral drug delivery but limited by its poor water solubility. Moreover, the formation of inclusion complexes remarkably increase water solubility of PTX with 146,149-fold higher than the mother drug. In addition, the  $\alpha$ -CD derivative also demonstrated up to 30,956-fold higher water

solubility than pure PTX. As we known, it is the best  $\alpha$ -CD-based carrier for PTX delivery. Furthermore, the anticancer ability is still maintained.

This study has expanded the strategy of folic acid (FA)-targeted delivery by combining the smart folate receptor (FR)-recycling function to achieve the significant enhancement of gene expression. We synthesized a new star-shaped cationic polymer consists of a  $\gamma$ -cyclodextrin ( $\gamma$ -CD) core and multiple oligoethylenimine (OEI) arms, conjugating with folic acid (FA) and incorporating with a biodegradable disulfide bond between polymer and target group for efficient targeted gene delivery. The synthesized cationic polymer, named  $\gamma$ -CD-OEI-SS-FA, could be efficiently cleaved under reductive condition similar to intracellular environment that reduces the disulfide linker, and then conjugated FA was readily released. The  $\gamma$ -CD-OEI-SS-FA polymers have good DNA condensation ability and lower cytotoxicity than PEI (25 kDa). Moreover, the  $\gamma$ -CD-OEI-SS-FA polymer can efficiently deliver pDNA into FR-positive cells through FR-mediated cellular uptake. The enhancement effects by structure modification of FA and disulfide bond were further demonstrated by FA competition and disulfide inhibitory tests.

Further studies focus on the drug and gene co-delivery to take advantage of the hydrophobic cavity of cyclodextrin. In detail, the inclusion complex between the star-shaped cationic  $\gamma$ -CD-OEI-SS-FA polymer and anticancer drug PTX was synthesized. The inclusion complex was stable in aqueous with 12% loading efficiency of PTX. The targeted delivery and FR recycling effect inducing by disulfide linker can be maintained. Moreover, introduction of PTX significantly increase the gene expression in luciferase assay and reduce the administration of polymer. Co-delivery of PTX and wild-type p53 gene with the cationic polymer shows large cell population at sub G1 and G2/M phase, demonstrating cell apoptosis and PTX-induced microtubule stabilization.

In general, the research of CD-OEI for PTX delivery greatly expands the

application of drug delivery using CDs. The cationic  $\gamma$ -CD-OEI-SS-FA carrier with FA-targeted and biodegradable capability may be a promising efficient gene delivery vector. Co-delivery of drug and gene has significant synergistic effect and it could be an efficient strategy for potential cancer gene therapy.

### 6.2. Future Work

As mentioned in the literature review, the unique structure of polyrotaxane has many interesting advantages for potential drug and gene delivery, such as the highly mobility of threaded cyclodextrins that could enhance the ligand-receptor interactions, the dethreading ability induced by cleavage of terminal groups may contribute to controlled release, and the easy chemical modification of threaded cyclodextrins. Synthesis of cationic polyroataxanes with target group folic acid and disulfide linker are promising structure that can keep the target effect and enhance the interaction with folate receptor on the malignant cell surface.

Many drug and gene delivery vectors suffered non-specifically adherent to normal cells and extracellular components, such as serum protein. This problem can be alleviated by shielding of the particle surface with hydrophilic uncharged molecule, such as PEG<sup>1</sup> or poly [N-2-(hydroxypropyl) methacrylamine] (PHPMA)<sup>2</sup>. The shield procedure can additionally reduce toxicity, prevent aggregation, and extend the half-life of polyplexes.<sup>3</sup> Therefore, structure modification with PEGylation may be promising tools to overcome this obstacle, and our synthesized cationic polymers still have many sites for further modification.

Although many types of folate conjugates have been tested by kinds of animal models, only six of folate-conjugated drugs have already entered clinic trials.<sup>4-9</sup> The parameters and barriers for *in vivo* delivery are higher and more sophisticates than those encountered *in vitro*, so it would be necessary to demonstrate the effect of drug and gene delivery carriers in animal test.

In general, additional improvements and experiments to improve the gene transfection efficiency and to prove the stability and efficiency in systemic administration *in vivo* are better to be investigated in future studies.

### 6.3. References

- (1) Ogris, M.; Brunner, S.; Schuller, S.; Kircheis, R.; Wagner, E., *Gene Ther* **1999**,*6*, 595-605.
- (2) Oupicky, D.; Howard, K. A.; Konak, C.; Dash, P. R.; Ulbrich, K.; Seymour, L. W., *Bioconjugate Chem* **2000**,*11*, 492-501.
- (3) Lee, M.; Kim, S. W., *Pharmaceut Res* **2005**,*22*, 1-10.
- (4) Leamon, C. P.; Parker, M. A.; Vlahov, I. R.; Xu, L. C.; Reddy, J. A.; Vetzal, M.; Douglas, N., *Bioconjug Chem* **2002**,*13*, 1200-1210.
- (5) Leamon, C. P.; Reddy, J. A.; Vlahov, I. R.; Westrick, E.; Parker, N.; Nicoson, J. S.; Vetzal, M., *International journal of cancer. Journal international du cancer* **2007**,*121*, 1585-1592.
- (6) Leamon, C. P.; Reddy, J. A.; Vlahov, I. R.; Westrick, E.; Dawson, A.; Dorton, R.; Vetzal, M.; Santhapuram, H. K.; Wang, Y., *Molecular pharmaceutics* **2007**,*4*, 659-667.
- (7) Lu, Y.; Low, P. S., *Cancer immunology, immunotherapy : CII* **2002**,*51*, 153-162.
- (8) Wang, S.; Luo, J.; Lantrip, D. A.; Waters, D. J.; Mathias, C. J.; Green, M. A.; Fuchs, P. L.; Low, P. S., *Bioconjug Chem* **1997**,*8*, 673-679.
- (9) Xia, W.; Low, P. S., *Journal of medicinal chemistry* **2010**,*53*, 6811-6824.